



DISSERTATION

Renewable Energy Generation when Supply Fluctuates Seasonally and the Effects of Learning

An Optimal Control Approach

ausgeführt zum Zwecke der Erlangung des akademischen Grades eines

Doktors der technischen Wissenschaften

unter der Leitung von

Ao.Univ.Prof. Dipl.-Ing. Dr.techn. Gernot Tragler

E105 - Institut für Wirtschaftsmathematik

sowie der Zweitbetreuung von

Univ.Prof. Dipl.-Ing. Dr.techn. Alexia Fürnkranz-Prskawetz

E105 - Institut für Wirtschaftsmathematik

eingereicht an der Technischen Universität Wien

Fakultät für Mathematik und Geoinformation

von

Dipl.-Ing. Elke Moser

Matrikelnr.: 0425707

Linzer Straße 372/2/6, 1140 Wien

Wien, 6. November 2014

(Elke Moser)

Kurzfassung

Angetrieben durch das starke Wirtschaftswachstum nimmt auch die weltweite Energienachfrage kontinuierlich zu. Der massive Verbrauch von fossilen Ressourcen treibt jedoch die Treibhausgasemissionen unweigerlich in die Höhe und fördert somit das Voranschreiten des Klimawandels. Die dringende Notwendigkeit einer maßgeblichen Veränderung in diesem Bereich ist daher deutlich gegeben. Um eine nachhaltige und saubere Energieversorgung zu gewährleisten, muss eine emissionsarme Energietechnologie gefunden werden, die gleichzeitig auch Versorgungssicherheit garantieren kann. Letzteres stellt bei den derzeitig verfügbaren erneuerbaren Technologien vermutlich die größte Herausforderung dar. Im Gegensatz zu fossilen Brennstoffen, die mehr oder weniger konstant vorhanden sind, sind erneuerbare Ressourcen oftmals starken Schwankungen unterlegen und lassen sich auch schwer prognostizieren. Die Wechselwirkungen aus überschüssiger und unzureichender Erzeugung sowie eingeschränkten Speichermöglichkeiten erschweren die Planbarkeit erneuerbarer Energieerzeugung deutlich. Ein weiteres Hindernis sind die hohen Investitionskosten, die bei erneuerbaren Technologien anfallen, während fossile Energieerzeugung zu wirtschaftlichen Preisen möglich ist. Diese hohen Kosten könnten allerdings nach einer gewissen Laufzeit durch das Ansammeln von Erfahrungswerten und Wissen reduziert werden. Da die meisten Entscheidungen in der Energieplanung jedoch auf den einhergehenden Kosten basieren und der Planungshorizont oft zu kurzfristig gesetzt ist, um solche Lerneffekte mit zu berücksichtigen, werden Investitionen in erneuerbare Energieerzeugung meist wieder in die Zukunft verschoben, was den möglichen Rahmen alternativer Energieerzeugung stark einschränkt.

Um diese Problematik näher zu untersuchen, befasst sich die vorliegende Doktorarbeit mit einer Reihe von optimalen Kontrollmodellen, welche die die Entscheidung eines Landes über die optimale Zusammensetzung eines Portfolios bestehend aus fossiler und erneuerbarer Energie zur Deckung des eigenen Energiebedarfes ermitteln. Hierfür wird das Angebot der fossilen Energie als konstant angenommen, während jenes der erneuerbaren Ressource saisonalen Schwankungen unterliegt. Um die erwähnte Kostenreduktion durch Lerneffekte in die Modelle mit einzubauen, wird das Konzept der Lernkurve verwendet. Welche Unterschiede sich aus der Berücksichtigung dieser Lerneffekte ergeben, zeigt die Analyse von drei unterschiedlichen Modellvarianten, wobei in der ersten die Investitionskosten unverändert bleiben, in der zweiten der treibende Aspekt durch Erfahrung gegeben ist, und in der dritten Variante ein weiterer Faktor in Form von Forschungs- und Entwicklungsprozessen mit eingebunden wird.

Abstract

Induced by the persistent and rapid economic growth, the worldwide demand for energy services is constantly increasing. The accompanying abundant use of fossil resources, however, strongly enhances green house gas emissions boosting the progress of climate change, which stresses the urgency of mitigation policies in this field. The probably biggest challenge along the path towards a more sustainable energy supply is to find a low-carbon energy technology that simultaneously guarantees energy security. For renewable energy generation, however, especially the second goal is hard to achieve as, in contrast to fossil resources, renewable resources strongly fluctuate and are often hard to predict. Consequently, the interplay of generated surpluses and shortfalls as well as limited storage possibilities complicate proper scheduling of renewable energy generation. Another major issue for renewable energy is given by the high costs. While conventional energy forms are competitive, renewable energy technology comes along with high investment costs that strongly restrict their profitability. These high costs would decline after some time in operation as experience and know-how improve the technical processes and hence foster the productivity. However, as the basis of energy planning decisions is mostly a matter of expenses and, in many cases, the planning horizon is too short to take these learning effects into account, investments for renewable energy technologies are often postponed into the future, which strongly restricts the scope of renewable energy generation.

To address this issue, this thesis deals with optimal control models that consider the energy planning decision of a small country optimizing a portfolio consisting of fossil and renewable energy to cover the country's energy demand. While fossil energy is assumed to be constantly available, renewable energy is fluctuating seasonally. To include the mentioned effect of cost reduction due to the accumulation of experience and knowledge, the concept of the learning curve is applied. To investigate the differences in the outcome depending on whether the mentioned learning effects are included or not in the decision process, three different model approaches are analyzed. In the first one the high investment costs of renewable energy capital remain unchanged over time, in the second one they are reduced by a so-called one-factor learning curve, where accumulated experience reduces costs, and in the third one a so-called two-factor learning curve is considered, where additionally R&D efforts foster the cost reduction.

Danksagung

Die Fertigstellung dieser Arbeit wäre nicht ohne die Unterstützung vieler Menschen möglich gewesen, bei denen ich mich an dieser Stelle herzlich bedanken möchte.

Zu Beginn sind meine beiden Betreuer Gernot Tragler und Alexia Fürnkranz-Prskawetz hervorzuheben, die mich über die gesamte Zeit mit Ideen und Anregungen begleiteten und mich stets motivierten. Ganz besonderer Dank gebührt Dieter Grass für seine große Unterstützung und hilfreichen Ratschläge bei numerischen Problemen und Unklarheiten. Ebenso geht mein Dank an meinen Zweitgutachter Richard F. Hartl für seine konstruktive Kritik und wertvollen Anmerkungen. Klaus Prettnner danke ich insbesondere für seine ökonomischen Motivationen.

Weiters möchte ich meine beiden Kollegen Christa Simon und Bernhard Skritek erwähnen. Der rege Gedankenaustausch während der gemeinsamen Kaffee-, Tee- und Mittagspausen war stets inspirierend und Quelle wertvoller Impulse für diese Arbeit.

Besonders möchte ich mich bei meinen Eltern bedanken, die mich in all meinen Plänen und Lebenslagen immer ausnahmslos unterstützen und somit wesentlich zum Abschluss dieser Arbeit beitrugen.

Diese Arbeit wäre auch nicht möglich gewesen ohne der motivierenden Zusprüche guter Freunde, die mich stets in meinem Vorhaben bekräftigten und mir so auch über die eine oder andere Hürde geholfen haben. Hier gilt ein spezielles Dankeschön an Wolfgang Haas für seine Unterstützung und Geduld während dieser Zeit.

Markus Waser danke ich insbesondere für seinen bedeutsamen Beitrag zur Verbesserung der Qualität und Lesbarkeit dieser Arbeit durch seine gewissenhaften Korrekturen.

Elke Moser

Declaration

I hereby certify that no other than the sources and aids referred to were used in this thesis. All parts which have been adopted either literally or in a general manner from other sources have been indicated accordingly.

I certify that the main contribution of this thesis, the investigation of the impact of learning effects on energy planning decisions as well as the challenge of seasonal fluctuations in the supply of renewable energy, is my own work.

Vienna, October 2014

Elke Moser

Contents

1	Introduction	1
1.1	Challenges of Renewable Energy Supply	1
1.2	The Concepts of Learning	2
1.2.1	Historical Background of the Learning Curve	3
1.2.2	One-Factor Learning Curve	4
1.2.3	Two-Factor Learning Curve	5
1.2.4	Learning Curves in Energy Systems	6
1.2.5	Forgetting by Not Doing	7
1.3	Formulation of the Problem	9
1.4	Software	11
1.5	Thesis Outline	11
1.6	Publications	12
2	The Basic Model	13
2.1	The Model	13
2.2	Solution	17
2.2.1	Canonical System and Necessary First Order Conditions	17
2.2.2	Periodic Solution	22
2.2.3	Stability	25
2.2.4	Numerical Continuation of Optimal Paths	30
2.3	Results	34
2.4	Sensitivity Analysis	38
2.4.1	Fossil Energy Price p_F	38
2.4.2	Degree of Efficiency η	44
2.4.3	Combined Effects	45
2.5	Fluctuating Energy Demand	48
2.6	Summary	52

3	The Effect of Learning by Doing	53
3.1	The Model	53
3.2	Solution	54
3.2.1	Canonical System and Necessary First Order Conditions	54
3.2.2	Periodic Solution	56
3.2.3	Stability	57
3.2.4	Optimal Paths	58
3.3	Results	61
3.3.1	Calculation of the Indifference Threshold Point	62
3.3.2	Economic Interpretation of the Indifference Threshold Point	66
3.3.3	Break-Even Analysis	69
3.4	Sensitivity Analysis	71
3.4.1	Fossil Energy Price p_F	71
3.4.2	Learning-by-Doing Coefficient α	84
3.4.3	Global Radiation Intensity	85
3.5	Summary	91
4	The Effect of Learning by Searching	93
4.1	The Model	93
4.2	Solution	94
4.2.1	Canonical System and Necessary First Order Conditions	94
4.2.2	Periodic Solution	98
4.2.3	Stability	100
4.2.4	Optimal Paths	102
4.3	Results	103
4.3.1	Calculation of the Indifference Threshold Curve	107
4.3.2	Economic Interpretation of the Indifference Threshold Curve	110
4.3.3	Break-Even Analysis	112
4.4	Sensitivity Analysis	115
4.4.1	Fossil Energy Price p_F	115
4.4.2	Global Radiation Intensity	128
4.5	Summary	130
5	Discussion and Conclusion	131
5.1	Methodological Aspects of Non-Autonomous Optimal Control Models	132
5.2	Economic Interpretation of the Results	133
5.3	Conclusion	137

Introduction

Facing the more frequent occurrence of natural disaster as a consequence of climate change, the rapid economic growth associated with a higher demand for energy services, either in form of power, heat, or transport, as well as the fact that the energy sector is one of the main contributors to the constant increase in greenhouse gas emissions (see IPCC, 2014), underlines the urgency of climate change mitigation policies to induce a restructuring of the current energy supply system. Therefore, one of the main challenges of the 21st century is to find a way to enable a sustainable, low-carbon energy supply providing the balance between energy security, economic development, and environmental protection. This, however, is not at all an easy task as renewable energy technologies exhibit some properties that strongly complicate a successful inclusion into the system, especially, if no proper political circumstances are given.

1.1 Challenges of Renewable Energy Supply

The probably most fundamental barrier for a successful inclusion of renewable energy technologies into the market is given by the high differences in investment costs compared to conventional energy forms. Whereas, for example, fossil energy is already properly set in the market and, consequently, competitive, the acquisition of new technology capital is very expensive as almost no experience with this technology exists, necessary work environments have to be adapted, and further research is needed to improve the performance. Therefore, in the short run the inclusion of a new technology would be too costly, as competitiveness with the already existing technologies is not given. In the long run, of course, the investment costs would decrease while experience improves the technological processes. In the literature, this effect is referred to as the learning curve and will be explained in more detail in the subsequent exposition. Whether energy planning

decisions are made long- or short-sighted can be crucial, because new technologies can only turn out to be profitable if their whole life-cycle and hence also these learning effects are considered in the decisions.

A second barrier for a shift towards a more sustainable energy supply is given by the fact that the renewable resources used for energy generation are subject to daily or seasonal fluctuations, which complicates proper scheduling, whereas the supply of fossil resources is more or less constant and predictable.

1.2 The Concepts of Learning

The incentives for developing and improving renewable energy technology have changed during the last decades. The original driving force has been the rapidly narrowing horizon of depletion of fossil fuels. However, due to the development of new extraction techniques and the discovery of new sources, the threats of global warming have become a more important issue. With energy generation being one of the major sources of greenhouse gas emissions, mitigation policies in form of investments in renewable energy technology try to reduce the emissions and slow down the global warming process. The available alternatives of energy generation in the future, however, strongly depend on structural and technological changes together with the accompanying investment decisions right now, because the development and the diffusion of a new technology is a time-intensive dynamic process (cf. Harmon, 2000). This underlines the importance of timely planning for energy technology decisions. As investment costs play a major role for such decisions and since these costs are very high for renewable technologies compared to the ones of conventional energy forms, investments are postponed until they get cheaper, hence strongly restricting the scale of alternative energy generation (cf. Rong-Gang, 2013; Berglund and Söderholm, 2006). Therefore, it is important to consider the whole life span of a new technology for energy planning decisions in order to include the diffusion process and the cost reduction that comes along with implementing the new technology.

In the literature of recent years, some important developments in macroeconomics and energy economics can be observed, dealing with the issue of technological change. While in previous modeling approaches technological change, if considered at all, has been included as an exogenous increase in energy conversion efficiency, more recently the aim has been to endogenously model technological change, especially in form of learning-by-doing effects sometimes also considered as technological learning (see, for example, Chakravorty et al., 2008, 2011; Messner, 1997; Reichenbach and Requate, 2012; Köhler et al., 2006).

1.2.1 Historical Background of the Learning Curve

The concept of the learning curve has been introduced by Wright (1936) who observed that in an airplane-manufacturing the number of working-hours spent for the production of an airframe is a decreasing function of the total number of the previously produced airframes of the same type. In other words, this means that the unit costs of labor declined with experience measured in cumulative output. However, in case that the rate of output is constant, this would imply that also the stimulus for learning would appear to be constant as well. Therefore, Arrow (1962) suggests to use cumulative gross investments in form of cumulative production of capital goods as a measure for experience. This implies that each new machine¹ used in production leads to a learning process with continual incentive, which makes a steady state growth in productivity possible. In 1968, the learning curve concept has also been applied in the field of strategic management (see BCG, 1970), and from then on has been used in several areas of research (cf. Kahouli-Brahmi, 2008). To give an example of application in energy economics, Neij (1997) used the learning curve approach to analyze prospects of diffusion and application of renewable energy technology with a focus on wind and photovoltaic. Although there exist concepts with different scopes of application and aggregation, they are all based on Arrow's explanation that learning by doing enables cost reduction and quality improvements (cf. Nemet, 2006).

Given the goal of achieving adequate technology policies to mitigate climate change, the implementation of endogenous technological change via the learning curve in models of future energy and macroeconomic scenarios is essential (see, for example, Grübler and Messner, 1998; Gerlagh and Van der Zwaan, 2003). The learning curve provides an important tool to measure the cost-effectiveness of policy decisions to support new technologies. It connects expected future costs with current investments so that the cost of the new technology depends on earlier developments reflected by the cumulative capacity. This comes along with the path dependence of technological competition.

The economic role and the importance of research and development (R&D) for technical processes has been investigated intensively in various forms in literature. Just to mention a few examples, see Cunha-e Sá et al. (2010), Rauscher (2009), Popp (2006), and Grimaud et al. (2011). Here, R&D is seen as the main driving force of technological change and innovation by generating new information. Cohen and Levinthal (1989) were among the first to bring up the idea of the dual

¹Arrow (1962) considers in his work capital goods with a fixed life time. Therefore, gross investments only incorporate the purchase of new machines. In case of capital goods depreciating exponentially, however, also the maintenance of already existing machines would be included in gross investments.

role of R&D in the sense of not only generating new information but also enhancing the ability to assimilate and exploit already existing information. With this new aspect, they identify R&D expenditures as a learning mechanism based on the knowledge propagated in a firm's environment. Since then, R&D expenditures have, next to accumulated experience, become an important learning factor for the cost reduction of technological processes.

In general, one can distinguish between two different learning curve concepts. On the one hand, there is the one-factor learning curve for which cumulative production of capital goods² is considered to be the driving aspect for the accumulation of experience and hence for the reduction of the investment costs. On the other hand, in the so-called two-factor learning curve, additional R&D efforts increase knowledge, which additionally contributes to the cost reduction. These two approaches are presented in more detail in what follows.

1.2.2 One-Factor Learning Curve

The one-factor learning curve empirically quantifies the impact of learning by doing on the production costs of an industry or a firm by considering the investment costs as a declining function of cumulative production of capital goods. In the literature, a variety of different functional forms modeling this interrelationship can be found, but the probably most common one is the log-linear function due to its simplicity and its observed good fit with data. In this case, the progressive decrease is explained by the so-called progress rate given by

$$PR = 2^{-\alpha},$$

where $\alpha > 0$ is the learning-by-doing coefficient. The progress rate corresponds to the percentage change in costs, when the cumulative production of capital goods is doubled. Therefore, a progress rate of 80% means that the costs are reduced to 80% of its previous value when the cumulative production of capital goods is twice as high. The reduction, in this case of 20%, is referred to as the learning-by-doing rate and is given by

$$LDR = 1 - PR = 1 - 2^{-\alpha}.$$

²Instead of cumulative production of capital goods, also cumulative output can be used as the driving factor for the learning effect, as originally suggested by Wright (1936). Both factors are possible approximating measures for knowledge (cf. Argote et al., 1990). However, in analogy to the approach which we later will use for our model, we already focus on capital goods.

The costs are then calculated as

$$C_t = C_0 \left(\frac{K_t}{K_0} \right)^{-\alpha}, \quad (1.1)$$

where C_t are the investment costs at time t , K_t is the cumulative production of capital goods at time t , K_0 is its initial level at time $t = 0$, and C_0 are the initial investment costs. This scaling expresses the fact that for an initially low cumulative production of capital goods, it takes more efforts and investments in order to produce a given output than for an initially high level (cf. Van der Zwaan et al., 2002). Taking the logarithm of Equation (1.1) yields an expression which can be estimated econometrically in order to get an estimate for α , and therefore for the learning-by-doing rate *LDR*. This, of course, strongly depends on the type of technology and is crucial for the speed of learning. A survey on estimates of learning rates for a set of energy technologies can be found in McDonald and Schrattenholzer (2001). Equation (1.1) is also referred to as the single- or one-factor-learning curve.

1.2.3 Two-Factor Learning Curve

The one-factor approach with cost development of a technology being a function of only one independent variable has a drawback from a methodological point of view as there exists no other policy instrument than purchasing in order to accelerate the technological progress (cf. Miketa and Schrattenholzer, 2004). In the so-called two-factor learning curve, as proposed by Kouvaritakis et al. (2000), the costs of investments are assumed to decline due to two types of learning, first learning by doing induced by the accumulation of experience, and second learning by searching as a result of accumulating knowledge. The quantitative relationship between technological performance and R&D expenditures is modeled in the same way as the relation between experience and cost reduction in the one-factor learning curve representation. Additional to the already introduced progression rate *PR* and learning-by-doing rate *LDR*, a second rate is included for the two-factor learning curve, which is called learning-by-searching rate and is given by

$$LSR = 1 - 2^{-\beta},$$

where β is the learning-by-searching coefficient. The interpretation is the following. Assume that there is no accumulated knowledge, then the meaning of the *LDR* is similar to the one-factor model describing the percentage cost reduction when cumulative production of capital goods doubles. On the other hand, if there is no cumulative production of capital goods, the *LSR* reflects the percentage cost reduction when the stock of knowledge doubles (cf. Miketa and Schrattenholzer,

2004). To model the cost reduction due to these two learning concepts in a symmetric way, the costs then are given in form of a Cobb-Douglas-type function as

$$C_t = C_0 \left(\frac{K_t}{K_0} \right)^{-\alpha} \left(\frac{K_{R_t}}{K_{R_0}} \right)^{-\beta}, \quad (1.2)$$

where K_{R_t} is the stock of knowledge accumulated by R&D efforts at time t and K_{R_0} is the initial knowledge stock at time $t = 0$.

1.2.4 Learning Curves in Energy Systems

Especially for the evolution of energy systems, technological learning plays an important role as the costs are the fundamental measure for the performance of a technology. Consequently, in order to improve a process and become competitive, experience is essential. A technology will not evolve unless experience can be accumulated with it (see Barreto and Kypreos, 1999). The same argument can be found in Wene (2000) where it is additionally stated that the opportunity to gain experience on the market is crucial for new energy technologies as, otherwise, its availability to the market is prematurely foreclosed.

To apply the learning curve concept in energy system models, the approach is used where cumulative production of capital goods is the driving factor for learning. The capital goods for energy technologies are given by the installed capacities. Focusing on renewable energy technologies, the fact that the supply of the renewable resource is exogenously determined and consequently, the cumulative output cannot directly be controlled, points out why cumulative capacity here is the better measure for experience. Figure 1.1 shows schematically how learning acquires the investment costs of a renewable technology through cumulative capacity. For a learning-by-doing rate of 16%, 20%, and 25%, the investment costs for the renewable energy technology are plotted. In contrast, one can see the investment costs of a conventional energy technology, here fossil energy taken as example. The so-called break-even point (BE) occurs when the new technology gets competitive with the conventional one. This means that the collected experience makes the new technology cost-efficient. As the learning-by-doing rate defines the speed of learning, this, of course, happens at a higher cumulative capacity the lower the learning-by-doing rate is. The area between the renewable and the fossil curve indicates the learning investments necessary to reach the break-even point. For more details on the idea that renewable energy technologies break even with fossil energy see Wene (2000).

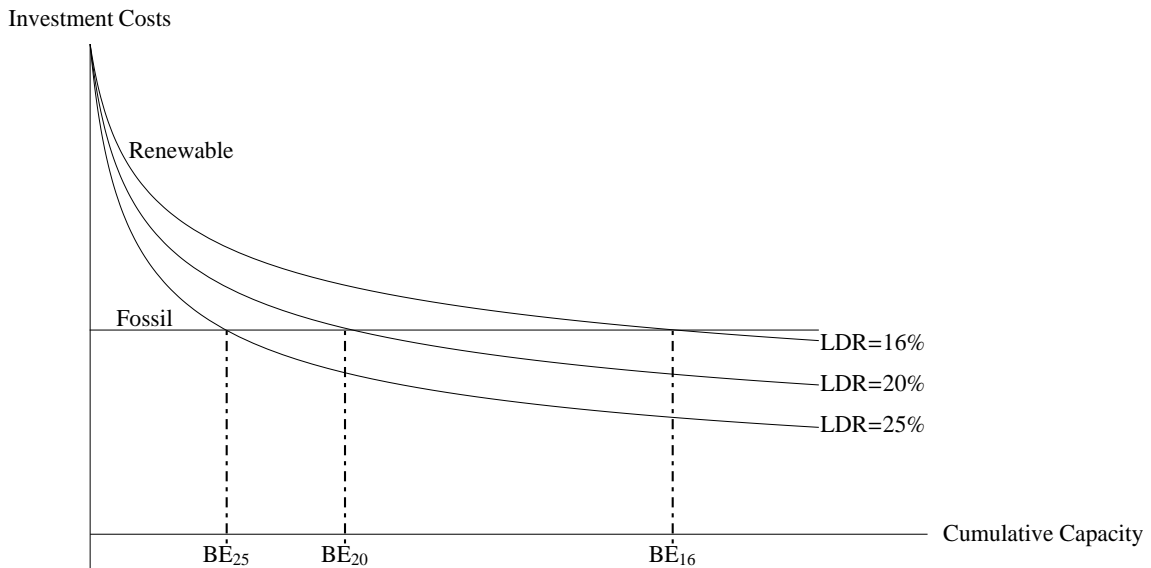


Figure 1.1: Break-even points for different learning rates.

1.2.5 Forgetting by Not Doing

In the learning concepts presented so far, cumulative output or gross investments in form of cumulative production of capital goods are considered to be the driving factors for the learning effect leading to a reduction of investment costs. Because these factors are non-negative and non-decreasing quantities, the accumulated experience along the learning process is assumed to be persistent in time and, hence, does not depreciate. This further implies that investment costs are monotonously decreasing. However, there exist references in the literature stating that investment costs do not always decrease over time, indicating that they possibly are not subject to pure learning. Such kind of negative learning effect, which in the literature is often referred to as organizational forgetting or forgetting by not doing, could be defined as the loss of knowledge caused by stopping to perform certain activities (Joosten et al., 1995). This can occur, for example, when the production process is interrupted. "Inventions don't just get adopted once and forever; they have to be constantly practiced and transmitted, or useful techniques may be forgotten" (Diamond, 1993). Baloff (1970) was among the first providing suggestive empirical evidence of a loss in production efficiency when production is paused. Keachie and Fontana (1966) discuss the phenomena of unlearning between intermittent production runs. They explain this phenomenon with the argument that in case of large time lags between the production lots, it is reasonable to assume that one would not follow the same learning curve at the point where one left, but investment costs

would have been increased back to a higher level again when production is resumed. Similarly, also Epple et al. (1991) present a counter-evidence for the hypothesis that knowledge becomes completely embodied in the technological process. They investigate a model on the transfer of knowledge acquired through learning by doing and show with their obtained results that not all knowledge is carried forward from one period to the next. Consequently, this implies that the conventional measure for learning overstates the persistence of learning (see also Argote et al., 1990; Argote and Epple, 1990). Focusing on the origin of the learning curve theory, the field of airplane-manufacturing, Benkard (2000) analyzes the dynamics of learning and the role of organizational forgetting in commercial aircraft production. The good fit of the obtained model results with the data underlines his assumption that learning can only take place when planes are produced and unless the production rates are not maintained, the gained experience starts to depreciate. Therefore, recent production experience seems to be more important for the determination of the current production efficiency than past production experience.

All these references underline the hypothesis, that experience gained from learning by doing does not remain forever. However, it is unclear what is the driving force behind this forgetting process. Benkard (2000) explains the depreciation of experience with the argument that experience acquired through learning by doing can be thought as accumulation of human capital and as periods of decreasing production rates are often accompanied by layoffs, this organizational human capital depreciates. Additional to highly variable production rates being a possible reason for organizational forgetting, also in Argote et al. (1990) it is supposed that rapid job turn over could be the major reason, where production workers are replaced by less experienced ones. However, their obtained model results show that knowledge depreciates more rapidly than the rate of job turn over which indicates the existence of some other significant factor which could be, beyond others, technological obsolescence, as they claim. Which aspect is more important for the process of forgetting further on depends on whether the production is more capital- or labor-intensive (see Benkard, 2000).

Also in models of energy technologies negative learning effects in form of forgetting can play an important role. McDonald and Schrattenholzer (2001) say that also in this field, indeed, interruptions in production and use can cause experience to be lost and unit costs to rise: "Unlike a fine wine, a technology design that is left on the shelf does not become better the longer it sits unused." While it is indisputable that the mechanism of forgetting by not doing finds its application in the R&D factor of the learning curve (see Wene, 2000), it seems reasonable to include it in the cumulative capacity factor as well (see Barreto, 2001). This is especially underlined when following Benkard (2000) in interpreting experience as human capital, which usually depreciates over time.

1.3 Formulation of the Problem

In order to analyze the challenges and chances of integrating renewable energy into the energy system as well as the differences in energy planning decisions when learning effects are included into the decision process, we consider as a benchmark the energy sector of a small country. The representative decision maker of this energy sector has to decide about the composition of a portfolio consisting of fossil and renewable energy with which the country's energy demand should be covered. In the literature many research papers can be found investigating the supply of a less pollutive or possibly even carbon free backstop technology, for example Hartley et al. (2010), Coulomb and Henriët (2011), and Van der Ploeg and Withagen (2012), or the transition to such a backstop technology as in Greiner et al. (2014) or Heinzl and Winkler (2011). What is however not included in these approaches is the fact that supply of renewable resources is not constant at all but strongly fluctuating due to climate or weather conditions. Focusing on solar energy as an example, we therefore postulate seasonal fluctuations in supply induced by the interplay of summer and winter. Further on, harvesting of the renewable energy resource is for free, but in order to use this resource, an appropriate capital is necessary, which accumulates by investments and hence comes at some costs. In contrast, for the supply of fossil energy it is postulated that the considered small country does not have own fossil energy resources and, consequently, fossil energy has to be imported for the current market price from other countries. Given these two different energy types, the representative energy-sector decision maker is looking for the optimal portfolio composition such that the energy demand of the country can be covered and no shortfalls occur. Proper forecasting of the energy demand is of course a really important and difficult issue in the energy supply sector. However, as the interest of this research rather lies on the qualitative composition of the portfolio than on proper prognosis methods, we postulate for simplicity that full information about the energy demand that has to be covered is available and no further uncertainties occur. We also follow Coulomb and Henriët (2011) and assume that it is stationary. In the literature, approaches can be found where the energy demand is considered to be dependent on the electricity price or on the GDP of the country, see for example Chakravorty et al. (2012). However, we here follow Messner (1997) and take the energy demand to be exogenously given. This allows us to focus on the supply side of renewable energy and on how a given demand may lead to an optimal division of supply between fossil and renewable energy.

In the first model approach, we consider a problem without including learning effects to see how the optimal portfolio composition looks like when the initial high investment costs for renewable energy capital remain unchanged over the whole planning period. The energy demand is first assumed to be constant over the year to clearly see the changes in the portfolio induced by the seasonal fluctuations. Sensitivity analysis then shows how the optimal composition of the portfolio changes, when the fossil energy price increases. In a second version, we model the energy demand seasonally fluctuating as well, where it either reaches its peak in winter due to heating, in summer due to air conditioning, or both.

Given this basic model approach, we then extend the model by first including a one-factor learning curve into the objective function. Instead of considering gross investments as suggested by Arrow (1962), we take net investments as the driving factor for the learning-by-doing effect, in order to simultaneously consider forgetting by not doing. As solar energy is a more capital-intensive than labor-intensive technology, forgetting then occurs as a result of insufficient maintenance activities. This effect is described in Sturm (1993) where difficulties in maintaining plants are considered to be a possible reason for negative learning effects in nuclear energy. The main difference between learning by doing based on gross and net investments is given by its economical interpretation. If the capital stock is assumed to depreciate exponentially, gross investments imply that experience is not only gained from investments in new machines but also in maintaining already existing machines. In the second approach with net investments, however, only buying new machines contributes to the learning process. Maintenance of already existing machines here is not considered to be an innovative activity providing additional knowledge. Further on, as net investments can, in contrast to gross investments, also decrease over time, they allow for the mechanisms of forgetting by not doing. In this first model extension, multiple solutions occur and an indifference threshold point separates the areas of attraction. Sensitivity analysis with respect to the fossil energy price, the learning-by-doing coefficient as well as different intensities of the supply of the renewable resource give insights how the optimal long-run solution behaves.

In the third approach we additionally introduce learning by searching by including a two-factor learning curve into the objective function and adding a second state to the model which represents the state of knowledge. This knowledge stock is accumulated by R&D investments which are considered as third control, but it also depreciates, describing the forgetting process. Also here, multiple solutions occur whose areas of attraction are separated in this case by an indifference threshold curve, and sensitivity analysis with respect to the fossil energy price and the intensity of the supply of the renewable resource is conducted.

As we include seasonal fluctuations into the models, we obtain non-autonomous optimal control problems with infinite horizon. In the first two approaches we have two controls and one state, while in the third approach we have three controls and two states. Due to the fact that the problem explicitly depends on time, the analysis differs from the usual steady-state analysis of autonomous problems.

1.4 Software

The considered optimal control problems are solved with Pontryagin's maximum principle (see, for example, Grass et al., 2008). Due to the complexity of the models, however, an analytical solution is only possible for some special cases, but cannot be found in general. Therefore, numerical methods are used which are explained in detail in the various chapters. As software for these calculations, MATLAB[®]7.5.0.342 (R2007b) has been used. The application of the shooting method that is presented and used in Chapters 3 and 4 in the course of the sensitivity analysis is carried out with CL_MATCONT for Matlab,³ see for more details Dhooge et al. (2006). Especially for the continuation of the optimal paths as well as the calculation of the indifference threshold points and curves in Chapters 3 and 4, additionally the MATLAB package OCMat developed by Dieter Grass has been employed.⁴

1.5 Thesis Outline

This thesis is organized as follows. In Chapter 2 we present and analyze the basic model where no learning effects are included. This first model approach as well as the obtained results provide the fundamental background for the analysis in the subsequent chapters. In Chapter 3 the first extension of the basic model with a one-factor learning curve is presented and analyzed, and the changes in the results compared to the basic model are discussed in detail. In Chapter 4 also the learning-by-searching effect is included into the model in form of a two-factor learning curve in the objective function. This model, which is extended by an additional control as well as an additional state, is analyzed and the economic interpretation of the newly obtained results is presented. Chapter 5 then summarizes and discusses the findings of all three model approaches, the differences and the economic interpretations as well as important methodological aspects for non-autonomous optimal control models that have arisen in the course of analyzing the models.

³Download from <http://www.matcont.ugent.be/> (accessed 01.06.2014)

⁴Download from http://orcos.tuwien.ac.at/research/ocmat_software/ (accessed 01.06.2014)

1.6 Publications

A summarized version of Chapter 2 presenting the first model approach without learning effects has been published in Moser et al. (2014) together with the co-authors Dieter Grass, Gernot Tragler, and Alexia Prskawetz in the peer-reviewed proceedings of the 9th International Conference on Large-Scale Scientific Computing 2013 in Sozopol, Bulgaria. Further on, a shortened version of Chapter 3 has been submitted to a refereed journal together with the co-authors Dieter Grass and Gernot Tragler.

The Basic Model

This chapter focuses on the formulation and the analysis of the basic model with no learning effects included. Beyond the obtained results, which will build the fundamental basis for the investigations in the subsequent chapters, also some theoretical aspects of solving non-autonomous optimal control models are presented.

2.1 The Model

We consider the energy sector of a small country in which both fossil and renewable energy can be used as perfect substitutes to cover an exogenously given energy demand. Due to the small size of the country it is assumed that there are no or at least not enough available fossil resources so that fossil energy has to be imported from other countries for the current market price. As far as renewable energy is concerned, generation is possible within the own country. In contrast to fossil energy, which is assumed to be constantly available, however, the supply of renewable energy fluctuates seasonally. In order to use this renewable energy resource, capital is necessary for the energy generation for which investments have to be undertaken. We consider for our model a representative energy-sector decision maker who chooses the optimal energy portfolio composition for the whole country. It is postulated that this decision maker has full information about the energy demand that has to be covered at each point of time. Therefore, he/she decides on the most cost-effective portfolio consisting of these two energy types that is used to cover the exogenously given demand, taking into account the seasonal fluctuations of renewable energy supply and the import costs of fossil energy. One important implication of the size of the country is, that this representative energy-sector decision maker is assumed to be a price taker, and accordingly his/her decision has no influence on the market price.

We take the considered fossil energy as an aggregate of fossil energy sources (e.g. coal, gas, etc.), and follow Chakravorty et al. (2006) in focusing on solar energy as renewable resource. To give an example for the seasonal supply, Figure 2.1a shows the average daily global radiation in Austria. One can clearly observe the seasonal differences that pose a challenge to a constant renewable energy supply over the whole year. Of course, saving of renewable energy would be supportive in the short-run, but as we are rather interested in long-run solutions and for this time frame saving possibilities are limited, we follow Chakravorty et al. (2006) in assuming that storage is not possible and focus only on the change in the portfolio composition. This means that the generated energy has to be used immediately or otherwise it is lost.

To include these seasonal fluctuations in our model a deterministic time-dependent function is used,

$$v_R(t) = v \sin^2(t\pi) + \tau,$$

which is plotted in Figure 2.1b. The period length of the seasonal fluctuations in our case is one year, τ is the minimal supply in winter, and v is the maximal increment during summer.¹ To get reasonable parameter values we used Austrian data (ZAMG, 2012) for estimation. Note that we only consider annual fluctuations and do not include daily fluctuations as well as changes due to weather conditions.

To convert solar radiation into energy, specific capital K_S in form of photovoltaic cells is necessary. This capital is accumulated by investments $I_S(t)$ and depreciates by a factor δ_S . The capital accumulation equation in our model reads as follows:

$$\dot{K}_S(t) = I_S(t) - \delta_S K_S(t). \quad (2.1)$$

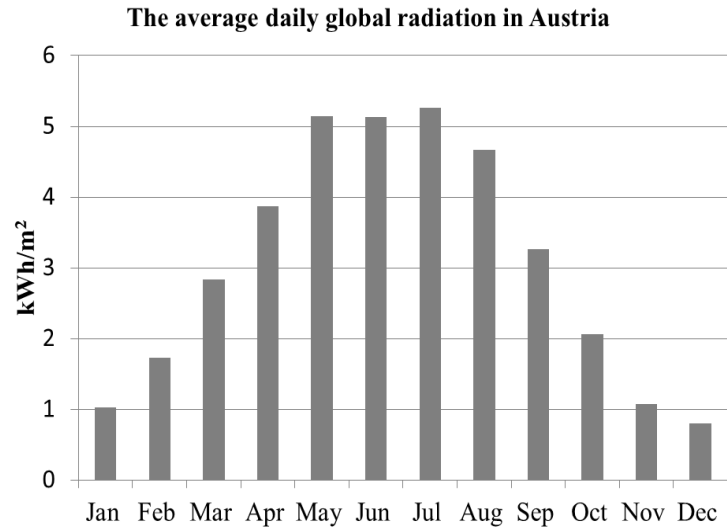
Given the available capital at each time and the current supply of global radiation, renewable energy is generated as

$$E_S(K_S(t), t) = (v \sin^2(t\pi) + \tau) K_S(t) \eta,$$

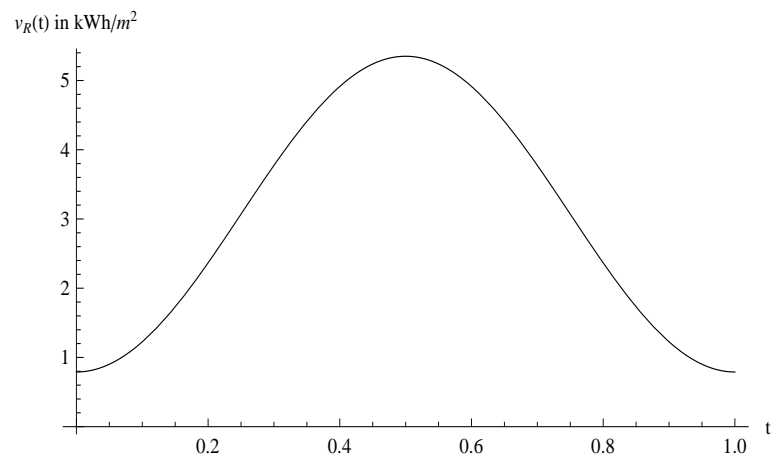
where η is the degree of efficiency (cf. Deshmukh and Deshmukh, 2008; Nema et al., 2009). For common photovoltaic cells that are currently on the market, η is about 20%. Note that this function explicitly depends on time t , which therefore makes the problem non-autonomous.

Since the representative energy-sector decision maker is assumed to have exact information about the required energy demand E and no further uncertainties are included, it is postulated that the demand has to be covered completely by the portfolio of fossil $E_F(t)$ and renewable

¹As usual, we let t denote the time argument.



(a)



(b)

Figure 2.1: **(a)** Average global radiation per month in Austria. **(b)** Deterministic function to describe the varying global radiation over one year, $t \in [0, 1]$.

$E_S(K_S(t), t)$ energy. Shortfalls are not allowed while surpluses are possible. However, as we do not include the possibility of storage, this implies that surpluses are lost and cannot be further used.² This balance is included in the model by the mixed-path constraint

$$E_F(t) + E_S(K_S(t), t) - E \geq 0.$$

Given these restrictions and the current market price p_F for fossil energy, the representative energy-sector decision maker determines the most cost-effective solution by minimizing total expenditures given by investment costs in renewable energy capital and import costs for fossil energy,

$$C(I_S(t), E_F(t)) = I_S(t)(b + cI_S(t)) + p_F E_F(t).$$

Note that we distinguish between linear investment and quadratic adjustment costs, where the latter ones arise from installation efforts (cf. Feichtinger et al., 2006; Rasmussen, 2001).

Summing up, we consider a non-autonomous optimal control model with infinite horizon, two controls representing the capital investments and the imported fossil energy, and one state describing the capital stock. This cost minimization problem is transformed to the equivalent maximization problem and, for a discount rate r , is given by

$$\max_{E_F(t), I_S(t)} \int_0^{\infty} e^{-rt} \left(-I_S(t)(b + cI_S(t)) - p_F E_F(t) \right) dt \quad (2.2)$$

$$\text{s.t.: } \dot{K}_S(t) = I_S(t) - \delta_S K_S(t), \quad (2.2a)$$

$$E_F(t) + E_S(K_S(t), t) - E \geq 0, \quad (2.2b)$$

$$E_S(K_S(t), t) = (\nu \sin^2(t\pi) + \tau) K_S(t) \eta, \quad (2.2c)$$

$$E_F(t), I_S(t) \geq 0. \quad (2.2d)$$

²In practice, of course, small surpluses generally would be traded on the market. However, in times of great surpluses as it sometimes occurs around Christmas due to the very low demand, prices often turn negative which also comes along with great losses. Therefore, we do not include this trading aspect in our model but consider such losses in form of sunk investment costs.

2.2 Solution

2.2.1 Canonical System and Necessary First Order Conditions

Let $(K_S^*(t), E_F^*(t), I_S^*(t))$ be an optimal solution of the control problem in (2.2), then according to *Pontryagin's maximum principle* for infinite time horizon problems (cf. Grass et al., 2008), there exists a continuous and piecewise continuously differentiable function $\lambda(t) \in \mathbb{R}$, also known as the *adjoint variable* or *costate*, and a constant $\lambda_0 \geq 0$ satisfying for all $t \geq 0$

$$(\lambda_0, \lambda(t)) \neq 0,$$

$$\mathcal{L}(K_S^*, E_F^*, I_S^*, \lambda, \lambda_0, \mu_1, \mu_2, \mu_3, t) = \max_{E_F(t), I_S(t)} \mathcal{L}(K_S^*, E_F, I_S, \lambda, \lambda_0, \mu_1, \mu_2, \mu_3, t),$$

where \mathcal{L} defines the *Lagrangian*³ which reads as

$$\begin{aligned} \mathcal{L}(K_S, E_F, I_S, \lambda, \lambda_0, \mu_1, \mu_2, \mu_3, t) &= \lambda_0 (-bI_S(t) - cI_S(t)^2 - p_F E_F(t)) + \lambda(t)(I_S(t) - \delta_S K_S(t)) \\ &+ \mu_1(t)(E_F(t) + (v \sin^2(t\pi) + \tau)K_S(t)\eta - E) + \mu_2(t)E_F(t) + \mu_3(t)I_S(t), \end{aligned}$$

with $\mu_1(t)$, $\mu_2(t)$, and $\mu_3(t)$ being the piecewise continuous *Lagrange multipliers* for the mixed-path constraint and the non-negativity conditions, respectively. Further on, at each point where the controls are continuous,

$$\dot{\lambda}(t) = r\lambda(t) - \frac{\partial \mathcal{L}(K_S^*, E_F^*, I_S^*, \lambda, \lambda_0, \mu_1, \mu_2, \mu_3, t)}{\partial K_S(t)}$$

is given and the complementary slackness conditions

$$\mu_1(t) (E_F^*(t) + E_S^*(K_S^*(t), t) - E) = 0 \quad , \quad \mu_1(t) \geq 0, \quad (2.3)$$

$$\mu_2(t) E_F^*(t) = 0 \quad , \quad \mu_2(t) \geq 0, \quad (2.4)$$

$$\mu_3(t) I_S^*(t) = 0 \quad , \quad \mu_3(t) \geq 0, \quad (2.5)$$

³Note that we omit the time argument in the function arguments of the Lagrangian for the ease of exposition.

have to be satisfied. The necessary first order conditions and the adjoint equation are given as follows:

$$\frac{\partial \mathcal{L}}{\partial I_S(t)} = -\lambda_0 b - 2\lambda_0 c I_S(t) + \lambda(t) + \mu_3(t) = 0, \quad (2.6)$$

$$\dot{\lambda}(t) = r\lambda(t) - \frac{\partial \mathcal{L}}{\partial K_S(t)} = (r + \delta_S)\lambda(t) - \mu_1(t)\eta(v \sin^2(t\pi) + \tau). \quad (2.7)$$

Further on, we require the limiting transversality condition

$$\lim_{t \rightarrow \infty} \lambda(t)e^{-rt} = 0 \quad (2.8)$$

to be satisfied. Note that the Lagrangian is linear in $E_F(t)$ and, consequently, a bang-bang solution occurs where $E_F(t)$ is determined by the switching function

$$\frac{\partial \mathcal{L}}{\partial E_F(t)} = -\lambda_0 p_F + \mu_1(t) + \mu_2(t)$$

so that

$$E_F(t) = \begin{cases} \infty \\ \text{singular} \\ 0 \end{cases} \text{ if } \frac{\partial \mathcal{L}}{\partial E_F(t)} \begin{cases} > \\ = \\ < \end{cases} 0.$$

Proposition 1. *Without loss of generality we can set $\lambda_0 = 1$ for the subsequent analysis.*

Proof. Let $\lambda_0 = 0$, then the Lagrangian is also linear in $I_S(t)$ and the switching functions for the two controls and the adjoint equation read as

$$\frac{\partial \mathcal{L}}{\partial E_F(t)} = \mu_1(t) + \mu_2(t), \quad (2.9)$$

$$\frac{\partial \mathcal{L}}{\partial I_S(t)} = \lambda(t) + \mu_3(t), \quad (2.10)$$

$$\dot{\lambda}(t) = (r + \delta_S)\lambda(t) - \mu_1(t)\eta(v \sin^2(t\pi) + \tau). \quad (2.11)$$

As $\mu_1(t), \mu_2(t) \geq 0$, it follows that in case of no fossil energy, $E_F(t) = 0$, $\mu_1(t) = \mu_2(t) = 0$ has to hold. For $E_F(t) > 0$ the complementary slackness condition in (2.4) implies that $\mu_2(t) = 0$. Moreover, however, also $\mu_1(t) = 0$ has to hold in this case which is obtained either from the complementary slackness condition in (2.5) if the mixed-path constraint in (2.2b) is satisfied with inequality, or from the switching function in (2.9) if it is satisfied with equality. In all cases, the

solution of the adjoint equation (2.11) is given by

$$\lambda(t) = \lambda(0)e^{(r+\delta_S)t}.$$

To satisfy the transversality condition in (2.8), $\lambda(0) = 0$ is the only feasible initial value. This, however, implies that $\lambda(t) = 0, \forall t$, which is contradictory to $(\lambda_0, \lambda(t)) \neq 0$. Therefore, $\lambda_0 > 0$ has to hold and adequate standardization yields

$$\tilde{\lambda}_0 = \lambda_0 \frac{1}{\lambda_0} = 1,$$

which proves the proposition. □

The necessary first order conditions and the adjoint equation are then given as follows:

$$\begin{aligned} \frac{\partial \mathcal{L}}{\partial I_S(t)} &= -b - 2cI_S(t) + \lambda(t) + \mu_3(t) = 0 \Leftrightarrow I_S(t) = \frac{\lambda(t) + \mu_3(t) - b}{2c}, \\ \dot{\lambda}(t) &= (r + \delta_S)\lambda(t) - \mu_1(t)\eta(v \sin^2(t\pi) + \tau), \end{aligned}$$

which yields the canonical system

$$\dot{K}_S(t) = \frac{\lambda(t) + \mu_3(t) - b}{2c} - \delta_S K_S(t) =: f^{K_S}(t, K_S(t), \lambda(t), \mu_3(t)) \quad (2.12)$$

$$\dot{\lambda}(t) = (r + \delta_S)\lambda(t) - \mu_1(t)\eta(v \sin^2(t\pi) + \tau) =: f^\lambda(t, \lambda(t), \mu_1(t)). \quad (2.13)$$

Note that the Lagrangian is concave in $I_S(t)$, and linear in $E_F(t)$ and $K_S(t)$. Further on, the partial derivatives of the objective function and the dynamics are continuous in their arguments, and the feasible region is convex. As, additionally, the transversality condition in (2.8) is required to be satisfied, this implies that for $(E_F^*(t), I_S^*(t), K_S^*(t))$ and $\lambda(t)$ satisfying Pontryagin's maximum principle and for all feasible $K_S(\cdot)$ the limiting transversality condition

$$\lim_{t \rightarrow \infty} \lambda(t)(K_S(t) - K_S^*(t)) \geq 0$$

has to hold and $(E_F^*(t), I_S^*(t), K_S^*(t))$ is an optimal solution. Consequently, not only the necessary but also the sufficient conditions are satisfied for the solutions we obtain in the following analysis.

Proposition 2. *A solution path in the interior of the feasible domain of this optimal control problem can never be optimal.*

Proof. Let $(E_F^*(t), I_S^*(t))$ be a solution of the optimal control problem in (2.2) which satisfies $\forall t \in (t_1, t_2)$ with $t_1 < t_2$

$$(E_F^*(t) + (v \sin^2(t\pi) + \tau)K_S^*(t)\eta - E) > 0, \quad (2.14)$$

$$E_F^*(t) > 0, \quad (2.15)$$

$$I_S^*(t) > 0, \quad (2.16)$$

with $K_S^*(t)$ and $\lambda^*(t)$ being the state and costate, respectively, solving the canonical system. That means, this solution lies in the interior of the feasible domain of the model (2.2). Then, from the complementary slackness conditions (2.3)-(2.5) we obtain $\mu_1^*(t) = \mu_2^*(t) = \mu_3^*(t) = 0 \forall t \in (t_1, t_2)$. As we have shown that $\lambda_0 = 1$, it holds for this case that

$$\frac{\partial \mathcal{L}}{\partial E_F(t)} = -p_F < 0.$$

Consequently, the maximum is reached at the lowest feasible control $E_F(t)$. This, however, implies that a solution $(E_F^*(t), I_S^*(t))$ that satisfies (2.16)-(2.14) is suboptimal as there always exists a solution with a lower control $E_F(t)$ and hence a better performance, which proves the proposition. \square

An important implication of Proposition 2 is that the optimal solution is reached either at the boundary

$$E_F^*(t) + (v \sin^2(t\pi) + \tau)K_S^*(t)\eta - E = 0$$

and/or at the boundary $E_F^*(t) = 0$. Moreover, despite the fact that we have got a bang-bang solution for fossil energy, $E_F^*(t)$ is continuous with respect to time, as for $E_F^*(t) > 0$ the mixed-path constraint has to be satisfied with equality.

As the proof of Proposition 2 shows, an interior solution with both controls $E_F(t), I_S(t) > 0$ and the mixed-path constraint of (2.2b) satisfied with inequality, can never be optimal as the cost of inefficient surpluses could immediately be reduced by decreasing the amount of fossil energy until either the mixed-path constraint is satisfied with equality or the fossil energy amount gets zero, which both corresponds to boundary cases. Hence, we can completely omit the interior solution and focus on the boundaries of the feasible domain. In total, we can distinguish between three of them:

- The *fossil* case: No investments in renewable energy capital are made,

$$E_F(t) > 0,$$

$$I_S(t) = 0,$$

$$E_F(t) + E_S(K_S(t), t) - E = 0.^4$$

- The *mixed* case: Both types of energy are used for the coverage,

$$E_F(t),$$

$$I_S(t) > 0,$$

$$E_F(t) + E_S(K_S(t), t) - E = 0.$$

- The *renewable* case: No fossil energy is used to cover the demand,

$$E_F(t) = 0,$$

$$I_S(t) > 0,$$

$$E_S(K_S(t), t) - E \geq 0.$$

Inserting the corresponding values of the controls and Lagrange multipliers yields the canonical systems for these boundary cases, which are given for the fossil case by

$$\dot{K}_S(t) = -\delta_S K_S(t), \quad (2.17)$$

$$\dot{\lambda}(t) = (r + \delta_S)\lambda(t) - p_F \eta (v \sin^2(t\pi) + \tau), \quad (2.18)$$

for the mixed case by

$$\dot{K}_S(t) = \frac{\lambda(t) - b}{2c} - \delta_S K_S(t), \quad (2.19)$$

$$\dot{\lambda}(t) = (r + \delta_S)\lambda(t) - p_F \eta (v \sin^2(t\pi) + \tau), \quad (2.20)$$

and for the renewable case by

$$\dot{K}_S(t) = \frac{\lambda(t) - b}{2c} - \delta_S K_S(t), \quad (2.21)$$

$$\dot{\lambda}(t) = (r + \delta_S)\lambda(t). \quad (2.22)$$

Figure 2.2 illustrates these three cases, where t^* is some fixed point of time during the year. If

⁴Note that for the fossil case the generated renewable energy $E_S(K_S(t), t)$ is still included in the energy balance equation. This is because renewable energy at the beginning of the path could still contribute to the portfolio if there is an initially positive capital stock. As no further investments are made, however, the capital stock will decline over time and the contribution of renewable energy gets negligibly small. If, in contrast, the initial capital stock is zero, the contribution is zero along the whole path.

the initial capital stock is zero and, furthermore, no investments are made, no renewable energy is generated at all and the whole energy demand has to be covered by fossil energy. As soon as capital is accumulated by investments, a mixture of the two energy types is used to cover the demand, which hence corresponds to the mixed case. If, however, the capital stock gets sufficiently high so that enough renewable energy can be generated to completely cover the demand, no further import of fossil energy is necessary. This finally corresponds to the renewable solution.

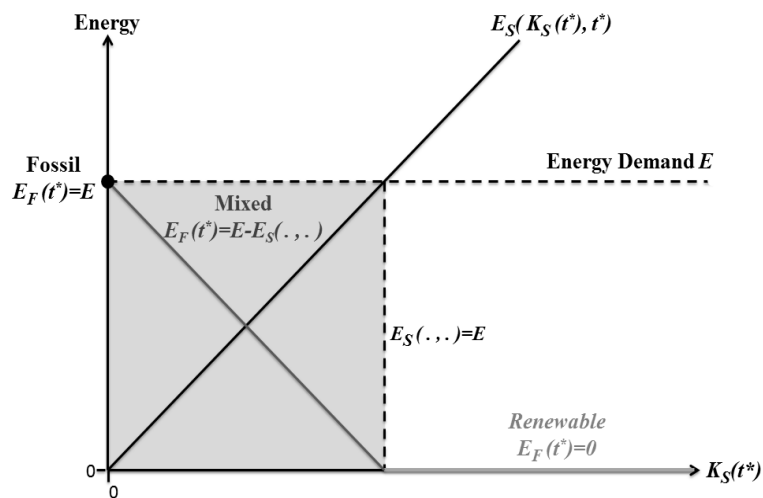


Figure 2.2: Fossil, mixed, and renewable solutions to cover the given energy demand.

2.2.2 Periodic Solution

The canonical system in (2.12)-(2.13) is not only non-autonomous, but in addition it is also periodic in t with period length 1, and therefore belongs to a special class of non-autonomous differential equation systems, also called *one-periodic differential equations*. Due to this periodicity, the most reasonable candidate for the optimal long-run solution of the problem in (2.2), which is the solution to which each optimal solution is converging over time, is given by a periodic solution with the period length of one year.⁵

⁵Note that this is in contrast to autonomous optimal control problems where the existence of periodic optimal solutions only is given under specific necessary and sufficient conditions, see for this Hartl (1993) and Han et al. (1994).

In order to find such candidates, we first determine the instantaneous equilibrium points, which are calculated for the general canonical system in (2.12)-(2.13) as

$$\begin{aligned}\dot{\lambda}(t) &= (r + \delta_S)\lambda(t) - \mu_1(t)\eta(v \sin^2(t\pi) + \tau) = 0 \\ \Leftrightarrow \lambda^{IEP}(t) &= \frac{\mu_1(t)\eta(v \sin^2(t\pi) + \tau)}{r + \delta_S} \\ \dot{K}_S(t) &= \frac{\lambda(t) + \mu_3(t) - b}{2c} - \delta_S K_S(t) = 0 \\ \Leftrightarrow K_S^{IEP}(t) &= \frac{\lambda^{IEP}(t) + \mu_3(t) - b}{2c\delta_S} = \\ &= \frac{\mu_1(t)\eta(v \sin^2(t\pi) + \tau)}{(r + \delta_S)2c\delta_S} + \frac{\mu_3(t) - b}{2c\delta_S}.\end{aligned}$$

Note that the curve of instantaneous equilibrium points is not a trajectory of the canonical system, unless $\{\dot{K}_S^{IEP}(t), \dot{\lambda}^{IEP}(t)\} = \{0, 0\}$, $\forall t$, see Ju et al. (2003). This special case, however, can not occur in our model approach. We solve the following boundary value problem using these instantaneous equilibrium points as starting solution,

$$\begin{aligned}\dot{K}_S(t) &= f^{K_S}(t, K_S(t), \lambda(t), \mu_3(t)), & \text{with } K_S(0) &= K_S(1), \\ \dot{\lambda}(t) &= f^\lambda(t, \lambda(t), \mu_1(t)), & \text{with } \lambda(0) &= \lambda(1).\end{aligned}$$

Solving this boundary value problem yields the periodic solution $(K_S^*(t), \lambda^*(t))$ that lies completely in one of the three boundary cases of the feasible domain. However, it can happen that the solution at some point leaves the current boundary of the feasible domain before the end of the period is reached. In this case, one cannot find a closed periodic solution along this boundary, but one has to switch to the corresponding canonical system of the next feasible boundary to end up with a periodic solution existing of several arcs. Therefore, a multi-point boundary value problem has to be solved. At each point of time where the constraints of the current region are violated, a switch to the proper region happens, meaning that the corresponding canonical system is used to continue the solution. For n switching times τ_1, \dots, τ_n and the boundary points τ_0 and τ_{n+1} , which satisfy

$$\tau_0 := 0 < \tau_1 < \tau_2 < \dots < \tau_{n-1} < \tau_n < 1 =: \tau_{n+1},$$

$n + 1$ arcs have to be calculated for which the continuity of the solution with respect to time at

each switch has to be guaranteed. We introduce an index

$$a_i = \begin{cases} 1, & \text{for the fossil region,} \\ 2, & \text{for the mixed region,} \\ 3, & \text{for the renewable region,} \end{cases} \quad (2.23)$$

which distinguishes between the canonical systems for the three boundary cases of the feasible domain described in (2.17)-(2.22) for each arc i with $i = 1, \dots, n+1$. In what follows, we use for simplicity the notation

$$\dot{K}_{S_i}(t) = f_{a_i}^{K_S}(t, K_{S_i}(t), \lambda_i(t), \mu_{3_i}(t)), \quad t \in [\tau_{i-1}, \tau_i], \quad (2.24)$$

$$\dot{\lambda}_i(t) = f_{a_i}^{\lambda}(t, \lambda_i(t), \mu_{1_i}(t)), \quad t \in [\tau_{i-1}, \tau_i], \quad (2.25)$$

for n switches along the periodic solution, $i = 1, \dots, n+1$, and $a_i \in \{1, 2, 3\}$. For the corresponding canonical system at arc i , it has to hold that

$$a_i \neq a_{i-1}, \quad (2.26)$$

$$|a_i - a_{i-1}| = 1, \quad (2.27)$$

which means that switches only can happen between neighboring regions in the sense that only one control condition changes at the switch. For the numerical solution of the system, for each arc i we use a time transformation so that it can be solved with fixed time intervals. This means that, in order to solve a system of equations as in (2.24)-(2.25),

$$\dot{x}(t) = f(t, x(t)), \quad t \in [\tau_{i-1}, \tau_i], \quad i = 1, \dots, n+1, \quad \tau_0 = 0, \quad \tau_{n+1} = 1,$$

we are looking for a time transformation $t = T(s)$ so that

$$\dot{y}(s) = \tilde{f}(s, y(s)), \quad s \in [i-1, i], \quad \text{with } y(s) = x(T(s)).$$

It turns out that the linear transformation

$$T(s) = (\tau_i - \tau_{i-1})(s - i) + \tau_i \quad (2.28)$$

satisfies the required conditions. Hence, in terms of the original dynamics this yields

$$\dot{y}(s) = \dot{x}(T(s)) = \frac{dx(T(s))}{ds} = \frac{dx(T(s))}{dT(s)} \frac{dT(s)}{ds} = f(T(s), y(s))(\tau_i - \tau_{i-1}).$$

Using this transformation, we have to solve for $i = 1, \dots, n+1$, $j = 1, \dots, n$, $s \in [i-1, i]$, $\tau_0 = 0$, $\tau_{n+1} = 1$ the multi-point boundary value problem

$$\dot{K}_{S_i}(s) = (\tau_i - \tau_{i-1}) f_{a_i}^{K_S}(T(s), K_{S_i}(s), \lambda_i(s), \mu_{3_i}(t)), \quad (2.29)$$

$$\dot{\lambda}_i(s) = (\tau_i - \tau_{i-1}) f_{a_i}^{\lambda}(T(s), \lambda_i(s), \mu_{1_i}(t)), \quad (2.30)$$

$$0 = (K_{S_j}(\tau_j), \lambda_j(\tau_j)) - (K_{S_{j+1}}(\tau_j), \lambda_{j+1}(\tau_j)), \quad (2.31)$$

$$0 = (K_{S_{n+1}}(1), \lambda_{n+1}(1)) - (K_{S_1}(0), \lambda_1(0)), \quad (2.32)$$

$$0 = c(a_j, a_{j+1}). \quad (2.33)$$

Equation (2.31) ensures, that the continuity of the state and the costate with respect to time at each switch is given. As the aim is to find a periodic solution, Equation (2.32) demands that the starting and the end point coincide. Equation (2.33) finally guarantees that the controls are continuous with respect to time as well. This condition is dependent on the involved regions as well as on the direction of the switch and for $j = 1, \dots, n$ is given as

$$c(a_j, a_{j+1}) = \left\{ \begin{array}{l} \lambda_j(\tau_j) - b = 0 \\ E_S(K_{S_j}(\tau_j), \tau_j) - E = 0 \end{array} \right\} \text{ if } \{a_j, a_{j+1}\} \in \left\{ \begin{array}{l} \{\{1, 2\}, \{2, 1\}\} \\ \{\{2, 3\}, \{3, 2\}\} \end{array} \right\}.$$

The periodic solution that solves this boundary value problem then is given by

$$(K_S^*(t), \lambda^*(t)) = \left((K_{S_1}^*(t), \lambda_1^*(t))_{0 \leq t < \tau_1}, (K_{S_2}^*(t), \lambda_2^*(t))_{\tau_1 \leq t < \tau_2}, \dots, (K_{S_{n+1}}^*(t), \lambda_{n+1}^*(t))_{\tau_n \leq t < 1} \right).$$

2.2.3 Stability

Due to the periodicity in t of the canonical system, its solutions have certain properties that are useful to determine their asymptotic behavior, which we will show in what follows. To do so, we first introduce the term *Poincaré map*, following the detailed demonstration in Hale and Koçak (1991). Let

$$\dot{x} = f(t, x), \quad (t, x) \in \mathbb{R} \times \mathbb{R}^n, \quad (2.34)$$

be the general notation of a 1-periodic canonical system. Further on, let $\phi(t, t_0, x_0)$ be the solution of (2.34) through the point $x_0 \in \mathbb{R}^n$ at time t_0 . Due to the periodicity, it holds that

$$\begin{aligned}\phi(t+1, t_0+1, x_0) &= \phi(t, t_0, x_0), \\ \phi(t+1, t_0, x_0) &= \phi(t, t_0, \phi(t_0+1, t_0, x_0)).\end{aligned}$$

We now define a scalar mapping that maps the initial value x_0 at time $t_0 = 0$ to the value of the solution $\phi(1, 0, x_0)$ given by

$$P : \mathbb{R}^n \mapsto \mathbb{R}^n, x_0 \mapsto \phi(1, 0, x_0).$$

This is the so-called Poincaré map associated with the periodic orbit of the system (2.34) and is also known as *time-one* or *period map*. Obviously, the initial value x_0 then is a fixed point of this map. Further on, the Poincaré map is monotone and differentiable with non-negative derivative (see for this Hale and Koçak, 1991). To illustrate the Poincaré map also graphically, the system (2.34) can be converted into the equivalent pair of autonomous differential equations,

$$\begin{aligned}\dot{\theta} &= 1, \\ \dot{x} &= f(\theta, x),\end{aligned}\tag{2.35}$$

where the first equation is periodic with any period and hence can be seen as differential equation on the unit circle \mathbb{S}^1 , while the second one is 1-periodic and consequently remains unchanged for all $\theta + k$ with any integer k . Therefore, the orbits and trajectories of (2.35) can conveniently be viewed along the cylindrical manifold $X = \mathbb{S}^1 \times \mathbb{R}^n$. When using the coordinates $(t(\text{mod } 1), x)$ and considering in this space the 1-dimensional cross-section

$$\Sigma = \{(t, x) \in X : t = 0\},$$

each orbit L_0 of the system (2.35) then crosses Σ transversally (cf. Kuznetsov, 1998), which can be seen in Figure 2.3. As the initial value x_0 is a fixed point of the Poincaré map, the stability properties of ϕ are the same as of x_0 . If $\phi(t, 0, x_0)$ is the solution of the system (2.34), with $\phi(0, 0, x_0) = x_0$, then

$$M(t) = \frac{\partial \phi(t, 0, x_0)}{\partial x_0}$$

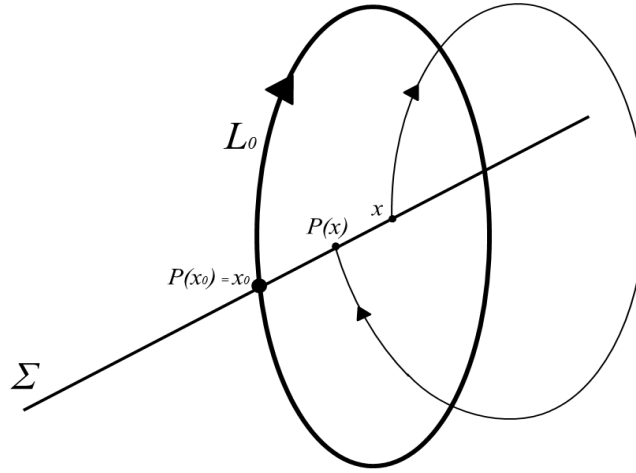


Figure 2.3: Poincaré map.

is the solution of the boundary value problem

$$\dot{y} = J(t)y, \quad y(0) = I_n, \quad (2.36)$$

where

$$J(t) = \frac{\partial f}{\partial x}(t, \phi(t, 0, x_0))$$

is the Jacobian matrix of the system (2.34) and I_n is the n -dimensional identity matrix. $M(t)$ is the fundamental matrix of the system (2.36) and is given by

$$M(t) = e^{J(t)}.$$

The differential equation in (2.36) is also called the *linear variational equation* about the solution $\phi(t, 0, x_0)$, as it describes the system of a perturbation $y(t)$ of the periodic solution,

$$x(t) = \phi(t, 0, x_0) + y(t).$$

Differentiating the Poincaré map $P(x_0) = \phi(1, 0, x_0)$ with respect to x_0 finally yields the Jacobian of the Poincaré map,

$$J_P = \frac{\partial P}{\partial x_0}(x_0) = \frac{\partial \phi(1, 0, x_0)}{\partial x_0} = M(1) = e^{J(1)}.$$

Consequently, the perturbation $y(t)$ decreases if all eigenvalues ξ_1, \dots, ξ_n of J_P are within the unit circle, $|\xi| < 1$, which implies that the solution $\phi(t, 0, x_0)$ is asymptotically stable. Further on, the eigenvalues are independent from the starting value x_0 , the periodic orbit L_0 , and Σ . One can see that these eigenvalues coincide with the ones of the matrix $M(1)$, which is called the *monodromy matrix*. ξ_1, \dots, ξ_n are also referred to as the *Floquet multipliers*, and the fundamental matrix can be represented in the so-called *Floquet form*

$$M(t) = e^{Rt}C(t),$$

where $C(t+1) = C(t)$ holds and $R \in \mathbb{C}^{n \times n}$ is a constant matrix whose eigenvalues are known as the *characteristic exponents* and the Floquet multipliers are given by the eigenvalues of the matrix e^R . For autonomous problems, the monodromy matrix always has 1 as eigenvalue which is called the *trivial Floquet multiplier*. The reason for this is that the tangent vector on the periodic orbit at x_0 is an eigenvector of the monodromy matrix with eigenvalue 1 (see Grass et al., 2008). The same applies also for non-autonomous problems if the canonical system is transformed to the $(n+1)$ -dimensional autonomous system of (2.35). Then, also here perturbations along the periodic orbit have eigenvalue 1 and the eigenvalues of the monodromy matrix are given by $1, \xi_1, \dots, \xi_n$ (see Guckenheimer and Holmes, 1990). If the trivial multiplier is the only eigenvalue of unity, the periodic solution is also hyperbolic, which implies that its stability can be determined from the linearization of the Poincaré map and hence from the remaining n eigenvalues (see Hale and Koçak, 1991).

In order to analyze the dynamic behavior of an obtained periodic solution $\Gamma(t)$ of the canonical system (2.12)-(2.13) with period length 1, we therefore calculate the monodromy matrix as the fundamental matrix solution of the variational equation

$$\begin{aligned} \dot{y} &= J(t)y, \\ y(0) &= \begin{pmatrix} 1 & 0 \\ 0 & 1 \end{pmatrix}, \end{aligned} \tag{2.37}$$

where $J(t)$ is the Jacobian matrix evaluated at the periodic solution $\Gamma(t)$,

$$J(t) = \begin{pmatrix} \frac{\partial f^{K_S}}{\partial K_S} & \frac{\partial f^{K_S}}{\partial \lambda} \\ \frac{\partial f^\lambda}{\partial K_S} & \frac{\partial f^\lambda}{\partial \lambda} \end{pmatrix} (\Gamma(t)).$$

For the case of mixed as well as renewable energy supply in the current model, this matrix reads

as

$$J(t) = \begin{pmatrix} -\delta_S & \frac{1}{2c} \\ 0 & r + \delta_S \end{pmatrix}.$$

Solving the differential equation in (2.37) yields the solution matrix, and therefore the monodromy matrix

$$M(1) = e^{J(1)} = \begin{pmatrix} e^{-\delta_S} & \frac{e^{r+\delta_S} - e^{-\delta_S}}{2c(r+2\delta_S)} \\ 0 & e^{r+\delta_S} \end{pmatrix}.$$

For the case where only fossil energy is used, the Jacobian matrix reads as

$$J(t) = \begin{pmatrix} -\delta_S & 0 \\ 0 & r + \delta_S \end{pmatrix},$$

which yields the monodromy matrix

$$Y = M(1) = e^{J(1)} = \begin{pmatrix} e^{-\delta_S} & 0 \\ 0 & e^{r+\delta_S} \end{pmatrix}.$$

Note that in both cases $J(t)$ only depends on parameters and therefore is independent of the periodic solution $\Gamma(t)$. We get for both monodromy matrices the eigenvalues

$$\xi_1 = e^{-\delta_S}, \quad \xi_2 = e^{r+\delta_S},$$

where the corresponding eigenvectors are given by

$$v_1 = \begin{pmatrix} 1 \\ 0 \end{pmatrix}, \quad v_2 = \begin{pmatrix} \frac{1}{2c(r+2\delta_S)} \\ 1 \end{pmatrix},$$

in the mixed and renewable case, and by

$$v_1 = \begin{pmatrix} 1 \\ 0 \end{pmatrix}, \quad v_2 = \begin{pmatrix} 0 \\ 1 \end{pmatrix},$$

in the fossil case. The eigenvalues of the monodromy matrix reflect the stability of the periodic solution. Let ξ_i , $i = 1, \dots, n$ be the eigenvalues of the monodromy matrix and let

$$n^+ := \{i : |\xi_i| < 1\}, \quad n^- := \{i : |\xi_i| > 1\},$$

be the sets of eigenvalues indicating stable (n^+) and unstable (n^-) directions, a periodic solution $\Gamma(t)$ is called of *saddle-type* if

$$|n^+||n^-| > 0$$

holds, which means that at least one of each type has to exist. If $|n^-| = 0$, the periodic solution is unstable (see Grass et al., 2008). As $0 < \delta_S < 1$ and $r + \delta_S > 0$ always holds, the two eigenvalues satisfy $\xi_1 = e^{-\delta_S} < 1$ and $\xi_2 = e^{r+\delta_S} > 1$. Due to the fact that the Jacobian matrix and therefore also the monodromy matrix is independent of the state and the control variables, this result implies that every periodic solution that we can find within one of the boundary regions is of saddle-type. Further on, as no eigenvalue $\xi_i = 1$, $i \in \{1, 2\}$ occurs, it even is a hyperbolic cycle, which guarantees that the behavior of the system near this periodic solution can be fully described by its linearization.

2.2.4 Numerical Continuation of Optimal Paths

In order to calculate a trajectory starting at an initial capital stock K_{S_0} , converging towards the optimal long-run periodic solution and lying completely within one of the boundaries of the feasible domain, a numerical continuation algorithm is needed. Let $\Gamma(t) = (K_S^*(t), \lambda^*(t))$ be a periodic solution of the model, then the goal is to find a solution path $(K_S(t), \lambda(t))$ which satisfies

$$0 = K_S(0) - K_{S_0}, \quad (2.38)$$

$$0 = F' \left(\begin{pmatrix} K_S(T_p) \\ \lambda(T_p) \end{pmatrix} - \begin{pmatrix} K_S^*(0) \\ \lambda^*(0) \end{pmatrix} \right), \quad (2.39)$$

where the matrix F is spanning the orthogonal complement to the stable eigenspace of the periodic solution (see Grass, 2012) and T_p is the truncation time of the path. The condition in (2.39) guarantees that the solution ends on the linearized stable manifold to which the vector F is orthogonal, cf. Figure 2.4 (for a more detailed theory on manifolds see Carr, 1982). Given the eigenspace determined in Section 2.2.3, the orthogonal complement to the stable eigenspace that is needed for the boundary value problem described in (2.38)-(2.39) is then calculated as

$$F = \begin{pmatrix} 0 \\ 1 \end{pmatrix}.$$

We normalize the time interval from $[0, T_p]$ to $[0, 1]$. Similar to the transformation we have

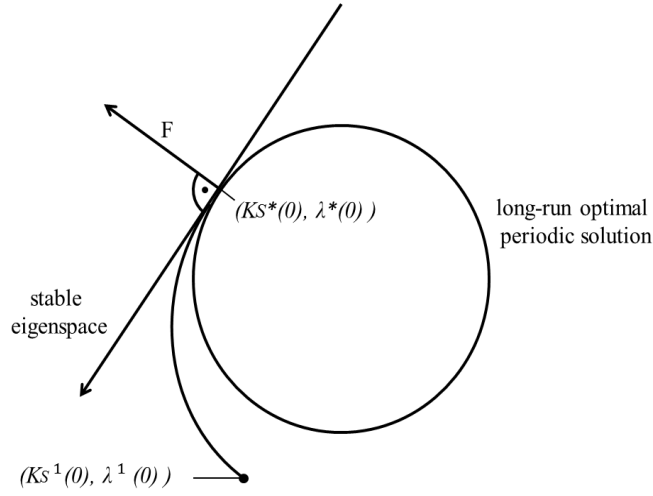


Figure 2.4: The stable eigenspace of the optimal long-run periodic solution, the orthogonal complement spanned by F , and a starting solution path starting at $K_S^1(0) = K_{S_0}^1$.

used in Section 2.2.2, we here set

$$T(s) = T_p s, \quad s \in [0, 1], \quad (2.40)$$

in order to transform a system of the form

$$\dot{x}(t) = f(t, x(t)), \quad t \in [0, T_p],$$

to the new system

$$\dot{x}(s) = \frac{dx(T(s))}{ds} = T_p f(T(s), x(s)), \quad s \in [0, 1].$$

To find a solution path that satisfies (2.38)-(2.39), the periodic solution is continued stepwise so that, after a finite number of steps, the target value K_{S_0} is reached. Starting with the initial value $K_{S_0}^1 = K_S^*(0)$ yields the trivial solution $\Gamma(t) = (K_S^*(t), \lambda^*(t))$, which is used as starting solution. Assume that we have N steps, then at each step $n = 1, \dots, N$ we have to find a solution path $(K_S^n(t), \lambda^n(t))$ so that

$$0 = K_S^n(0) - K_{S_0}^n, \quad (2.41)$$

$$0 = F' \left(\begin{pmatrix} K_S^n(1) \\ \lambda^n(1) \end{pmatrix} - \begin{pmatrix} K_S^*(0) \\ \lambda^*(0) \end{pmatrix} \right). \quad (2.42)$$

A simple strategy to deduce from one starting point $(K_S^{n-1}(0), \lambda^{n-1}(0), K_{S_0}^{n-1})$ a prediction of the next starting point $(K_S^n(0), \lambda^n(0), K_{S_0}^n)$ is given by linear interpolation (Euler method),

$$\begin{pmatrix} \hat{K}_S^n(0) \\ \hat{\lambda}^n(0) \\ \hat{K}_{S_0}^n \end{pmatrix} = \begin{pmatrix} K_S^{n-1}(0) \\ \lambda^{n-1}(0) \\ K_{S_0}^{n-1} \end{pmatrix} + h_{n-1} v_{n-1}, \quad \text{with } \|v_{n-1}\| = 1,$$

where h_{n-1} is the $(n-1)$ st step width and v_{n-1} is the tangential vector which can be approximated by the secant vector

$$v_{n-1} \approx \frac{1}{h_{n-1}} \left(\begin{pmatrix} K_S^{n-1}(0) \\ \lambda^{n-1}(0) \\ K_{S_0}^{n-1} \end{pmatrix} - \begin{pmatrix} K_S^{n-2}(0) \\ \lambda^{n-2}(0) \\ K_{S_0}^{n-2} \end{pmatrix} \right).$$

As at each step the system has 3 unknowns $(K_S^n(0), \lambda^n(0), K_{S_0}^n)$ but only 2 equations, it is thus under-determined. Therefore, an additional equation

$$g(K_S^n(0), \lambda^n(0), K_{S_0}^n) = 0,$$

is needed. One possibility is to set

$$g(K_S^n(0), \lambda^n(0), K_{S_0}^n) = K_{S_0}^n - \hat{K}_{S_0}^n,$$

which means that the predicted target value $\hat{K}_{S_0}^n$ and consequently also $K_S^n(0)$ is fixed and the corresponding $\lambda^n(0)$ has to be found. In geometric terms, this means that a solution is searched along a 1-dimensional hyperplane which is orthogonal to the chosen K_S -coordinate and that this solution is given by the intersection point of this hyperplane and the solution path. This algorithm works as long as the solution path is not bending back, as in this case the Jacobian matrix of the enlarged system is singular in this point. This problem gets obvious in Figure 2.5a. Having this drawback in mind, we use a slightly adapted version of this algorithm by searching for a solution along a hyperplane which is not orthogonal to the K_S -coordinate but to the secant vector v_n instead, and runs through the predicted point $(\hat{K}_S^n(0), \hat{\lambda}^n(0), \hat{K}_{S_0}^n)$. Formally, this is given by the equation

$$g(K_S^n(0), \lambda^n(0), K_{S_0}^n) = v'_{n-1} \left(\begin{pmatrix} \hat{K}_S^n(0) \\ \hat{\lambda}^n(0) \\ \hat{K}_{S_0}^n \end{pmatrix} - \begin{pmatrix} K_S^n(0) \\ \lambda^n(0) \\ K_{S_0}^n \end{pmatrix} \right).$$

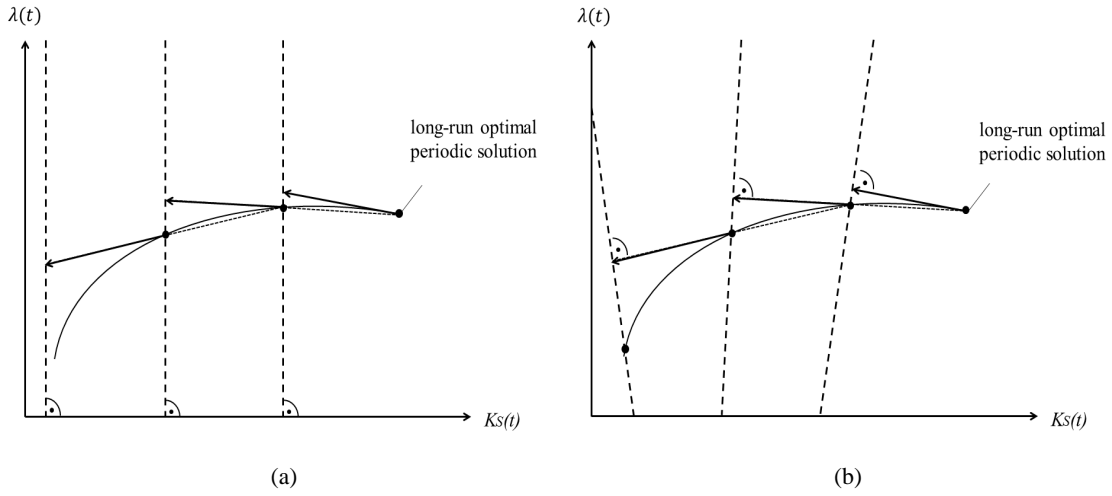


Figure 2.5: Algorithm where a solution is searched along a hyperplane orthogonal to **(a)** the K_S -coordinate, **(b)** the tangential vector. The latter one allows back-bending of the solution path.

With this method, the Jacobian matrix of the enlarged system does not further get singular and, hence, back-bending of the solution path causes no problems, see Figure 2.5b. To control the step width h_n , we use simple step width regulation, which means that the step width depends on the number of Newton iterations. If this number is high, the step width is reduced, if it is low, the step width is increased, and if it is moderate, the step width does not change.

To sum up, we solve at each step the following boundary value problem for $s \in [0, 1]$:

$$\begin{aligned}
 \dot{K}_S(s) &= T_p f^{K_S}(T(s), K_S(s), \lambda(s), \mu_3(s)), \\
 \dot{\lambda}(s) &= T_p f^\lambda(T(s), \lambda(s), \mu_1(s)), \\
 0 &= K_S^n(0) - K_{S_0}^n, \\
 0 &= F' \left(\begin{pmatrix} K_S^n(1) \\ \lambda^n(1) \end{pmatrix} - \begin{pmatrix} K_S^*(0) \\ \lambda^*(0) \end{pmatrix} \right), \\
 0 &= v'_{n-1} \left(\begin{pmatrix} K_S^{n-1}(0) \\ \lambda^{n-1}(0) \\ K_{S_0}^{n-1} \end{pmatrix} + h_{n-1} v_{n-1} - \begin{pmatrix} K_S^n(0) \\ \lambda^n(0) \\ K_{S_0}^n \end{pmatrix} \right).
 \end{aligned}$$

The solution at the N -th step yields the path leading from the initial state K_{S_0} , if feasible, into the optimal long-run periodic solution.

2.3 Results

For the numerical analysis we use the parameter values summarized in Table 2.1. Figure 2.6 shows

Interpretation	Parameter	Value	Interpretation	Parameter	Value
Investment costs	b	0.6	Depreciation rate	δ_S	0.03
Adjustment costs	c	0.3	Degree of efficiency	η	0.2
Energy demand	E	2000	Maximal radiation increment	ν	4.56
Fossil energy price	p_F	0.08	Minimal radiation in winter	τ	0.79
Discount rate	r	0.04			

Table 2.1: Parameter values used for the numerical analysis.

the optimal long-run periodic solution that corresponds to the case with both types of energy used to cover the energy demand. The black arrow marks the starting point in winter. Here, global radiation is weak and therefore the benefit of the capital stock with respect to renewable energy generation is low. Also investments are kept on a low level. However, as global radiation goes up in spring and the benefit of the capital stock increases, investments increase as well in the first quarter of the year in order to accumulate capital. The capital stock and the renewable energy generation then grow and reach a peak during summer which coincides with the maximum of global radiation. Note that investments during the second quarter of the year already decline again to stop the increase of the capital stock at this peak. In the third quarter of the year, also the capital stock decreases and renewable energy generation goes down. Finally, in winter, increasing investments let the capital stock level out at its initial value.

Figure 2.7 shows a phase portrait in the state-control space for this periodic solution. The trajectories (gray) lead cyclically into the periodic solution (black), where the left one starts at an initially lower and the right one at an initially higher capital stock. Along the left path one can see that the periodical investments lead to accumulation of the capital stock over time. However, to understand this fluctuating investments in more detail, one has to distinguish between investments for acquisition and investments for maintenance effort. Remember that we have included depreciation in the state equation in (2.1), so over time maintenance activities are necessary to keep the capital in a good condition. Figure 2.8 shows this aspect in more detail. It depicts the ratio of depreciation and total investments to illustrate maintenance activities. While at the beginning of the path starting at an initially lower capital stock almost all investments are used to accumulate capital, more and more is invested relatively in maintenance the closer the path comes to the optimal long-run periodic solution, in which investments and depreciation are perfectly balanced. Along

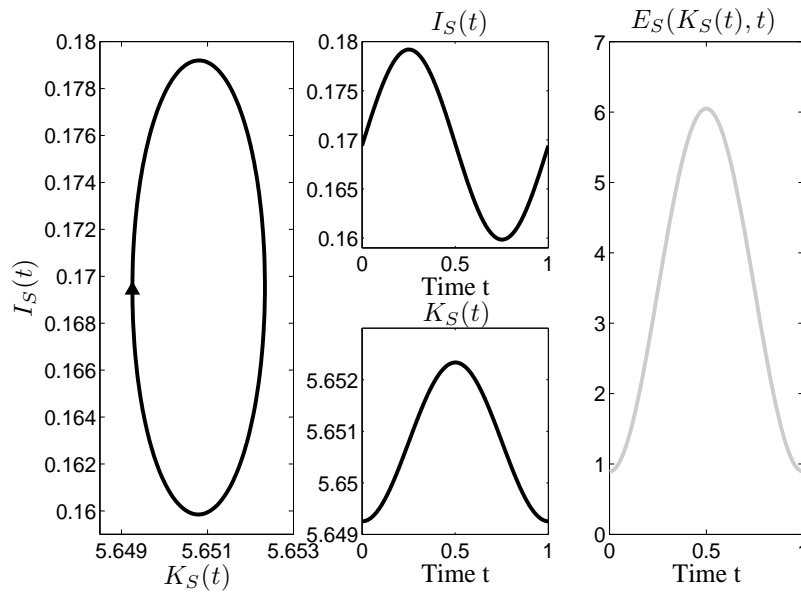


Figure 2.6: Periodic solution (left box), time paths for investments and capital over one year (two boxes in the middle) and renewable energy generation (right box) for a fossil energy price $p_F = 0.08$.

the path starting at the initially higher capital stock, the investment path follows exactly the opposite direction. Here, the initial capital stock is higher than optimal, so no investment for acquisition are made along the whole path and all investments are used for maintenance only. However, as the capital stock should decline towards the optimal level, investments are lower than depreciation (underinvestments) and full compensation of depreciation is reached only in the optimal long-run periodic solution.

Considering the proportions of fossil and renewable energy that are used in this scenario to cover the given energy demand, Figure 2.9 shows that the vast majority of the demand is covered by fossil energy and that the maximal contribution of renewable energy for this parameter set is very low at about 0.3% during summer only. This comes due to the fact that fossil energy with $p_F = 0.08$ is comparably cheap and, hence, high investments in renewable energy are too costly and therefore not worthwhile.

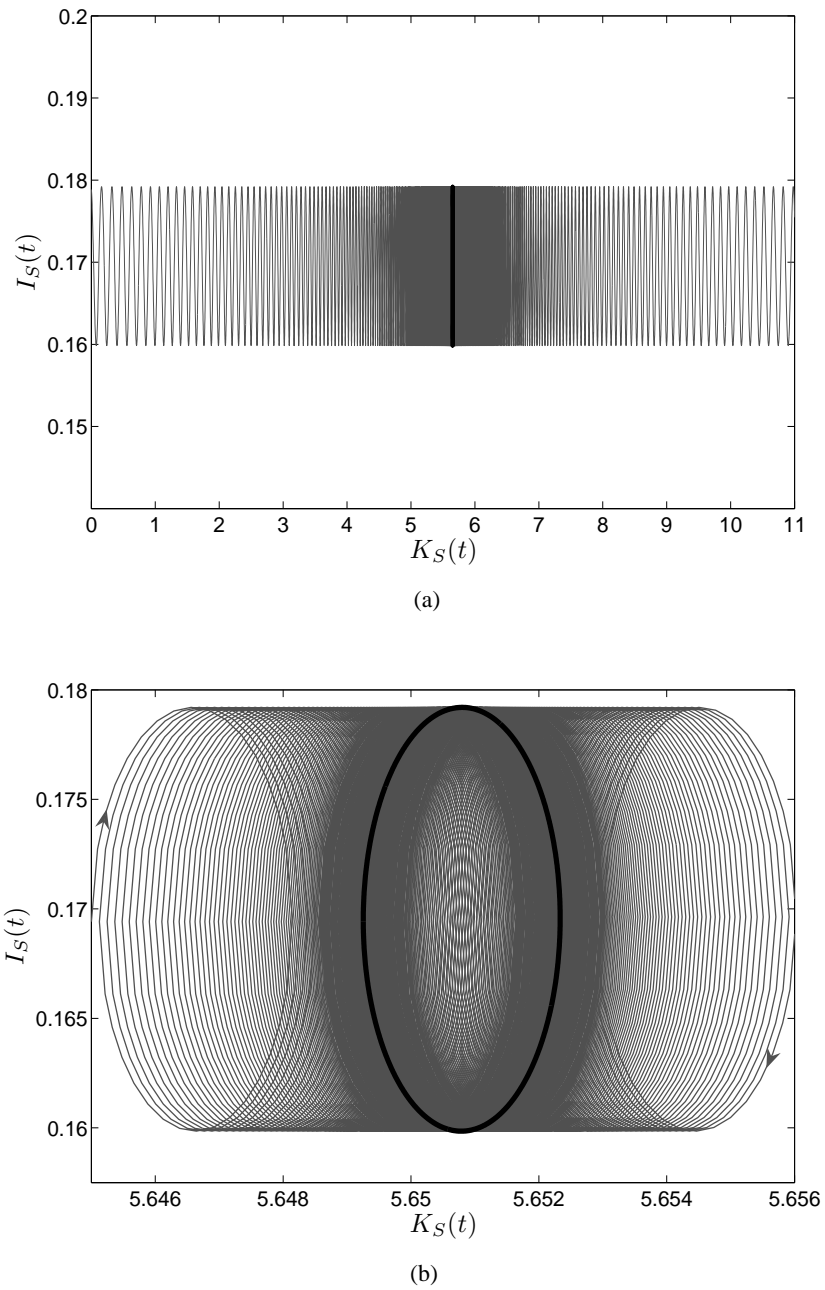


Figure 2.7: (a) Phase portrait for a fossil energy price $p_F = 0.08$ showing the trajectories (gray) leading into the optimal long-run periodic solution (black). (b) Zoom.

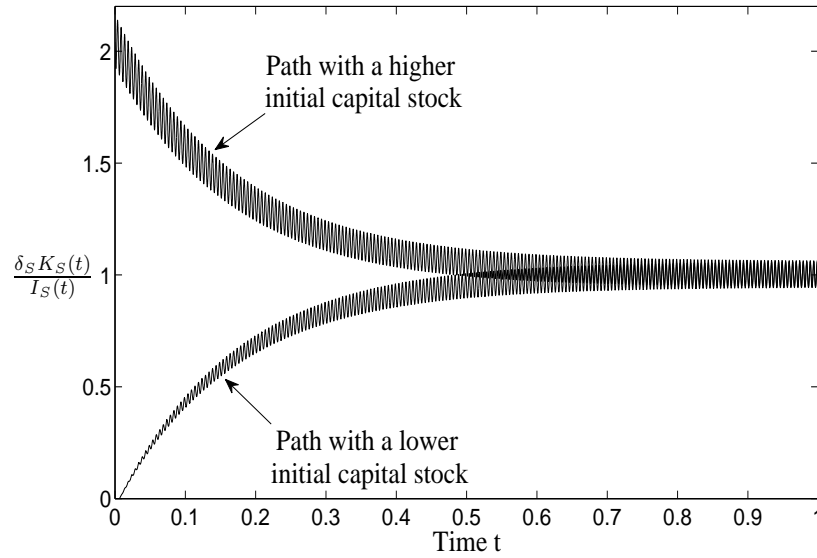


Figure 2.8: Maintenance investments along the solution paths leading into the periodic solution for a fossil energy price $p_F = 0.08$: Share of total investments along the path from an initially lower capital stock as well as underinvestments along the path for an initially higher capital stock, respectively.

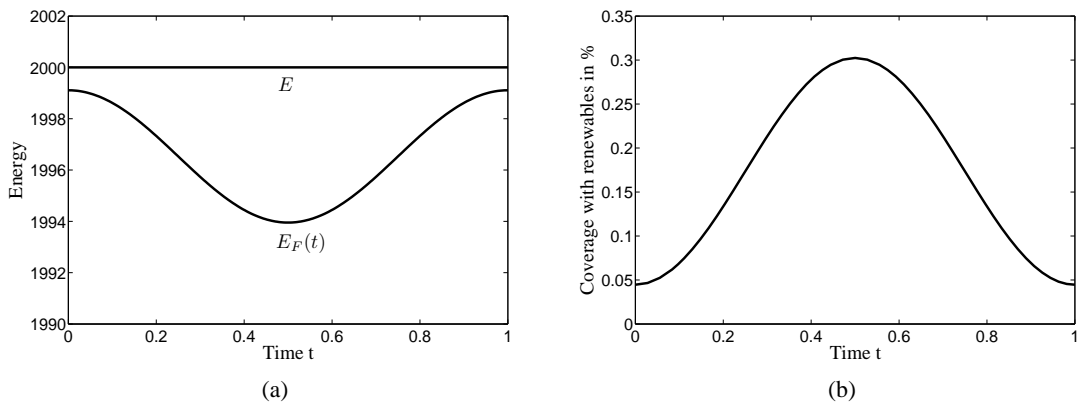


Figure 2.9: **(a)** Energy demand and optimal long-run fossil energy amount for a fossil energy price $p_F = 0.08$. **(b)** Coverage of the energy demand with renewable energy in percent.

2.4 Sensitivity Analysis

The results of the scenario presented in Section 2.3 have shown that for the parameter set of Table 2.1, the contribution of renewable energy to cover the exogenous energy demand is very low. These results immediately lead to the question, which mechanisms could foster renewable energy generation. The fossil energy price is certainly one of the factors that may induce a higher use of renewable energy. As long as the costs for importing fossil energy are low, investments in renewable energy capital are not very profitable. Therefore, the question is whether an increase in this price would lead to higher investments in renewable energy capital and, further on, whether there exists a price limit at which fossil energy is so expensive that the whole demand is covered only with renewable energy. Considering the interaction of technological improvements for discovery methods of new fossil resource reservoirs on the one hand and for extraction methods on the other hand, it is unclear how long fossil resources will be available for energy generation in the future. Therefore, scarcity alone cannot be seen as the driving force for an increasing fossil energy price. But considering the historical development as well as the aspect that enforced climate mitigation policies will sooner or later make fossil energy more costly, an increasing fossil energy price seems to be a reasonable assumption.

The second aspect that is supposed to have a positive effect on renewable energy generation is of course the degree of efficiency η . Technological progress driven by research and development will possibly enable a more efficient renewable energy generation in the future. Therefore, an interesting question is how the optimal portfolio in our model changes if renewable energy is generated with a higher efficiency η . Could this increase possibly compensate for the higher investment costs?

To investigate these two aspects we conduct a sensitivity analysis in this section by solving the optimal control problem for varying parameter values.

2.4.1 Fossil Energy Price p_F

First, we focus on the impact of an increasing fossil energy price p_F on the optimal portfolio composition. To do this, we start with a very low fossil energy price and increase it step by step, using numerical continuation to investigate how the optimal long-run solution changes. The results are shown graphically in Figures 2.10-2.14 for increasing values of p_F . In each figure, the box on the left hand side shows the solution in the state-control space. The two boxes in the middle depict the time paths for investments $I_S(t)$ and capital stock $K_S(t)$, respectively, and the box on the right hand side illustrates the composition of the energy portfolio with renewable energy shown as gray

line, fossil energy as black line, and the energy demand as black dashed line.

To begin with, we solve the problem for a fossil energy price $p_F = 0.01$. Note that this price is even lower than in the previous scenario of Section 2.3. Hence, fossil energy here is so cheap that nothing at all is invested in renewable energy capital and the whole energy demand is covered by fossil energy in the long run. This corresponds to the case in Section 2.2.1 which we called the fossil solution. As one can see in Figure 2.10, the optimal long-run solution in $K_S(t)$ and $I_S(t)$ coincides with the origin as no investments are made over the year and therefore no capital stock is accumulated. Note that we assume an initial capital stock of zero, so that no investments imply no renewable energy generation. But even in case of an initially positive capital stock, zero investments would lead to $K_S(t) \approx 0$ in the long run as well. The fossil energy amount fully covers the energy demand in this scenario and therefore, these two lines coincide in the right box of Figure 2.10, while renewable energy generation is constantly zero.

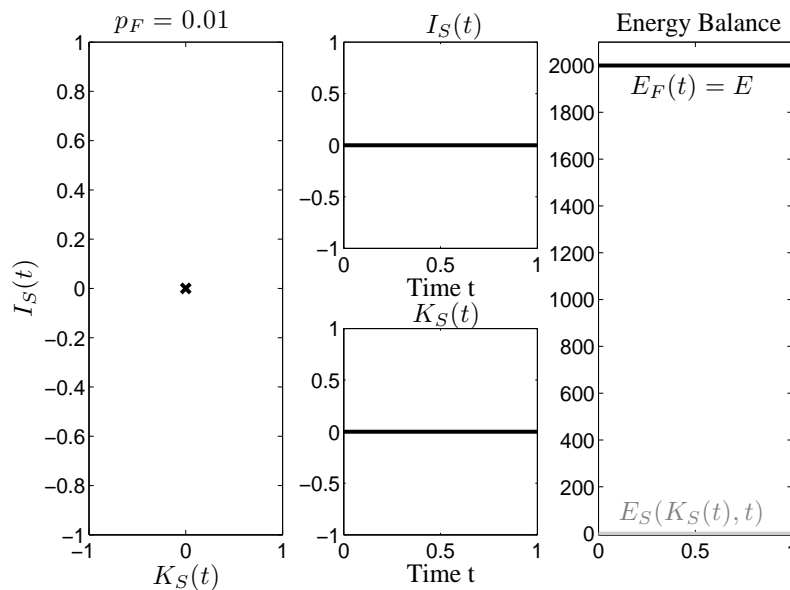


Figure 2.10: Solution for a fossil energy price $p_F = 0.01$: Fossil solution over the whole year with zero investments $I_S(t) = 0$, zero capital stock $K_S(t) = 0$, no renewable energy generation, and hence fossil energy imports of $E_F(t) = E$.

If the fossil energy price is slightly increased, however, renewable energy is used as additional energy source for the portfolio. At $p_F = 0.06785$ an interesting aspect can be observed. As already mentioned in Section 2.3, the benefit of the capital stock with respect to renewable energy generation is the highest in summer, when global radiation reaches its maximum. Due to the still

very low fossil energy price, however, a too high capital stock outside of this period is not cost-effective. Therefore, it is only worthwhile to invest in renewable energy capital shortly before the summer period to slightly increase renewable energy capital (or to do some maintenance to keep it in a good condition) in order to optimally utilize the high global radiation at this time. During the rest of the year, however, investments are again set to zero and the demand is almost completely covered by the cheaper fossil energy. Hence, for this fossil energy price we find a periodic solution that consists of three arcs, two with zero investments corresponding to the fossil case, and one with positive investments corresponding to the mixed case. This is shown in Figure 2.11, where the black line depicts the arc of the mixed solution with both types of energy used for the coverage, and the black dashed line corresponds to the arcs where no investments are made and almost the whole demand is covered by fossil energy.⁶ As the contribution of renewable energy generation to cover the given energy demand still is very low, the energy balance looks quite similar to the one in Figure 2.10, where the black dashed line for the energy demand and the black line for the fossil energy amount have been identical. Although they are pretty close also in this case, they are numerically not equal as the zoom in Figure 2.11 shows. The price interval for which this mixed-arc-solution exists is very small, $p_F \in [0.06785, 0.06897]$.

For a higher fossil energy price, investments are made over the whole year, and they still are higher shortly before the summer period in order to fully utilize the high global radiation as in the previous case. Figure 2.12 shows the optimal long-run periodic solution for $p_F = 2.7$, which corresponds completely to the mixed case, meaning that both types of energy are used over the whole year to cover the demand. In contrast to Figure 2.11, where the renewable energy generation is so low that it hardly can be seen in the graph, one already can observe in Figure 2.12 that the generation increases with the fossil energy price. More and more investments are made and the additional fossil energy amount during the summer period is reduced. During the winter period, however, a high amount of fossil energy is still required due to the low global radiation in this time.

Increasing the fossil energy price even further leads to an increased renewable energy generation until finally, at $p_F = 3.9468$, it reaches exactly the demand at the peak of global radiation in summer. At this point, a switch to the complete renewable case happens. What is only one oscillation point at the beginning develops to an interval when the price is increased further. In this interval, which always is around the point of time of maximal global radiation, the energy demand

⁶The capital stock of course is not immediately zero if there are no further investments, but due to the fact that the capital stock is not very high even during summer and depreciation reduces the stock if there are no investments, renewable energy generation during the winter months is negligibly low.

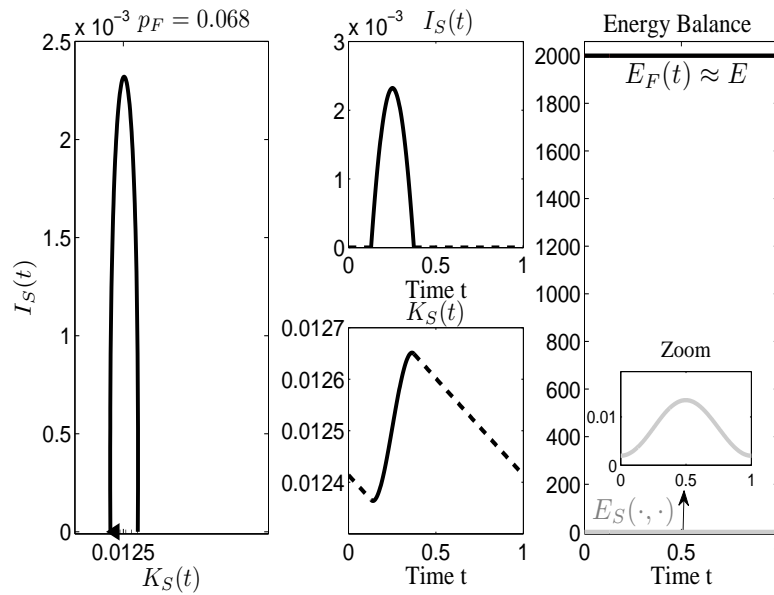


Figure 2.11: Periodic solution for a fossil energy price $p_F = 0.068$ with three arcs: Mixed solution with positive investments $I_S(t)$ and positive fossil energy imports $E_F(t)$ (solid line), and fossil solution with zero investments $I_S(t) = 0$ and fossil energy imports of $E_F(t) = E$ (dashed line).

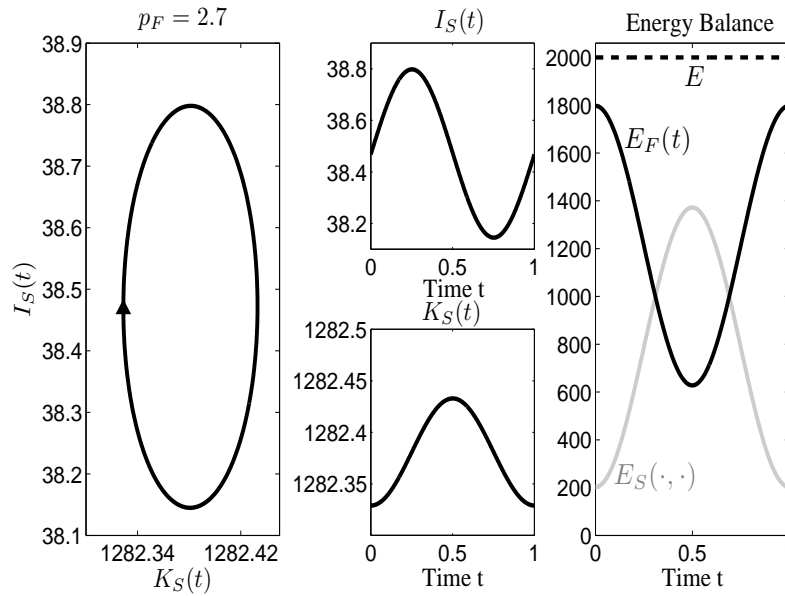


Figure 2.12: Periodic solution for a fossil energy price $p_F = 2.7$: Mixed solution with positive investments $I_S(t)$ and positive fossil energy imports $E_F(t)$ over the whole year.

can be covered fully by renewable energy while fossil energy in addition is not further needed. Figure 2.13 shows this scenario for a fossil energy price $p_F = 5.5$. At the beginning of the year, investments increase in order to accumulate enough capital for spring and summer, where global radiation increases and reaches its maximum. However, as surpluses during summer are not profitable, investments already decrease again during spring in order to avoid a too high capital stock during this time. As global radiation still is relatively high in autumn, however, the capital stock should also not get too small and, therefore, an increase in investments can be observed over the summer period. Due to the low global radiation in winter, however, they decrease again in autumn as a high capital stock is not further profitable there and, finally, at the end of the year they go up again to accumulate capital for the spring and summer period. Considering the energy portfolio in the right box, one can see the surpluses that are generated during the summer period. As the possibility of storage is omitted in our approach, these surpluses are lost but the energy supply in this period is independent of fossil energy. For this scenario we find again a periodic solution that consists of three arcs, the black parts corresponding to the arcs of the mixed solutions and the gray one displaying the renewable solution arc in-between.

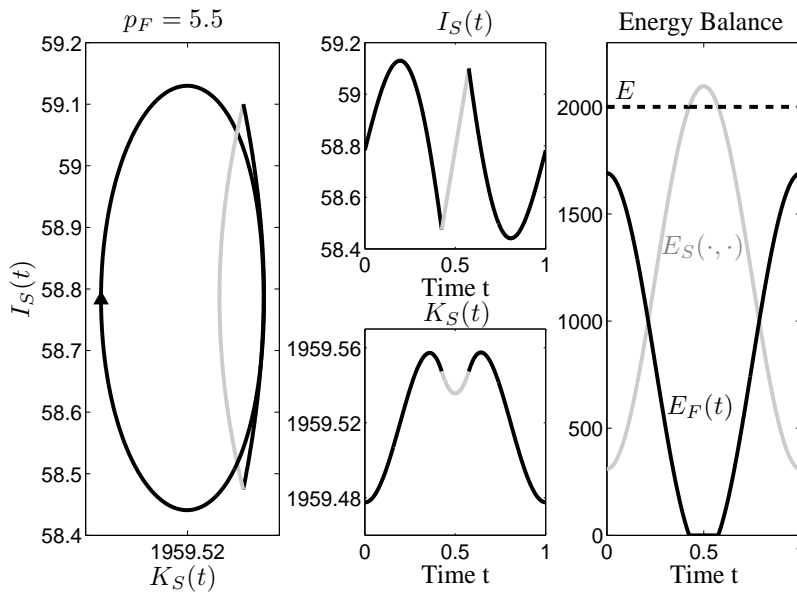


Figure 2.13: Periodic solution for a fossil energy price $p_F = 5.5$ with three arcs: Mixed solutions with positive investments $I_S(t)$ and positive fossil energy imports $E_F(t)$ (black solid lines), and renewable solution with positive investments $I_S(t)$ and zero fossil energy imports $E_F(t) = 0$ (gray solid line).

The interval in which renewable energy is sufficient to cover the energy demand increases, the further the fossil energy price goes up. However, it turns out that this happens at a decreasing speed, and during winter fossil energy still is necessary to cover the shortfalls, even if the fossil energy price is already very high. Figure 2.14 shows the optimal long-run solution for a really high fossil energy price $p_F = 10$. One can see that, despite the high surpluses in summer, there is only little improvement in renewable energy generation in winter.

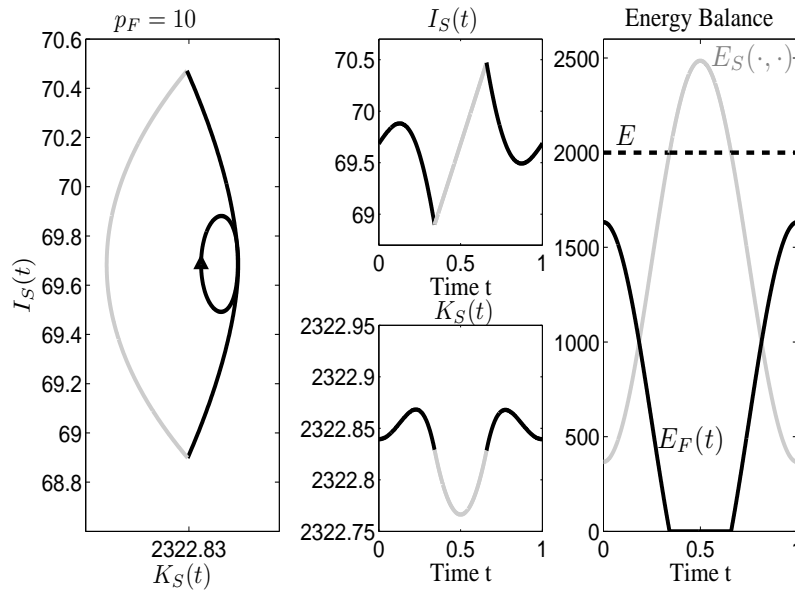


Figure 2.14: Periodic solution for a fossil energy price $p_F = 10$ with three arcs: Mixed solutions with positive investments $I_S(t)$ and positive fossil energy imports $E_F(t)$ (black solid lines), and renewable solution with positive investments $I_S(t)$ and zero fossil energy imports $E_F(t) = 0$ (gray solid line).

To give an insight into how the costs over the whole period vary with the obtained portfolio compositions of different price scenarios, Figure 2.15 shows the occurring costs for the solutions at $p_F = 0.01$, $p_F = 0.068$, $p_F = 2.7$, and $p_F = 5.5$. Note that the cost function

$$C(E_F(t), I_S(t), t) = I_S(t) \left(b + c I_S(t) \right) + p_F E_F(t)$$

evaluated along the optimal long-run periodic solution is considered here, and not the accumulated and discounted costs over the whole time period, as it is given in the objective function. The advantage of this analysis is that the changes in the costs of the portfolio composition over the seasons can be shown in more detail. One can see that the pure fossil portfolio at $p_F = 0.01$

compared to the fossil and mixed portfolio at $p_F = 0.068$ hardly differs in the annual costs as fossil energy is very cheap and the contribution of renewable energy generation is too low to cause a remarkable reduction of costs during the summer period. For the portfolio at $p_F = 2.7$, this is significantly different. Here, a strong decline of the costs during summer can be observed as the renewable energy generation compensates for the more expensive fossil energy amount. On the other side, it also points out how expensive the winter gets due to the low global radiation and the high fossil energy price. This is even worse for the portfolio at $p_F = 5.5$. However, during summer here the costs drop down even below the cost curve of the portfolio at $p_F = 2.7$, as no fossil energy is used anymore. This strong reduction underlines on the one hand the cost-reducing potential of renewable energy if supply is sufficient, while on the other hand, however, it illustrates the strongly reduced benefit due to the high costs in winter where supply is too low.

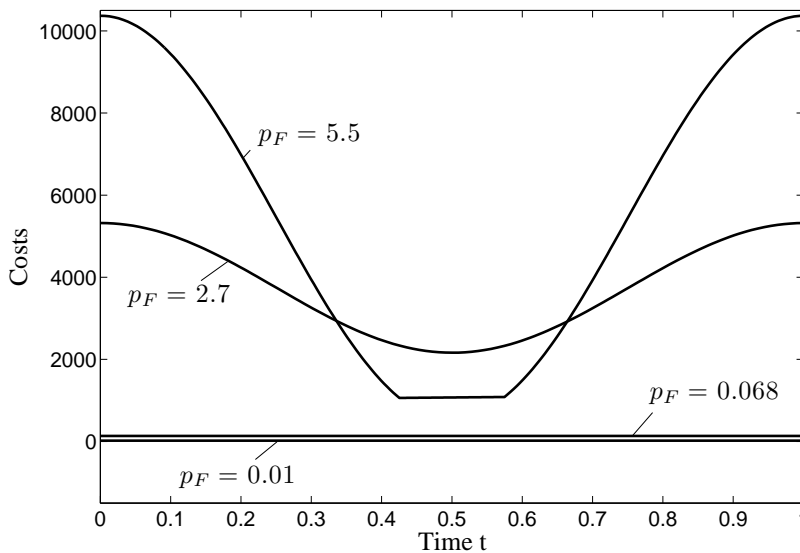


Figure 2.15: Development of the cost function along the optimal long-run periodic solutions for different fossil energy price scenarios.

2.4.2 Degree of Efficiency η

To investigate how an increase in efficiency could change the portfolio composition, we conduct the analogous analysis as in the previous section with respect to the degree of efficiency η . For that purpose, we let the fossil energy price be fixed at $p_F = 2$ and start with an initially low degree of efficiency $\eta = 0.1$, which is then increased step by step to demonstrate the changes in

the portfolio composition. The results of this analysis can be seen in Figure 2.16. Figure 2.16a shows that even for a comparably high fossil energy price, a low efficiency degree of 10% makes investments in renewable energy capital not profitable. As the output of the generation is too low to compensate for the high investment costs, fossil energy is still used to cover the major share of the energy demand. If the degree of efficiency is increased up to 25%, as shown in Figure 2.16b, an improvement in renewable energy generation can be observed. While fossil energy still costs the same, the investments into renewable energy capital have become more worthwhile as the output of generation has increased. Finally, Figure 2.16c shows the result for an efficiency of 40%, which is already very high for photovoltaic cells. One can see, however, that this improvement changes the situation completely. For this case we can find again a periodic solution consisting of three arcs, where the arcs in winter and spring correspond to the mixed case and the one in summer to the renewable case with renewable energy being sufficient for the coverage of the demand. This extreme scenario was chosen to demonstrate the changes in the solution and to underline the aspect that improvements in renewable energy technologies' efficiency indeed could play a major role along the path towards a more sustainable energy generation in the future.

2.4.3 Combined Effects

The previous two sections have illustrated the impact of a change in the fossil energy price as well as in the efficiency of renewable energy technology on the optimal long-run solution. However, a further interesting aspect is what happens with the portfolio if both changes happen simultaneously, and whether these two effects reinforce or dampen each other. In this section we will focus on this 2-dimensional parameter variation. The sensitivity analysis with respect to the fossil energy price p_F has shown that there exist price levels at which the optimal long-run solution changes from a pure one-arc periodic solution to a periodic solution consisting of several arcs. At the first price boundary, the pure fossil solution changes to a mixed-arc solution with three arcs, two corresponding to the fossil and one to the mixed case. At the second one, the optimal long-run periodic solution lies completely at the feasible boundary of the mixed case, while at the third one, the pure mixed solution changes to a mixed-arc solution with two arcs corresponding to the mixed and one to the renewable case. For the analysis of the combined effects we start at a very low efficiency $\eta = 0.05$, increase it step by step, and derive at each efficiency level these price boundaries. Figure 2.17 illustrates these results, where the black solid line describes the

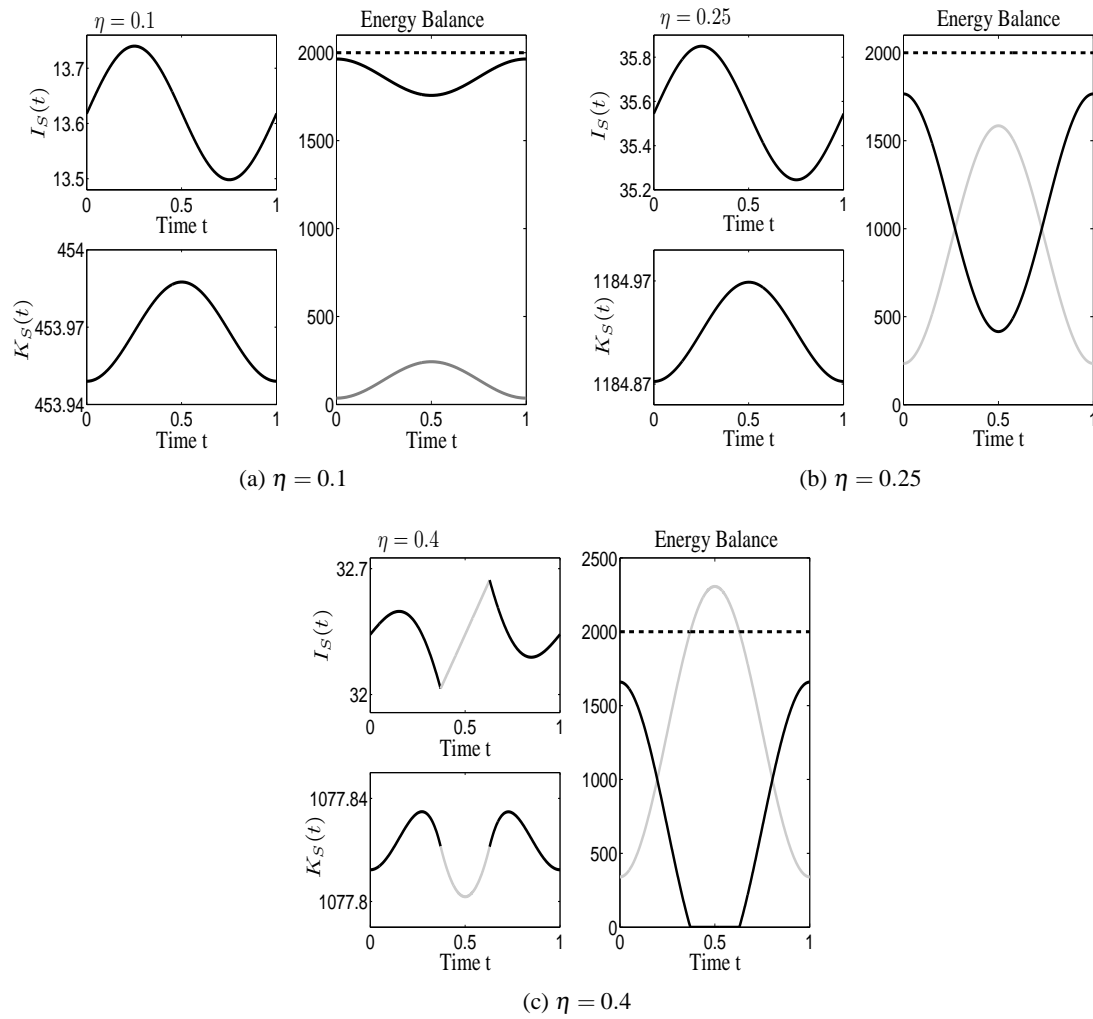


Figure 2.16: Periodic solution for different degrees of efficiency η .

price boundary from the fossil to the mixed solution,⁷ and the gray solid line the one from the mixed solution to the combined mixed and renewable solution. For a low level of η it can be seen that the region for the mixed solution is very large,⁸ and the increase in the fossil energy price that would be necessary to reach the mixed/renewable area would have to be extremely high. As renewable energy technology here is not efficient enough, also the fossil area is comparatively large. The higher efficiency gets, however, the smaller is this area and the lower the necessary price increase has to be to make using renewable energy as additional source profitable. Also the price boundary for the transition to the mixed/renewable case decreases with efficiency. As the output of the renewable energy capital grows, renewable energy gets already sufficient at a lower fossil energy price. These results show that the two effects reinforce each other, which underlines the importance of financial and technological incentives for a cleaner energy supply.

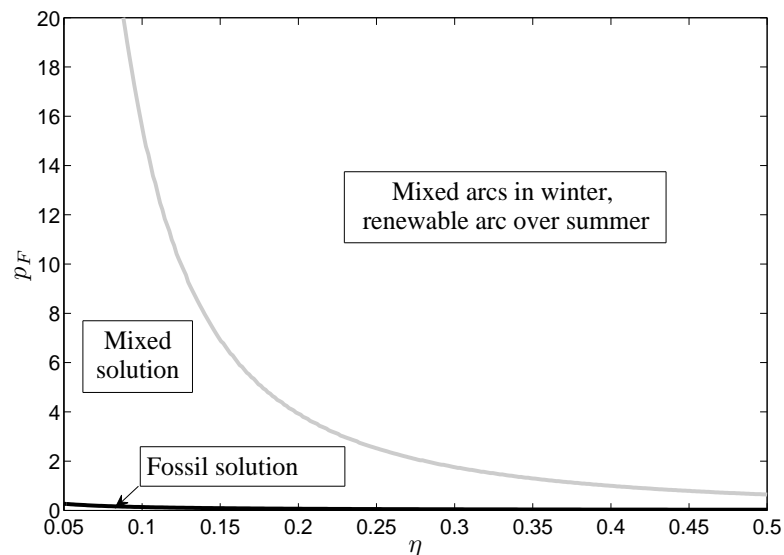


Figure 2.17: Combined effects with changes in both the fossil energy price as well as efficiency.

It, of course, does not come at a surprise that an increase in the fossil energy price as well as an increase in efficiency improve the profitability of investments into renewable energy capital within the considered portfolio. However, this sensitivity analysis shows the extent of these changes and

⁷Note that of course there is in fact also the boundary from the fossil case to the combined case with a fossil and a mixed arc, but as the price interval in which this transition happens is so small, we omitted this boundary in the figure for the sake of clarity.

⁸For the sake of lucidity we had to cut off the second price boundary for these low levels as they are really high. For the initial value of $\eta = 0.05$ it lies above $p_F = 60$.

how they interact. As renewable energy technology has high investment costs, its competitiveness strongly depends on the price of conventional energy types. These results underline that for example penalties on CO₂ intensive technologies indeed could be a strong incentive for renewable energy investments, as they increase this price and therefore support the renewable technology to penetrate the market. Further on, simultaneous R&D activities might improve the efficiency of the renewable energy technology and could enforce this aspect to accelerate the process towards a more sustainable energy generation in the future.

2.5 Fluctuating Energy Demand

So far we have postulated that the energy demand is well known and constant over the whole year. This, of course, is a strong simplification. In reality, the proper prediction of the exact energy amount that has to be supplied is one of the biggest challenges of energy trading companies due to the strong fluctuations between different hours of the day but also between seasons. In middle and northern European countries for example, the energy demand during the winter months can be one and a half times as high as the one during summer due to heating, lighting, drying laundry, etc. This behavior, of course, is exactly reverse to the supply of global radiation. In countries of the south, however, an opposite situation can be observed. While the winter months there are not so cold and hence the necessary heating effort is very low, the summer months are so hot that air conditioning strongly increases the energy demand during this time. This period of high demand coincides with the high supply of global radiation, which makes it easier to cover it with renewable energy. Due to the impact of climate change on temperature increase, however, some areas with a winter peak regime tend to slowly approach a summer peak regime instead, see IPCC (1998). Consequently, along the transition the demand can also be a mixture of these two shapes where both, a summer peak due to air conditioning and a winter peak due to heating, occur. Also in Austria, where the winter peak is definitely dominant, the above-average temperatures in summer especially in recent years have induced a small air conditioning summer peak as well.

To account for such fluctuations in energy demand we extend the model presented in (2.2) by including an energy demand that is seasonally fluctuating. We still omit, however, daily fluctuations. To model the varying energy demand with a deterministic function, we use a cosine function given by

$$E(t) = E_a + \frac{E_a}{3} \cos(2t\pi)$$

for a country with the peak of energy demand during winter, where E_a is considered to be the

average annual demand for which we use the level of the fixed energy demand of the previous approach. The new demand is shown in Figure 2.18a. We further use

$$E(t) = E_a - \frac{E_a}{3} \cos(2t\pi)$$

for a country with the peak of energy demand during summer as shown in Figure 2.18b, and finally

$$E(t) = E_a + \frac{E_a}{3} \cos(4t\pi)$$

for a country with both peaks as shown in Figure 2.18c.

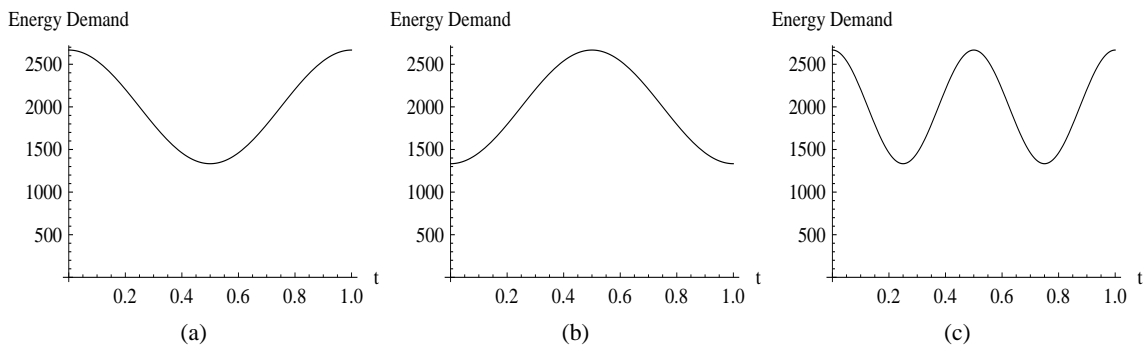


Figure 2.18: Seasonally fluctuating energy demand with **(a)** a peak during the winter period, **(b)** a peak during the summer period, **(c)** both peaks.

Applying the same analysis as in Section 2.4, it turns out that also in case of a fluctuating energy demand one can find a time interval during summer where renewable energy is sufficient to cover the demand. However, this happens at different fossil energy prices as compared to our results in Section 2.4. Figure 2.19 shows the result for a country with a higher demand in winter. One can see that during the summer period the demand is so low that already at a comparatively low fossil energy price the energy demand is reached with renewable energy. During winter, however, the peak is so high that the required amount of fossil energy is huge even if fossil energy gets very expensive, due to the low global radiation in these months.

In contrast to this, Figure 2.20 shows the result for a country in the south with a peak during summer. For the same fossil energy price as used for Figure 2.19, one can easily see that here renewable energy is far away of being sufficient for the very high demand. Therefore, no such interval of a pure renewable solution exists for this price. During winter, however, the additional amount of fossil energy is comparatively low as the demand here goes down.

Investigating the case with two demand peaks yields a very interesting case. Figure 2.21 shows the optimal long-run periodic solution for this approach for a fossil energy price $p_F = 7.5$. As one can see, we no longer have a solution that consists of three arcs but instead of even five arcs. Starting in winter, the peak caused by heating requires a high amount of fossil energy to cover the demand while renewable energy generation only contributes little, as it also is the case in the other two scenarios. In spring, the energy demand goes down and, as in the countries having only the winter peak, at some point of time renewable energy gets sufficient and the system changes to the solution using only renewable energy. However, this does not persist for long as the demand at the summer peak is too high to let renewable energy remaining to be sufficient, so again fossil energy is needed to cover the shortfalls. In autumn, the summer peak declines again and, as for the countries having only the winter peak, renewable energy generation is sufficient here. But similar to spring, the winter peak ends this interval of sufficiency and fossil energy is necessary again to cover the high demand.

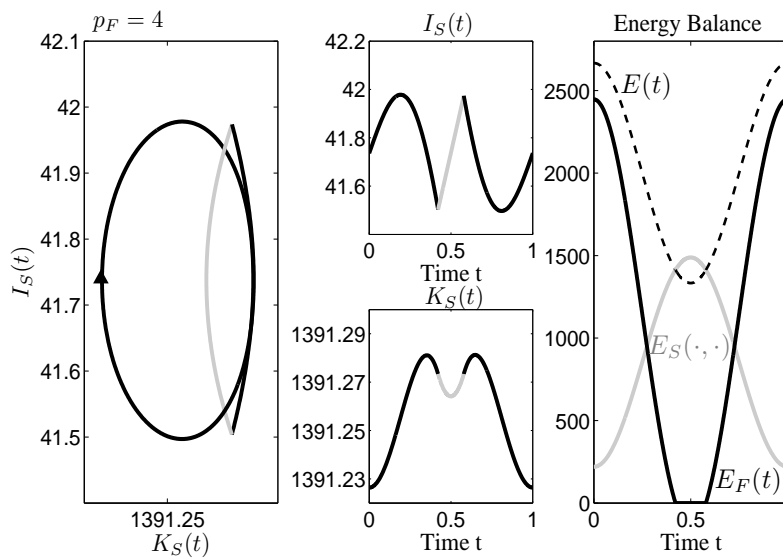


Figure 2.19: Periodic solution for a fossil energy price $p_F = 4$ with three arcs, for a seasonally fluctuating energy demand with a peak during the winter period: Mixed solutions with positive investments $I_S(t)$ and positive fossil energy imports $E_F(t)$ (black solid lines), and renewable solution with positive investments $I_S(t)$ and zero fossil energy imports $E_F(t) = 0$ (gray solid line).

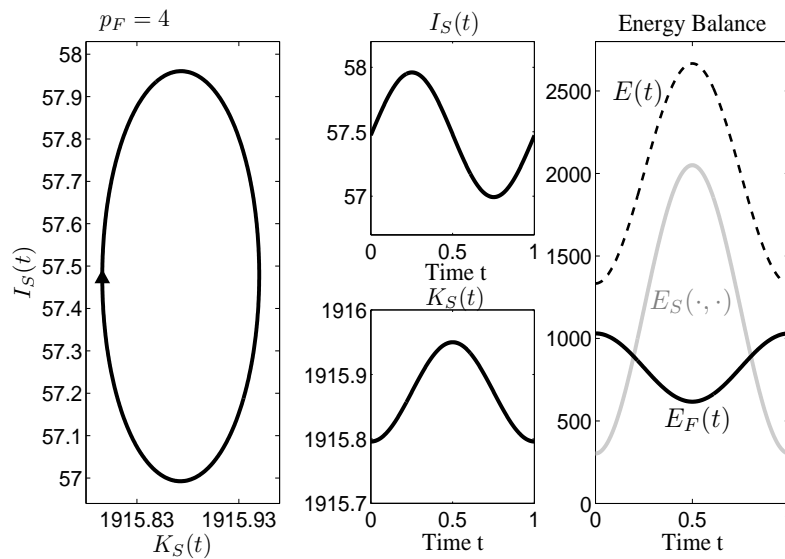


Figure 2.20: Periodic solution for a fossil energy price $p_F = 4$, for a seasonally fluctuating energy demand with a peak during the summer period: Mixed solution with positive investments $I_S(t)$ and positive fossil energy imports $E_F(t)$ (black solid line) over the whole year.

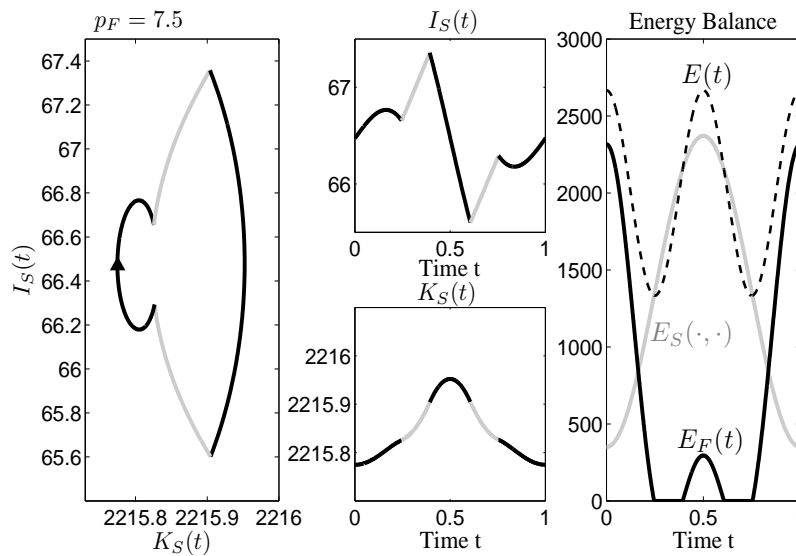


Figure 2.21: Periodic solution for a fossil energy price $p_F = 7.5$ with five arcs for a seasonally fluctuating energy demand with both, a winter and a summer peak: Mixed solutions with positive investments $I_S(t)$ and positive fossil energy imports $E_F(t)$ (black solid lines), and renewable solutions with positive investments $I_S(t)$ and zero fossil energy imports $E_F(t) = 0$ (gray solid lines).

2.6 Summary

In this chapter we have investigated the impact of the fossil energy price on the optimal portfolio composition consisting of fossil and renewable (solar) energy in a small country. We postulated that the supply of the renewable resource is varying seasonally, and the energy demand is well known and constant over the year in the first approach, while in the second one it is assumed to be seasonally fluctuating.

The sensitivity analysis of this non-autonomous optimal control problem with respect to the fossil energy price p_F has shown that a higher fossil energy price indeed is an incentive for more investments in renewable energy capital. However, an autarkic renewable energy supply is not possible, as the global radiation during the winter period is too low to be sufficient, no matter how high the fossil energy price is. While independence on fossil energy can be achieved during some time interval in summer in which global radiation is high and even surpluses can be generated, the shortfalls in winter always have to be covered by fossil energy. The potential of solar energy is even reduced, if the energy demand is postulated to be fluctuating over the year, either with a peak in winter or in summer.

These results underline one of the major challenges of renewable energy generation, which is given by the non-constant supply as well as the high investment costs which make it difficult to be competitive with the conventional energy types. In our model approach, these investment costs were kept constant. However, it is well known that in reality there exist some experience effects, which positively influence renewable energy generation. This means that the more renewable energy is generated, the lower are the costs necessary for renewable energy capital. This aspect will be considered as extension of the model in the next chapter.

The Effect of Learning by Doing in Renewable Energy Generation

As already presented in the introduction in Chapter 1, a common approach to include learning effects into energy planning decision problems is given by the so-called learning curve. In this chapter the first extension of the basic model analyzed in Chapter 2 will be considered by including a one-factor learning curve into the objective function of the optimal control problem. The obtained results will show that this change indeed causes a remarkable difference in the optimal long-run solution of the model.

3.1 The Model

Before we extend the basic model with a one-factor learning curve, we first make some assumptions about its functional form. While Equation (1.1) only is defined for an initially installed capacity of $K_0 > 0$, we extend this approach by allowing also a complete start-up with renewable energy, meaning $K_0 = 0$. To do so, we follow Berglund and Söderholm (2006) who present a learning curve formula without explicitly modeling the initially installed capacity. Further on, we add an additional term ε defining the initial investment costs when the cumulative capital stock is zero, as done in Hartley et al. (2010). The new learning curve then reads as

$$C_t = C_0(K + \varepsilon)^{-\alpha}.$$

The cumulative capacity in our model approach is reflected by the capital stock $K_S(t)$. Applying this on the cost function of the model approach presented in Chapter 3 yields the new cost function

$$C_t = I_S(t) (b + cI_S(t)) (K_S(t) + \varepsilon)^{-\alpha}.$$

This specification further implies that a rapid increase in the renewable energy capital stock is costly, which is relevant for the speed of the economy's shift to renewable energy generation (cf. Rasmussen, 2001).

The extended version of the model (2.2) then reads as

$$\max_{E_F(t), I_S(t)} \int_0^{\infty} e^{-rt} \left(-I_S(t) (b + cI_S(t)) (K_S(t) + \varepsilon)^{-\alpha} - p_F E_F(t) \right) dt \quad (3.1)$$

$$\text{s.t.: } \dot{K}_S(t) = I_S(t) - \delta_S K_S(t), \quad (3.1a)$$

$$E_F(t) + E_S(K_S(t), t) - E \geq 0, \quad (3.1b)$$

$$E_S(K_S(t), t) = (\nu \sin^2(t\pi) + \tau) K_S(t) \eta, \quad (3.1c)$$

$$E_F(t), I_S(t) \geq 0. \quad (3.1d)$$

3.2 Solution

3.2.1 Canonical System and Necessary First Order Conditions

As for the model in the previous approach we use the maximum principle for infinite time horizon problems (cf. Grass et al., 2008) and consider the Lagrangian

$$\begin{aligned} \mathcal{L}(K_S, E_F, I_S, \lambda, \lambda_0, \mu_1, \mu_2, \mu_3, t) &= \lambda_0 \left(-bI_S(t) + cI_S(t)^2 \right) (K_S(t) + \varepsilon)^{-\alpha} - p_F E_F(t) \\ &+ \lambda(t) (I_S(t) - \delta_S K_S(t)) + \mu_1(t) (E_F(t) + (\nu \sin^2(t\pi) + \tau) K_S(t) \eta - E) \\ &+ \mu_2(t) E_F(t) + \mu_3(t) I_S(t), \end{aligned}$$

with $\lambda(t) \in \mathbb{R}$ being, again, a continuous and piecewise continuously differentiable function and a constant $\lambda_0 \geq 0$, so that for all $t \geq 0$

$$(\lambda_0, \lambda(t)) \neq 0,$$

$$\mathcal{L}(K_S^*, E_F^*, I_S^*, \lambda, \lambda_0, \mu_1, \mu_2, \mu_3, t) = \max_{E_F(t), I_S(t)} \mathcal{L}(K_S^*, E_F, I_S, \lambda, \lambda_0, \mu_1, \mu_2, \mu_3, t),$$

and satisfying the limiting transversality condition in (2.8). As before, $\mu_1(t)$, $\mu_2(t)$, and $\mu_3(t)$ are the piecewise continuous Lagrange multipliers for the mixed-path constraint in (3.1b) and the non-negativity constraints, respectively. As the only difference between this model and the one in Chapter 2 lies within the objective function, we have to consider the same complementary slackness conditions as in (2.3)-(2.5), and also Proposition 1 still holds. Hence, we can set for the

following $\lambda_0 = 1$ without loss of generality. The necessary first order conditions then read as

$$\frac{\partial \mathcal{L}}{\partial I_S(t)} = -b(K_S(t) + \varepsilon)^{-\alpha} - 2cI_S(t)(K_S(t) + \varepsilon)^{-\alpha} + \lambda(t) + \mu_3(t) = 0 \quad (3.2)$$

$$\Leftrightarrow I_S(t) = \frac{(K_S(t) + \varepsilon)^\alpha (\lambda(t) + \mu_3(t)) - b}{2c},$$

$$\begin{aligned} \dot{\lambda}(t) &= \lambda(t)r - \frac{\partial \mathcal{L}}{\partial K_S(t)} = (r + \delta_S)\lambda(t) - \alpha(b + cI_S(t))I_S(t)(K_S(t) + \varepsilon)^{-\alpha-1} \\ &\quad - \mu_1(t)\eta(v \sin^2(t\pi) + \tau). \end{aligned} \quad (3.3)$$

Note that in this model approach only the necessary but not the sufficient conditions are considered to be satisfied as the satisfaction of the sufficient conditions cannot be generally proven. Consequently, the solutions that we can find are basically extremal but not necessarily optimal. Nevertheless, based on the economic interpretation of these solutions and the comparability to the results of Chapter 2, it makes sense to assume that they are in fact optimal.¹ Due to the linearity of the Lagrangian in $E_F(t)$, the optimal fossil energy amount is determined by the switching function

$$\frac{\partial \mathcal{L}}{\partial E_F(t)} = -p_F + \mu_1(t) + \mu_2(t).$$

As the changed costs for renewable energy capital do not affect the fossil costs in the objective function, Proposition 2 also applies for this approach and, therefore, we only focus on the three boundary cases of the feasible domain, given by the fossil case with no investments in renewable energy capital, the mixed case where both types of energy are used for the coverage, and finally the renewable case where no more fossil energy is needed in addition to renewable energy. Inserting the corresponding values for the Lagrange multipliers yields the three different canonical systems. For the fossil case, it is given by

$$\dot{K}_S(t) = -\delta_S K_S(t), \quad (3.4)$$

$$\dot{\lambda}(t) = \lambda(t)(r + \delta_S) - p_F \eta(v \sin^2(t\pi) + \tau), \quad (3.5)$$

¹Note, however, that $\frac{\partial^2 \mathcal{L}}{\partial I_S(t)^2} = -2c(K_S(t) + \varepsilon)^{-\alpha} < 0$ holds and, consequently, the Lagrangian is at least strictly concave with respect to $I_S(t)$ and the first order condition (3.2) indeed delivers a maximum.

for the mixed case by

$$\dot{K}_S(t) = \frac{\lambda(t)(K_S(t) + \varepsilon)^\alpha - b}{2c} - \delta_S K_S(t), \quad (3.6)$$

$$\dot{\lambda}(t) = \alpha(K_S(t) + \varepsilon)^{-\alpha-1} \left(\frac{b^2 - (K_S(t) + \varepsilon)^{2\alpha} \lambda(t)^2}{4c} \right) - p_F \eta (v \sin^2(t\pi) + \tau) + \lambda(t)(r + \delta_S), \quad (3.7)$$

and for the renewable case by

$$\dot{K}_S(t) = \frac{\lambda(t)(K_S(t) + \varepsilon)^\alpha - b}{2c} - \delta_S K_S(t), \quad (3.8)$$

$$\dot{\lambda}(t) = \alpha(K_S(t) + \varepsilon)^{-\alpha-1} \left(\frac{b^2 - (K_S(t) + \varepsilon)^{2\alpha} \lambda(t)^2}{4c} \right) + \lambda(t)(r + \delta_S). \quad (3.9)$$

3.2.2 Periodic Solution

To find the periodic solutions of this model, we first calculate the instantaneous equilibrium points, $\{K_S^{IEP}(t), \lambda^{IEP}(t)\}$. In contrast to Chapter 2, they cannot be calculated analytically for this approach. We therefore use the numerical results as starting solution for the boundary value problem that has to be solved for the calculation of a periodic solution consisting of one arc. Denoting the canonical system generally as

$$\begin{aligned} \dot{K}_S(t) &= f^{K_S}(t, K_S(t), \lambda(t), \mu_3(t)), \\ \dot{\lambda}(t) &= f^\lambda(t, K_S(t), \lambda(t), \mu_1(t)), \end{aligned}$$

this boundary value problem reads as

$$\begin{aligned} \dot{K}_S(t) &= f^{K_S}(t, K_S(t), \lambda(t), \mu_3(t)), & \text{with } K_S(0) &= K_S(1), \\ \dot{\lambda}(t) &= f^\lambda(t, K_S(t), \lambda(t), \mu_1(t)), & \text{with } \lambda(0) &= \lambda(1). \end{aligned}$$

Note that in contrast to the approach in Chapter 2, $\dot{\lambda}(t)$ here also depends on the state $K_S(t)$.

For the calculation of a periodic solution consisting of several arcs, we use the linear time transformation $T(s)$ of (2.28) and solve for $i = 1, \dots, n+1$, $j = 1, \dots, n$, $s \in [i-1, i]$, and the switching times as well as the boundary points,

$$\tau_0 := 0 < \tau_1 < \tau_2 < \dots < \tau_{n-1} < \tau_n < 1 =: \tau_{n+1},$$

the multi-point boundary problem

$$\begin{aligned} \dot{K}_{S_i}(s) &= (\tau_i - \tau_{i-1}) f_{a_i}^{K_S}(T(s), K_{S_i}(s), \lambda_i(s), \mu_{3_i}(t)), \\ \dot{\lambda}_i(s) &= (\tau_i - \tau_{i-1}) f_{a_i}^{\lambda}(T(s), K_{S_i}(s), \lambda_i(s), \mu_{1_i}(t)), \\ 0 &= (K_{S_j}(\tau_j), \lambda_j(\tau_j)) - (K_{S_{j+1}}(\tau_j), \lambda_{j+1}(\tau_j)), \\ 0 &= (K_{S_{n+1}}(1), \lambda_{n+1}(1)) - (K_{S_1}(0), \lambda_1(0)), \\ 0 &= c(a_j, a_{j+1}), \end{aligned}$$

where a_i defines again the region type, see (2.23). The conditions to guarantee the continuity of the controls with respect to time are given for $j = 1, \dots, n$ as

$$c(a_j, a_{j+1}) = \left\{ \begin{array}{l} (K_{S_j}(\tau_j) + \varepsilon)^\alpha \lambda_j(\tau_j) - b = 0 \\ E_S(K_{S_j}(\tau_j), \tau_j) - E = 0 \end{array} \right\} \text{ if } \{a_j, a_{j+1}\} \in \left\{ \begin{array}{l} \{\{1, 2\}, \{2, 1\}\} \\ \{\{2, 3\}, \{3, 2\}\} \end{array} \right\}.$$

3.2.3 Stability

As in Chapter 2, we calculate the monodromy matrix in order to analyze the dynamic behavior of the obtained periodic solutions. Determining the Jacobian matrix for the fossil case yields

$$J(t) = \begin{pmatrix} -\delta_S & 0 \\ 0 & r + \delta_S \end{pmatrix},$$

which is equal to the one of the model in Chapter 2 and, therefore, also the monodromy matrix is the same, given by

$$M(1) = e^{J(1)} = \begin{pmatrix} e^{-\delta_S} & 0 \\ 0 & e^{r+\delta_S} \end{pmatrix}, \quad (3.10)$$

with the eigenvalues

$$\xi_1 = e^{-\delta_S} < 1, \quad \xi_2 = e^{r+\delta_S} > 1. \quad (3.11)$$

This implies that also in the current model approach, every fossil solution that can be found is of saddle-type. Calculating the Jacobian matrix for the mixed and the renewable case yields

$$J(t) = \begin{pmatrix} -\delta_S + \frac{\alpha(K_S(t)+\varepsilon)^{\alpha-1}\lambda(t)}{2c} & \frac{(K_S(t)+\varepsilon)^\alpha}{2c} \\ -\frac{\alpha(K_S(t)+\varepsilon)^{-\alpha-2}(b^2(1+\alpha)+(\alpha-1)(K_S(t)+\varepsilon)^{2\alpha}\lambda^2)}{4c} & r + \delta_S - \frac{\alpha(K_S(t)+\varepsilon)^{\alpha-1}\lambda(t)}{2c} \end{pmatrix}.$$

Note that the Jacobian matrix and, therefore, also the monodromy matrix are no longer independent of the periodic solution $\Gamma(t)$, as it has been the case in Chapter 2. Consequently, a general statement on the stability of the mixed and renewable periodic solutions is not possible in this approach.

3.2.4 Optimal Paths

The goal in this section is, again, to calculate a trajectory that starts at an initial capital stock K_{S_0} and leads into the considered optimal long-run periodic solution. While in Section 2.2.4 we have used a secant method where the solution has been searched orthogonally to the secant vector, we will here use a more established method called *Moore-Penrose method*. The advantage of this method compared to the previous one is a better tracking of the solution curve, especially if there are strong changes in direction. Assume again that we have N continuation steps and therefore have to solve at each step $n = 1, \dots, N$ the system

$$\begin{aligned} 0 &= K_S^n(0) - K_{S_0}^n, \\ 0 &= F' \left(\begin{pmatrix} K_S^n(1) \\ \lambda^n(1) \end{pmatrix} - \begin{pmatrix} K_S^*(0) \\ \lambda^*(0) \end{pmatrix} \right), \end{aligned} \quad (3.12)$$

as noted in equations (2.41)-(2.42). In Section 2.2.4 we already have mentioned that this system is undetermined as we have 3 unknowns, $(K_S^n(0), \lambda^n(0), K_{S_0}^n)$, but only 2 equations and, therefore, an additional equation is necessary. While this additional condition $g(\cdot) = 0$ has been fixed to calculate the new starting point of the path in Section 2.2.4, the idea of the Moore-Penrose method is to adapt this function at every Newton iteration along a continuation step of the discretized system.

For simplicity, let $A(x)$ denote the undetermined equation system in (3.12), and let $x_i = (K_S^n(t), \lambda^n(t))$ be the point on the curve we are looking for at the i -th step of the continuation process. Hence,

$$A(x_i) = 0$$

holds. Consider now the n -th step of the Newton method used for searching this x_i , which is given by

$$A_x(x_i^n)(x_i^{n+1} - x_i^n) = -A(x_i^n), \quad (3.13)$$

where subscripts here denote the partial derivative. As the inverse $(A_x(x_i^n))^{-1}$ of such an undetermined problem does not exist, the Moore-Penrose pseudo inverse could be used. With the

Moore-Penrose method, however, the calculation of this matrix can be avoided by adding an additional row vector to the matrix $A_x(x_i^n)$. Assume that we have the next predicted point on the curve given by

$$\hat{x}_i = x_{i-1} + hv_i,$$

where h is the step width and v_i is the tangent vector (possibly approximated by the secant vector), as used for the continuation process in Section 2.2.4. If we are looking for the point x_i on the curve and in addition require that this is the nearest to \hat{x}_i , we have to solve the minimization problem

$$\begin{aligned} \min_{x_i} & \|x_i - \hat{x}_i\| \\ \text{s.t.} & A(x_i) = 0, \end{aligned}$$

which is equivalent to the solution of the system

$$\begin{aligned} A(x_i) &= 0 \\ w_i'(x_i - \hat{x}_i) &= 0, \end{aligned}$$

where w_i is the tangent vector at point x_i . The n -th step of the Newton method then is given by solving the extended system

$$\begin{pmatrix} A_x(x_i^n) \\ (w_i^n)' \end{pmatrix} (x_i^{n+1} - x_i^n) = \begin{pmatrix} -A(x_i^n) \\ 0 \end{pmatrix} \quad (3.14)$$

$$\begin{pmatrix} A_x(x_i^n) \\ (w_i^{n-1})' \end{pmatrix} w_i^n = \begin{pmatrix} 0 \\ 1 \end{pmatrix}. \quad (3.15)$$

Equation (3.14) yields a solution of (3.13) under the condition that the vector between two such sequent solution points of the Newton method, $(x_i^{n+1} - x_i^n)$, is orthogonal to the vector w_i^n . Equation (3.15) assures that w_i^n is a tangential vector to x_i^n , and the vector product $\langle w_i^{n-1}, w_i^n \rangle = 1$ guarantees that the direction along the curve is sustained and the vector is normalized. Geometrically, with the Moore-Penrose method a solution of $A(x_i) = 0$ is searched in a hyperplane that is orthogonal to the previous tangent vector, calculated in each iteration step, as one can see in Figure 3.1. Note that also here the enlarged Jacobian matrix can be inverted and hence back-bending is no problem neither. For more details on this method see Allgower and Georg (1997) and Dhooge et al. (2006).

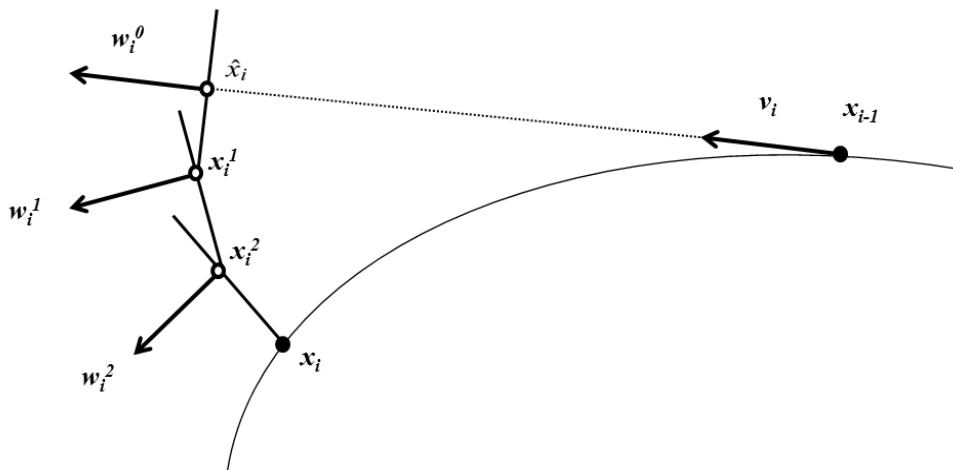


Figure 3.1: One continuation step with Moore-Penrose method (cf. Dhooge et al., 2006).

3.3 Results

We start the following analysis by setting the parameters as in Table 3.1. In contrast to the results of

Interpretation	Parameter	Value	Interpretation	Parameter	Value
Investment costs	b	0.6	Depreciation rate	δ_S	0.03
Adjustment costs	c	0.3	Initial investment costs	ε	1
Energy demand	E	2000	Degree of efficiency	η	0.2
Fossil energy price	p_F	0.051	Maximal radiation increment	v	4.56
Discount rate	r	0.04	Minimal radiation in winter	τ	0.79
LD* coefficient	α	0.25			

*... learning by doing

Table 3.1: Parameter values used for the numerical analysis.

Chapter 2, in this approach we can find even multiple periodic solutions for the current parameter values. One of them corresponds to the fossil case with zero investments $I_S(t)$ and a fossil energy amount $E_F(t) = E$. Two other ones correspond to the mixed case with both controls greater than zero, where one is with high investment and therefore a high capital stock and the second one is with lower investments and a lower capital stock close to the fossil periodic solution.

As we have shown analytically in equations (3.10) and (3.11), the fossil solution is always of saddle-type. To investigate the stability of the other two mixed solutions, we calculate the eigenvalues of the monodromy matrix, which shows that the lower mixed solution is an unstable focus, while the higher one is also of saddle-type. The solutions are shown in Figure 3.2 and, together with the corresponding eigenvalues, are summarized in Table 3.2. The time-control paths as well as the time-state paths for the two periodic solutions being of saddle-type are shown in more detail in Figure 3.3, where Figure 3.3a corresponds to the fossil energy amount $E_F(t)$, Figure 3.3b to the renewable energy investments $I_S(t)$, and Figure 3.3c to the renewable energy capital stock $K_S(t)$. Note that, also here, the capital stock is slightly fluctuating over the year, similar to the results obtained in Chapter 2. In fact, forgetting by not doing already occurs during these fluctuations as maintenance investments are slightly insufficient in the short-term. However, as these fluctuations are really small, this forgetting process is negligibly small as well.

Summing up, we have two periodic solutions of saddle-type whose areas of attraction are probably separated by an indifference threshold point induced by the unstable focus in-between. Indifference threshold points are points in the state space at which the paths leading into two different optimal long-run solutions have the same objective value. Therefore, at these points one is indifferent between these solutions. Indifference threshold points are sometimes also referred to

as DNSS points and originate from Skiba (1978), Sethi (1977, 1979), Dechert (1983) and Dechert and Nishimura (1983). For more details on indifference threshold points see also Grass et al. (2008), Kiseleva and Wagener (2010), and Kiseleva (2011).

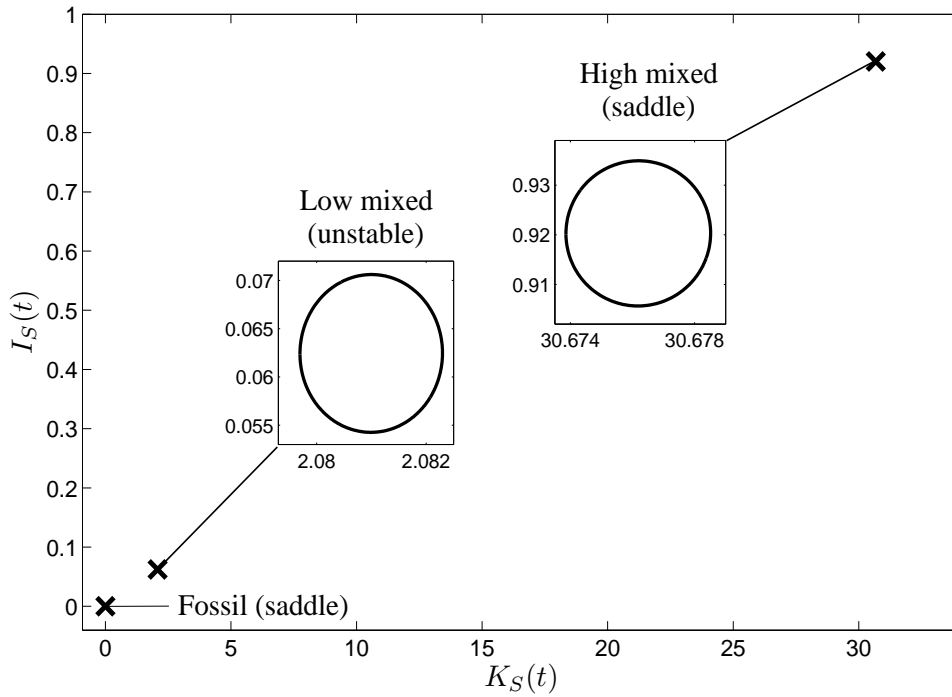


Figure 3.2: The three detected periodic solutions for a fossil energy price $p_F = 0.051$ in the state-control space.

Solution	$K_S^*(0)$	$E_F^*(0)$	$I_S^*(0)$	Eigenvalues	Objective function (in 10^3)
Fossil	0.0000	2000.00	0.0000	{0.9704, 1.0725}	-2.4500
Low mixed	2.0797	1999.67	0.0623	{1.0182+0.0645i, 1.0182-0.0645i}	-2.4491
High mixed	30.6739	1995.15	0.9201	{0.9827, 1.0591}	-2.4351

Table 3.2: Multiple periodic solutions for $p_F = 0.051$.

3.3.1 Calculation of the Indifference Threshold Point

Whether such an indifference threshold point exists or one of the two periodic solutions of saddle-type is dominant, therefore has to be analyzed. While this can rather easily be done for autonomous optimal control models, the approach for non-autonomous control models is a little bit different.

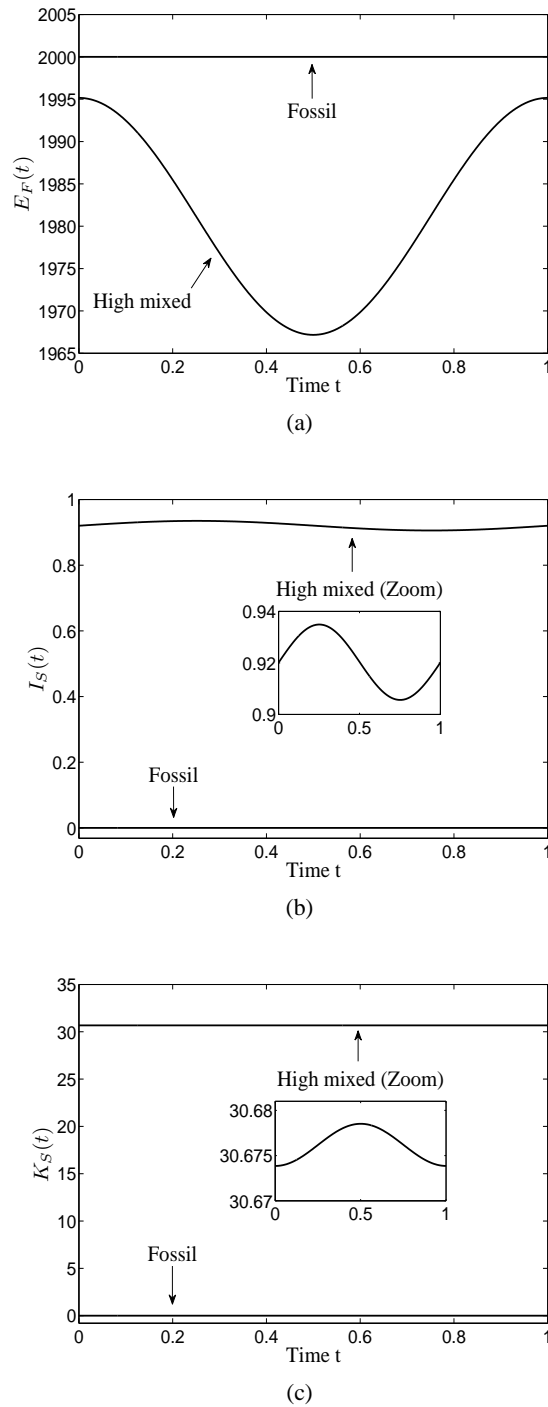


Figure 3.3: Time-control paths for the two detected periodic solutions of saddle-type for a fossil energy price $p_F = 0.051$ in (a) fossil energy $E_F(t)$, and (b) renewable energy investments $I_S(t)$, as well as the time-state paths in (c) renewable energy capital $K_S(t)$.

Let

$$H(x(t), u(t), \lambda(t)) = F(x(t), u(t)) + \lambda(t)f(x(t), u(t))$$

generally define the current value Hamiltonian of an autonomous optimal control model with infinite horizon where $x(t)$ are the states, $u(t)$ are the controls, $\lambda(t)$ are the costates, $F(\cdot, \cdot)$ is the instantaneous objective function and $f(\cdot, \cdot)$ describes the dynamics. Assume that all the necessary regularity conditions for applying the maximum principle are satisfied, which are the continuity of the objective function and the dynamics with respect to the controls and to time and their continuous differentiability with respect to the states. Let further Ω define the feasible domain, and let

$$H^0(x(t), \lambda(t)) = \max_{u \in \Omega} H(x(t), u(t), \lambda(t))$$

denote the maximized Hamiltonian. Then, for each trajectory for which there exists a continuous $\lambda(t)$ so that

$$\dot{\lambda}(t) = r\lambda - \frac{\partial H}{\partial x} \quad \text{and} \quad H(x^*(t), u^*(t), \lambda(t)) = \max_{u \in \Omega} H(x^*(t), u(t), \lambda(t))$$

are satisfied along with the condition

$$\lim_{t \rightarrow \infty} e^{-rt} H^0(x(t), \lambda(t)) = 0,$$

the value of the objective function is given by

$$\int_0^{\infty} e^{-rt} F(x(t), u(t)) dt = \frac{1}{r} H^0(x(0), \lambda(0)). \quad (3.16)$$

For more details on this see Feichtinger and Hartl (1986). The proof, which is also given there, is built up on the aspect that $\frac{dH}{dt} = \frac{\partial H}{\partial t} + r\lambda f = r\lambda f$ as the partial derivative of the Hamiltonian with respect to time t is zero for autonomous problems, and that along each trajectory that satisfies the optimality conditions, the values of H and H^0 coincide.

For a non-autonomous problem, however, the relation in (3.16) does not hold as the partial derivative of the Hamiltonian with respect to time is non-zero. Consequently, no such relation can be found, and in order to get the objective values for a given trajectory, we have to calculate it along the whole path. To do so, we therefore introduce an additional differential equation to the canonical system, which is given by

$$\dot{c}(t) = e^{-rt} \left(-I_S(t) \left(b + cI_S(t) \right) \left(K_S(t) + \varepsilon \right)^{-\alpha} - p_F E_F(t) \right), \quad \text{with } c(0) = 0, \quad (3.17)$$

and include it into the boundary value problem for the continuation process. The last value, $c(T_p)$, where T_p is the truncation time of the path, yields the objective value. However, as this only is the objective value for the time interval $[0, T_p]$, we further on have to add the weighted remaining tail of the periodic solution for $[T_p, \infty)$. If $F_p(t)$ is the objective value evaluated along the path at each point of time t , $c(t)$ is the accumulated objective value along the path given by the solution of the differential equation in (3.17) on $[0, t]$, and $F_{per}(t)$ is the objective value along the periodic solution at each point of time t , the total objective value OV is given by

$$\begin{aligned}
OV &= \int_0^{T_p} e^{-rt} F_p(t) dt + \int_{T_p}^{\infty} e^{-rt} F_{per}(t) dt = \\
&= c(T_p) + \sum_{i=0}^{\infty} \int_{T_p+i}^{T_p+i+1} e^{-rt} F_{per}(t) dt = \\
&= c(T_p) + \sum_{i=0}^{\infty} e^{-r(T_p+i)} \underbrace{\int_0^1 e^{-rt} F_{per}(t) dt}_{=:c_{per}} = \\
&= c(T_p) + e^{-rT_p} \sum_{i=0}^{\infty} e^{-ri} c_{per} = \\
&= c(T_p) + \frac{e^{-rT_p}}{1 - e^{-r}} c_{per}. \tag{3.18}
\end{aligned}$$

Hence, we have to add the second term in (3.18) to the so far calculated objective values of the paths. While for autonomous problems it would be sufficient to evaluate (3.16) along the paths of the last continuation step and compare these objective function values in order to see whether an indifference threshold point occurs or one periodic solution is dominant, the comparison of the objective function values for non-autonomous problems is not time invariant. Therefore, the objective values at the truncation time of the paths at each continuation step for the current initial state value have to be considered.

If both periodic solutions are not dominant, an indifference threshold point has to exist in-between separating the areas of attraction. To investigate this, we continue the trajectories of both periodic solutions to each other as far as possible until one of the subsequent 3 cases occurs:

1. The continuation process aborts as the path reaches another boundary of the feasible domain;
2. the path is bending back;
3. the other periodic solution is reached.

The results of these continuations can be seen in Figure 3.4a. The path starting at the high mixed periodic solution is bending back while the one starting at the fossil periodic solution gets infeasible at some point. Here, the path can be continued into the mixed case. However, this further continuation is not necessary in the current case as there occurs already a sufficiently large overlap in the state K_S for the "pure paths" (i.e. paths lying completely within the same boundary of the feasible domain as the periodic solution to which they lead). The next step to find the indifference threshold point is to compare the objective function values along the two paths. For the two periodic solutions of our model approach these final objective value curves are shown in Figure 3.4b. The intersection yields the indifference threshold point, which for the current parameter set lies at $K_S^{ITP} = 1.6477$.

3.3.2 Economic Interpretation of the Indifference Threshold Point

The occurrence of an indifference threshold point is an important result of this analysis and is a consequence of the model extension with learning by doing. While in the first model considered in Chapter 2 the optimal long-run periodic solution only depends on the current fossil energy price, it here also depends on the initial capital stock at which the optimization process is started.

Figure 3.5 shows how the indifference threshold point separates the areas of attraction of the mixed and the fossil periodic solution. If the initial capital stock lies exactly on the indifference threshold point K_S^{ITP} , the paths to both periodic solutions are equally expensive. Consequently, the decision maker is indifferent between increasing investments $I_S(t)$ and moving towards the mixed periodic solution with a higher capital stock and a lower fossil energy amount during the summer period on the one hand, and stopping investments and moving towards the fossil periodic solution on the other hand. If the initial capital stock is higher than the indifference threshold point K_S^{ITP} , it is optimal to move up towards the mixed periodic solution and, if it is lower, the fossil periodic solution is optimal. The reason for this change lies within the learning-by-doing effect. If the initial capital stock is high enough, the reduction of the investment costs due to the learning-by-doing effect can compensate for the cost of additional capital accumulation, and therefore it is optimal to increase the capital stock which even reinforces this effect, although at a decreasing rate. If, however, the initial capital stock is low, the learning-by-doing effect on the investment costs is too weak to sufficiently reduce the high costs. Therefore, it is profitable to reduce investments and hence the capital stock while increasing the share of fossil energy until, finally, the fossil optimal periodic solution is reached and the whole demand is covered by fossil energy in the long run. Note that along this path forgetting by not doing occurs. As no further investments

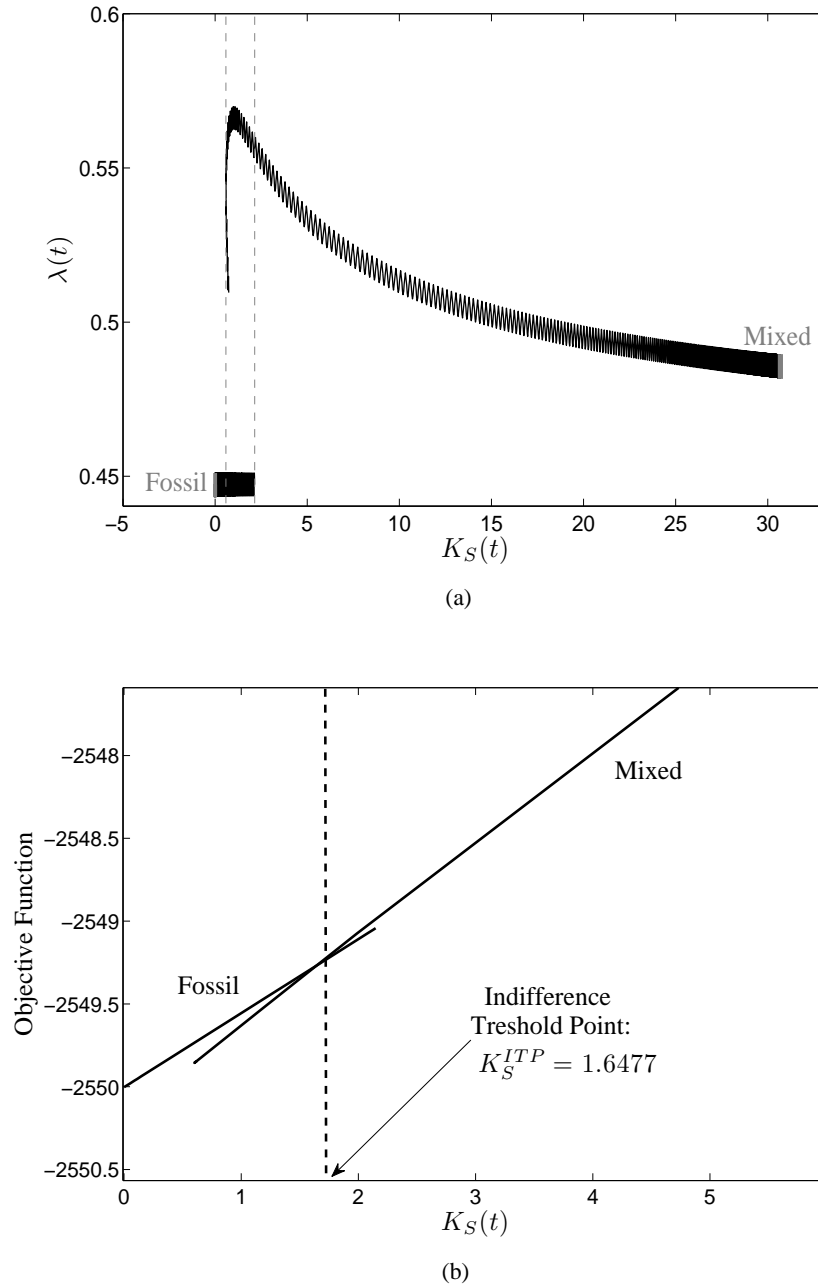


Figure 3.4: Search for the indifference threshold point for a fossil energy price $p_F = 0.051$: **(a)** Overlap of trajectories leading into the two periodic solutions. **(b)** Indifference threshold point: Intersection of the objective function values.

are made, the accumulation of new capital but also the maintenance of existing capital stops and, hence, the capital stock decreases. Simultaneously, due to forgetting by not doing investment costs increase again until, finally, at the fossil solution they are as high as for a complete start-up with renewable energy. The occurring separation of the areas of attraction dependent on the initial state is also known as history dependence, as the optimal long-run periodic solution is determined by the accumulation effort of renewable energy capital in the past.

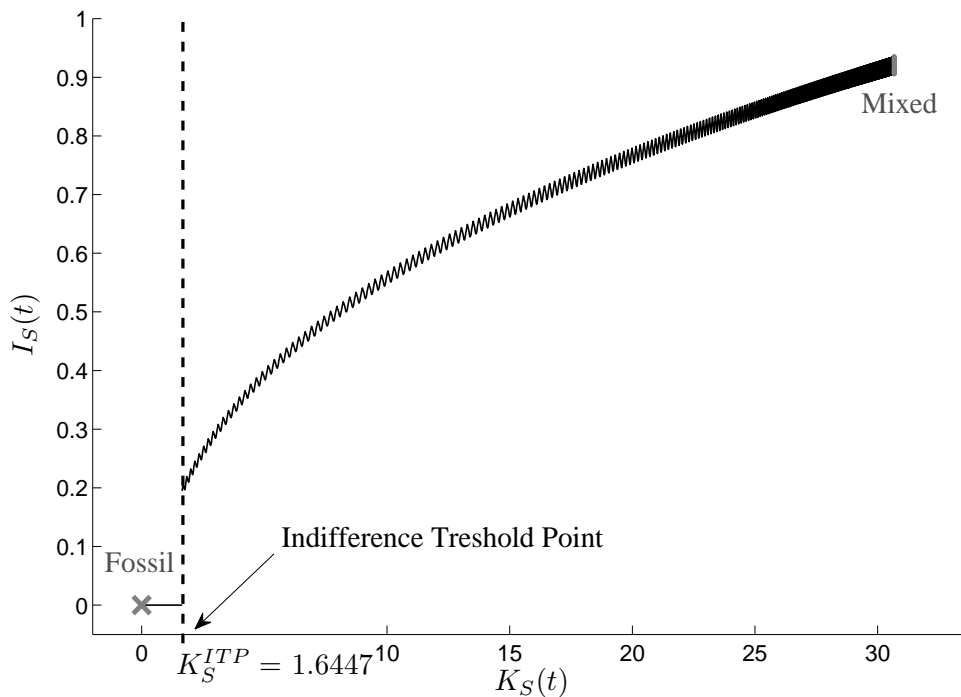


Figure 3.5: Indifference threshold point and the separated areas of attraction of the two periodic solutions for a fossil energy price $p_F = 0.051$.

This result points out the difficulty of introducing a new energy technology into the market. While conventional energy types are already competitive and have low prices due to the high experience accumulated over years, the investment costs for new technologies are very high. As no experience exists at the beginning, these high investment cost would have to be paid over some period of time during which the new technology definitely is not profitable, until finally at least some reduction due to accumulated experience is achieved. This aspect underlines the importance of subsidies and other kind of financial support that is necessary during the start-up period to help new technologies getting over this barrier. In our model approach, where no such subsidies

are included, it therefore would never be optimal to start with the renewable energy technology from the very beginning. If no experience exists to reduce the initially high investment costs, fossil energy is always less cost intensive and, as no further restrictions are included such as CO₂ performance standards, no switch to a cleaner energy technology would happen. Only, if there is already a sufficiently high level of experience when optimization is started, further investments are profitable.

3.3.3 Break-Even Analysis

Figure 1.1 has shown how the investment costs of a new technology decrease due to the effect of learning by doing. As accumulated experience improves the necessary processes and hence reduces the financial effort, the technology gets more profitable. However, it can take a long time until full competitiveness with the conventional technology is achieved, which happens at the so-called break-even point.

To analyze the extent of the learning-by-doing effect on the investment costs in our model approach, we compare the costs of renewable energy generation with the fossil energy price p_F by calculating the investment costs per unit of generated renewable energy (in the following referred to as unit investment costs) at time t along the path leading into the optimal long-run periodic solution, given by the term

$$\frac{(bI_S^*(t) + cI_S^*(t)^2) (K_S^*(t) + \varepsilon)^{-\alpha}}{(\nu \sin^2(t\pi) + \tau) K_S^*(t) \eta}. \quad (3.19)$$

$K_S^*(t)$ and $I_S^*(t)$ are the state and the corresponding investments along the optimal path leading into the optimal long-run periodic solution. The results can be seen in Figure 3.6. As the generation of renewable energy occurs in the denominator of Equation (3.19) and fluctuates in time along with the available global radiation, the unit investment costs also vary over the period. However, a clearly decreasing tendency can be observed as soon as capital is accumulated. The black horizontal line in Figure 3.6 shows the fossil energy price p_F . At the beginning of the path, the unit investment costs are very high. Especially in winter they are almost the eight-fold of the fossil energy price p_F . The reasons for this are the initially high investment costs of the renewable energy technology together with the low initial capital stock and hence the low amount of generated renewable energy. In summer, however, one can see that the unit investment costs are lower as global radiation is high and therefore more renewable energy is generated. Very early along the path even the fossil energy price level is reached during summer. As the path proceeds, investments accumulate new capital and therefore the learning-by-doing effect as well as the generated renewable energy increase. This leads to declining unit investment costs both in winter and summer and also

the margin between them decreases until finally the optimal long-run periodic solution is reached. Here, the unit investment costs in summer are already far below the fossil energy price level while in winter they are still above it. However, over the whole year the benefit of the portfolio mixture is high enough to let the combination of fossil and renewable energy be optimal.

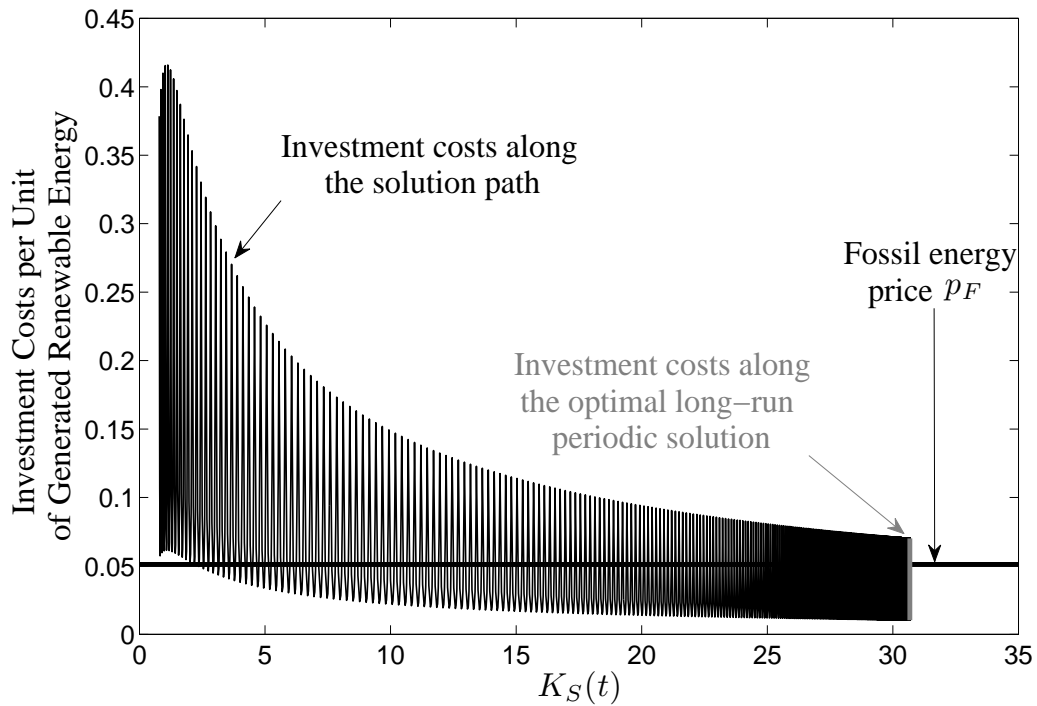


Figure 3.6: Investment costs per unit of generated renewable energy along the path leading into the mixed optimal long-run periodic solution for a fossil energy price $p_F = 0.051$.

3.4 Sensitivity Analysis

The analysis of the previous section has shown that the learning-by-doing effect can imply history dependence of the optimal long-run periodic solution. The driving force for this dependence is given by the cost-effectiveness of renewable energy generation with respect to conventional energy technologies. However, there are several factors beyond historical capital accumulation activities that influence this cost-effectiveness. First of all, of course, the fossil energy price p_F plays a major role, reflecting the economic performance of the fossil technology. Further on, it is essential how strong the cost decreasing influence of the learning-by-doing effect is on the investment costs of renewable energy. Besides that, also the performance of the renewable energy generation is important which is determined for example by site-specific factors such as the supply of global radiation. To analyze how the obtained results of the previous section change when these factors vary, we conduct in this section a sensitivity analysis with respect to the fossil energy price p_F , the learning-by-doing coefficient α , and different sets of the parameters τ and ν that determine the site-specific global radiation intensity.

3.4.1 Fossil Energy Price p_F

In the first step, we focus on the influence of the fossil energy price on the optimal portfolio composition. Similar to the analysis in Section 2.4 we will use numerical continuation with respect to the fossil energy price p_F to investigate how the results change when fossil energy gets more expensive. We start with considering the calculation of the indifference threshold point for a fossil energy price $p_F < 0.051$, as at this price some interesting aspects occur.

Calculation of the Indifference Threshold Point for $p_F < 0.051$

For $p_F = 0.05$, Figure 3.7a shows the longest possible continuation of the paths leading into the fossil and the mixed periodic solutions, respectively, both lying completely on the corresponding boundary of the feasible domain. Also here, an overlap can be found. However, considering the objective function values within this interval as shown in Figure 3.7b, one can see that here no intersection occurs. Consequently, the pure fossil path has to be continued further along the mixed feasible boundary to obtain the indifference threshold point.

As the continuation process has been aborted because the path gets infeasible, a solution path consisting of several arcs has to be calculated. Assume again that N continuation steps are necessary in order to get a path starting at the initial capital stock K_{S_0} and leading into the periodic

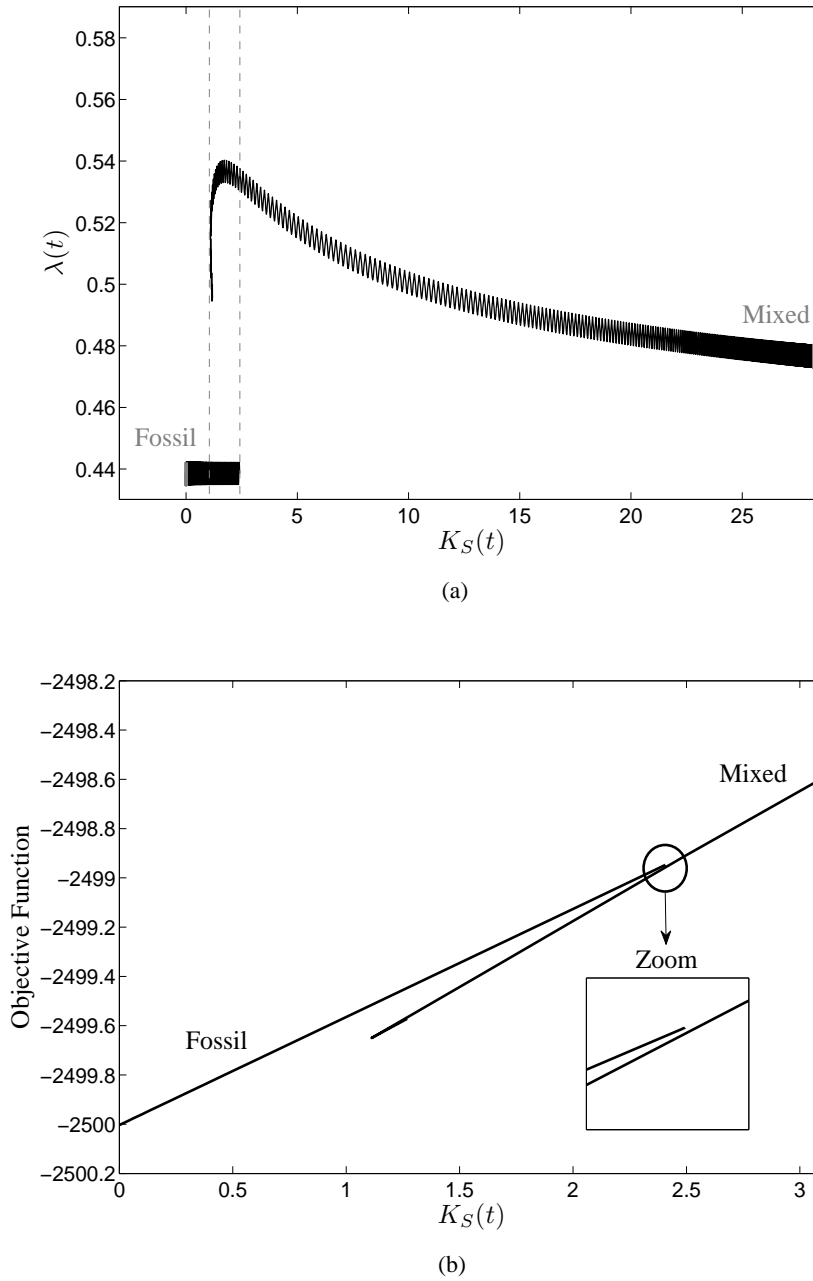


Figure 3.7: Search for the indifference threshold point for a fossil energy price $p_F = 0.05$:
(a) Overlap of trajectories leading into the two periodic solutions. **(b)** Indifference threshold point:
 No intersection of the objective function values occurs so far.

solution. Then, at each step $n = 1, \dots, N$, the number of necessary arcs are defined by the number of violations of the feasible boundary conditions along the path. Let I_n denote the number of necessary arcs for the n -th continuation step and let

$$\tau_0^n := 0 < \tau_1^n < \tau_2^n < \dots < \tau_{I_n-1}^n < 1 =: \tau_{I_n}^n$$

be again the switching times. Similar to Section 2.2.2 where we have searched for a long-term optimal periodic solution consisting of several arcs, also here the multi-arc solution is defined by a boundary value problem that guarantees the continuity of the solution with respect to time at each switch. While we required in Section 2.2.2 that the starting and the end point coincide in order to get a solution that is periodic, we here have to assure that the starting point and the end point are equal to the current initial capital stock $K_{S_0}^n$ and the starting point of the periodic solution, respectively. We use again the following index,

$$a_i = \begin{cases} 1, & \text{for the fossil region,} \\ 2, & \text{for the mixed region,} \\ 3, & \text{for the renewable region,} \end{cases}$$

in order to distinguish between the three different boundary cases of the feasible domain. Also here only switches between neighboring regions are feasible. As for this continuation we first have to transform the interval $[0, T_p]$ to $[0, 1]$ with T_p being the truncation time of the path, and then to $[i-1, i]$ for each arc $i = 1, \dots, I_n$, we combine the time transformations of (2.28) and (2.40) to

$$T(s) = T_p((\tau_i - \tau_{i-1})(s - i) + \tau_i). \quad (3.20)$$

Then, at each continuation step $n = 1, \dots, N$, a path is searched that consists of I_n arcs and that solves for $i = 1, \dots, I_n$ and for $j = 1, \dots, I_n - 1$ the boundary value problem

$$\dot{K}_{S_i}(s) = T_p(\tau_i - \tau_{i-1})f_{a_i}^{K_S}(T(s), K_{S_i}(s), \lambda_i(s), \mu_{3_i}(t)), \quad (3.21)$$

$$\dot{\lambda}_i(s) = T_p(\tau_i - \tau_{i-1})f_{a_i}^{\lambda}(T(s), K_{S_i}(s), \lambda_i(s), \mu_{1_i}(t)), \quad (3.22)$$

$$0 = K_{S_j}^n(\tau_j) - K_{S_{j+1}}^n(\tau_j), \quad (3.23)$$

$$0 = \lambda_j^n(\tau_j) - \lambda_{j+1}^n(\tau_j), \quad (3.24)$$

$$0 = c(a_j, a_{j+1}), \quad (3.25)$$

$$0 = K_{S_1}^n(0) - K_{S_0}^n, \quad (3.26)$$

$$0 = F' \left(\begin{pmatrix} K_{S_{I_n}}^n(1) \\ \lambda_{I_n}^n(1) \end{pmatrix} - \begin{pmatrix} K_S^*(0) \\ \lambda^*(0) \end{pmatrix} \right), \quad (3.27)$$

where $\{\dot{K}_{S_i}(s), \dot{\lambda}_i(s)\}$ are the corresponding dynamics of the canonical system for the arc i and (3.25) guarantees again the continuity of the controls with respect to time,

$$c(a_j, a_{j+1}) = \left\{ \begin{array}{l} (K_{S_j}(\tau_j) + \varepsilon)^\alpha \lambda_j(\tau_j) - b = 0 \\ E_S(K_{S_j}(\tau_j), \tau_j) - E = 0 \end{array} \right\} \text{ if } \{a_j, a_{j+1}\} \in \left\{ \begin{array}{l} \{\{1, 2\}, \{2, 1\}\} \\ \{\{2, 3\}, \{3, 2\}\} \end{array} \right\}.$$

Figure 3.8a shows the obtained path for $p_F = 0.05$ that consists of three arcs, so here $I_N = 3$. The gray line shows the pure fossil path lying completely at the fossil feasible boundary, where no investments for renewable energy capital are made and the whole energy demand is covered by fossil energy in the long run. At $K_S(t) = 2.432$, however, the corresponding Lagrange multiplier μ_3 gets negative and hence the fossil path is no longer feasible. Here, the switch happens to the mixed arc with positive investments in renewable energy and the demand covered by a mixed portfolio of the two available energy types. This arc can be seen as black line in Figure 3.7a. However, very soon at $K_S(t) = 2.455$, the investments $I_S(t)$ gets zero again and a switch back to the fossil feasible boundary is necessary. Calculating the objective function values for this extended continuation of the fossil path finally leads to an intersection with the objective function value of the mixed-path and hence to an indifference threshold point $K_S^{ITP} = 2.4601$, as one can see in Figure 3.8b.

The resulting phase portrait can be seen in Figure 3.9, where the indifference threshold point separates the areas of attraction of the two periodic solutions. Comparing this result with the phase portrait in Figure 3.5, one can see that a slight reduction in the fossil energy price p_F has induced a shift of the indifference threshold point to the right. Consequently, the historical capital accumulation effort has to be higher in order to make further investments into renewable energy capital worthwhile. Otherwise, the cost reducing impact of the learning-by-doing effect is too weak to make renewable energy profitable in the portfolio and, hence, the whole energy demand is covered by fossil energy in the long run.

While we had only one long-term optimal periodic solution in Section 2.4 and therefore calculated the solutions for different fossil energy prices separately in order to analyze the impact of a changing fossil energy price p_F on the optimal portfolio composition, we here will use numerical continuation to get all initial points of the periodic solutions as a curve in p_F .

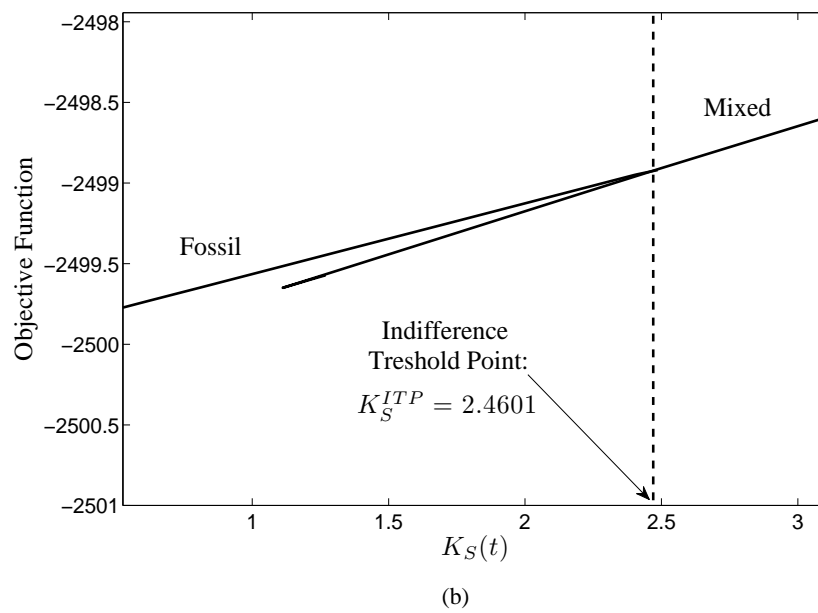
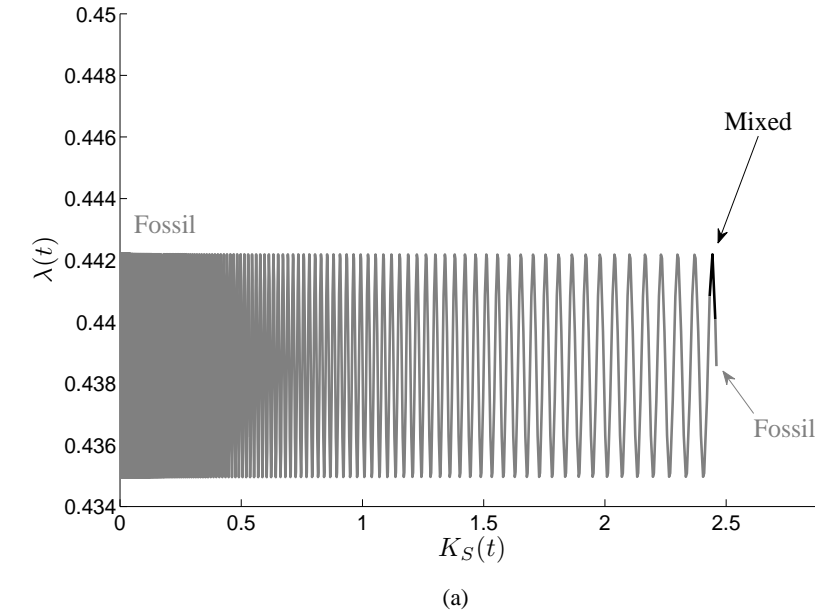


Figure 3.8: Search for the indifference threshold point for a fossil energy price $p_F = 0.05$: **(a)** Path consisting of three arcs (fossil (gray line), mixed (black line), and again fossil) leading into the fossil periodic solution. **(b)** Indifference threshold point: intersection of the objective values.

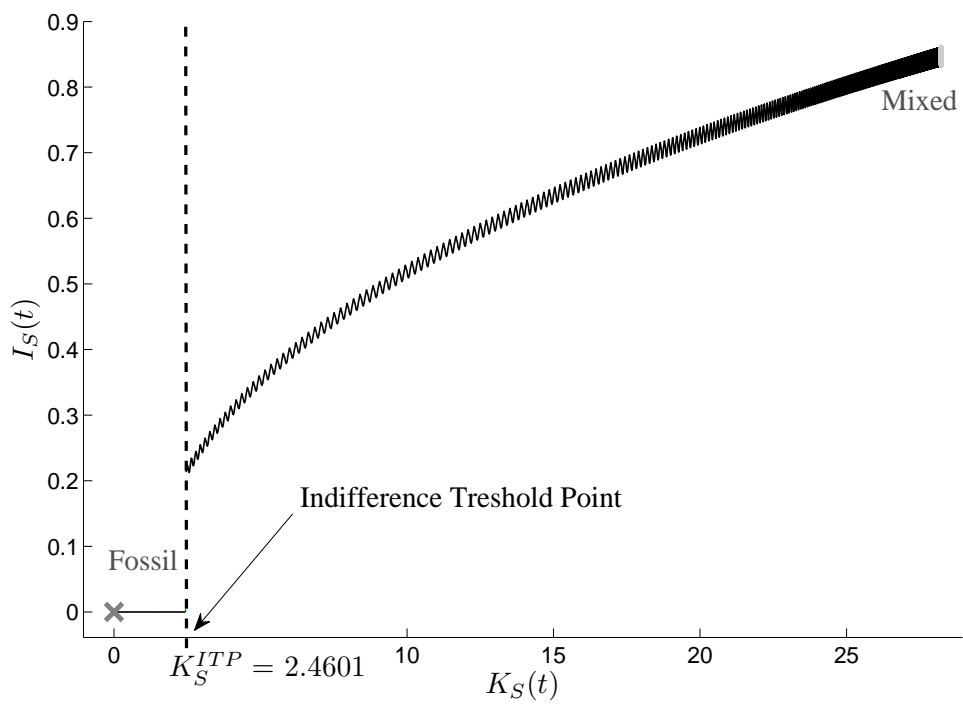


Figure 3.9: Indifference threshold point and the separated areas of attraction of the two periodic solutions for a fossil energy price $p_F = 0.05$.

The goal is to find, for each fossil energy price p_F , periodic solutions $\Gamma(t) = (K_S^*(t), \lambda^*(t))$ with period length 1, for which it holds that

$$\begin{aligned} K_S^*(0) &= K_S^*(1), \\ \lambda^*(0) &= \lambda^*(1). \end{aligned}$$

Hence, for each parameter p_F the boundary value problem

$$\begin{aligned} \dot{K}_S(t) &= f^{K_S}(t, K_S(t), \lambda(t), \mu_3(t)), \\ \dot{\lambda}(t) &= f^\lambda(t, K_S(t), \lambda(t), \mu_1(t)), \\ K_S^*(0) - K_S^*(1) &= 0, \\ \lambda^*(0) - \lambda^*(1) &= 0, \end{aligned}$$

would have to be solved. Instead, however, we transform this boundary value problem into a finite-dimensional equation system.

We consider for this a sufficiently differentiable perturbation of the 1-periodic differential canonical system, in the following again generally denoted as $\dot{x} = f(t, x)$, which is given by

$$\dot{x} = F(p, t, x), \tag{3.28}$$

where $p \in \mathbb{R}$ is some parameter and F is defined as

$$F : \mathbb{R} \times \mathbb{R} \times \mathbb{R}^n : (p, t, x) \mapsto F(p, t, x),$$

with

$$F(0, t, x) = f(t, x) \quad \text{and} \quad F(p, t+1, x) = F(p, t, x).$$

Let $P(p, x)$ denote the Poincaré map of the perturbed system in (3.28), then regardless of the specific form of (3.28) the Poincaré map is a monotone map. Hence, to study local bifurcations of a solution $\phi(t, 0, x_0)$ of a 1-periodic system $\dot{x} = f(t, x)$, a fixed point of the Poincaré map $P(p, x)$ in the neighborhood of x_0 for sufficiently small values of the parameter p has to be found (Hale and Koçak, 1991). To do so, we use a single shooting method. Let $\phi_p(t, 0, x_0)$ be the solution of (3.28) at time t with the initial point x_0 . Such a solution should be numerically computable by

using some ordinary differential equation (ODE)-solver. Then, the equation system

$$\phi_p(1, 0, x_0) - x_0 = 0$$

has to be solved which can be done by a Newton-like method. If the periodic solution has no eigenvalue equal to 1 and the hyperplane with the starting values is a transversal cross-section to the periodic solution, the Newton iterations converge to the periodic solution for any sufficiently close approximation. In other words, this method is searching for a point on this hyperplane Σ that is a fixed point of the corresponding Poincaré map, as shown in Figure 3.10 where L_0 and L_p denote the periodic orbits, respectively. For further details on this method see Kuznetsov (1998).

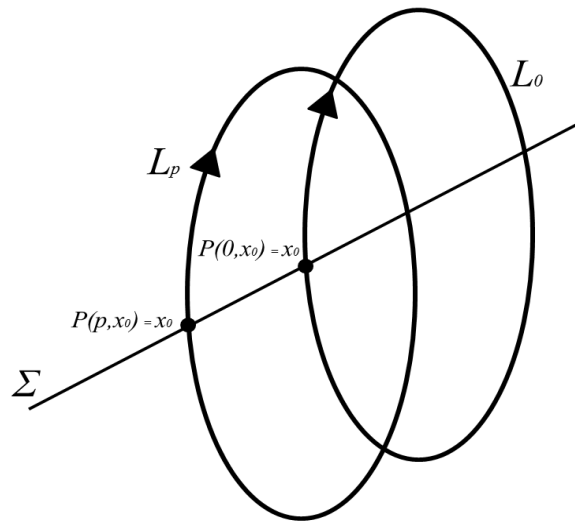


Figure 3.10: Shooting method to locate periodic solutions.

Bifurcation Analysis

We now continue the obtained periodic solutions along the p_F -axis and investigate how they change. Note that we always consider in the following the bifurcation of the canonical system, not of the optimal system. Therefore, also the changes in the unstable as well as the dominated periodic solutions are shown. The results can be seen in Figure 3.11, where the starting points $K_S(0)$ of the periodic solutions are plotted as gray line for the fossil solution and as black line for the mixed solutions. If the fossil energy price is very low, the optimal long-run periodic solution is given by the fossil periodic solution as the investment costs into renewable energy capital are

so high that they are not profitable and hence no investments at all are made and the whole energy demand is covered only with fossil energy in the long run.

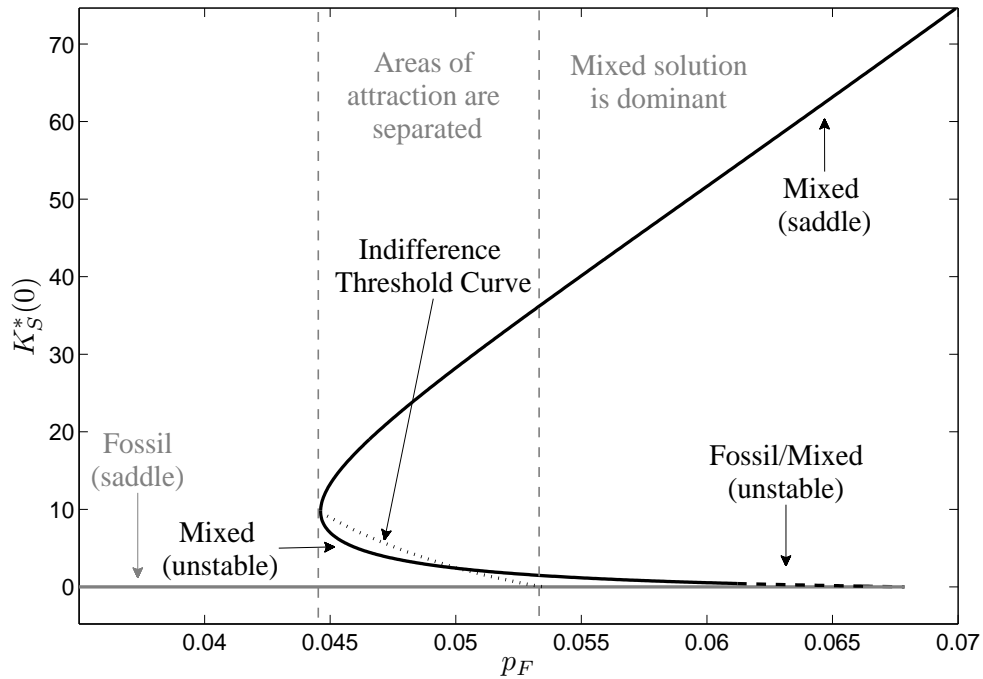


Figure 3.11: Bifurcation diagram of the canonical system with respect to the fossil energy price $p_F \leq 0.07$.

Starting at a fossil energy price $p_F = 0.0446$, there exist also the two mixed periodic solutions, where the lower one is unstable and the upper one is of saddle-type. The areas of attraction of the fossil and the upper mixed periodic solutions are separated by indifference threshold points summarized in the indifference threshold curve plotted as black dotted line. At the beginning, it lies above the unstable mixed long-run solution. As fossil energy in this area still is comparatively cheap, the historical efforts of renewable energy capital accumulation have to be comparably high in order to make further investments in renewable energy capital profitable. If the fossil energy price further increases, the indifference threshold curve declines due to the fact that renewable energy capital investments are profitable already at a lower historical capital accumulation effort. For a fossil energy price $0.0466 \leq p_F \leq 0.0501$, the fossil path has to be continued to a multiple arc solution path similar to the one in Figure 3.8a in order to obtain the indifference threshold point.

At $p_F = 0.0501$, the indifference threshold curve intersects with the unstable mixed periodic solution. From then on, the areas of attraction are separated below this periodic solution, and the continuation of the fossil path to a multiple arc solution path is not necessary any more to yield the indifference threshold point. If the fossil energy price further increases, the indifference threshold curve declines further as investments in renewable energy capital get profitable at a lower initial capital stock until finally, at $p_F = 0.0535$, it coincides with the fossil periodic solution.

For a fossil energy price $0.0535 \leq p_F \leq 0.0679$, still all three periodic solutions exist, but the high mixed one dominates the fossil one, as here fossil energy alone would be too expensive to cover the demand. Concerning the unstable mixed solution in-between the two periodic solutions of saddle-type, it is mixed at the beginning but turns into a multi-arc solution with two mixed arcs and one fossil arc in-between at $p_F = 0.0612$, as investments decline with the fossil energy price until they finally get zero.

As one can see in Figure 3.11, the fossil solution only exists to some specific fossil energy price. The reason for this is that the Lagrange multiplier $\mu_3(t)$ becomes negative. This can easily be shown by considering the analytical solution of the fossil canonical system in (3.4)-(3.5). Together with the transversality condition which we already have defined in (2.8), the fossil solution for $\lambda(t)$ is given by

$$\lambda(t) = \frac{p_F \eta ((4\pi^2 + (r + \delta_S)^2)(v + 2\tau) + (r + \delta_S)v(2\pi \sin(2\pi t) - (r + \delta_S) \cos(2\pi t)))}{2(r + \delta_S)(4\pi^2 + (r + \delta_S)^2)}. \quad (3.29)$$

With the Lagrange multiplier,

$$\mu_3(t) = b(K_S(t) - \varepsilon)^{-\alpha} - \lambda(t), \quad (3.30)$$

the fossil energy price at which (3.30) is zero and therefore the pure fossil periodic solution is not further existent, is given by

$$\bar{p}_F(K_S(t), t) = \frac{2b(r + \delta_S)(4\pi^2 + (r + \delta_S)^2)(K_S(t) + \varepsilon)^{-\alpha}}{\eta ((4\pi^2 + (r + \delta_S)^2)(v + 2\tau) + (r + \delta_S)v(2\pi \sin(2\pi t) - (r + \delta_S) \cos(2\pi t)))}.$$

This price is a function of the state $K_S(t)$ and time t . When the fossil energy price p_F increases, the first violation of $\mu_3(t) \geq 0$ occurs at a peak of the periodic fluctuations in $\lambda(t)$. This is because the derivative of (3.30) with respect to $\lambda(t)$ is negative. Calculating the time t_{max} at which this occurs for the first time and inserting this together with $K_S(t_{max}) = 0$ into $\bar{p}_F(\cdot, \cdot)$ yields for the current parameter set the maximal fossil energy price $\bar{p}_{F_{max}} = 0.0678$ until which the pure fossil periodic

solution exists. For higher values of p_F a pure fossil solution is not further feasible. However, a fossil-mixed solution still can be feasible if the part along which the Lagrange multiplier would be negative is replaced by a mixed arc. If the fossil energy price p_F is further increased, however, the interval in which a fossil arc is not feasible any more increases as well and, as soon as the Lagrange multiplier is negative already at the minimum of the periodic fluctuations in $\lambda(t)$, also no feasible fossil-mixed solution can be found any more. For the current parameter set this occurs at $\bar{p}_{F_{min}} = 0.069$. For a fossil energy price $p_F > \bar{p}_{F_{min}}$, the optimal long-run periodic solution is given by the high mixed periodic solution.

Figure 3.12 shows what happens if the fossil energy price p_F increases even above 0.07. As renewable energy generation progressively gets profitable due to the reduced investment costs by the accumulated experience as well as compared to the more expensive fossil energy, a strong increase in renewable energy capital can be observed. However, still both energy types are needed over the whole period in order to cover the given energy demand.

At $p_F = 0.5613$, renewable energy capital is so high that during summer, when global radiation reaches its maximum, the demand even can be covered without fossil energy. At this point, the feasible boundary of the mixed case is reached and from this fossil energy price on, a periodic solution exists that consists of two mixed arcs and a renewable arc in-between. Along this mixed/renewable solution, the demand over some time interval in summer is covered only by renewable energy, while in winter fossil energy still is needed in addition, as already shown in in the results of Chapter 2. If the fossil energy price raises even further, there is still an increase in the stock of renewable energy capital, however, obviously at a decreasing rate. The reason for this is that the marginal benefit of an additional unit of renewable energy capital declines. Remember the results in Chapter 2 which have shown that along the renewable arc also surpluses are generated that are not used. Therefore, a further increase of the capital stock only is profitable along the mixed arcs, where there is still potential to decrease the necessary amount of fossil energy by slightly raising renewable energy generation. But as global radiation at the switching times separating the arcs gets lower, the closer they are to 0 and 1, more and more renewable energy capital would be necessary to induce this effect. In contrast to the model approach in Chapter 2, here the investment costs of renewable energy capital also decline with a growing capital stock due to learning by doing, which reduces at least the financial effort for this compensation, but, nevertheless, this saturation effect is still obvious.

Figure 3.11 further on shows that a turning point occurs at $p_F = 0.044$ in the mixed solution. To investigate how the optimal vector field changes here, we consider the local behavior of the monodromy matrix in what follows.

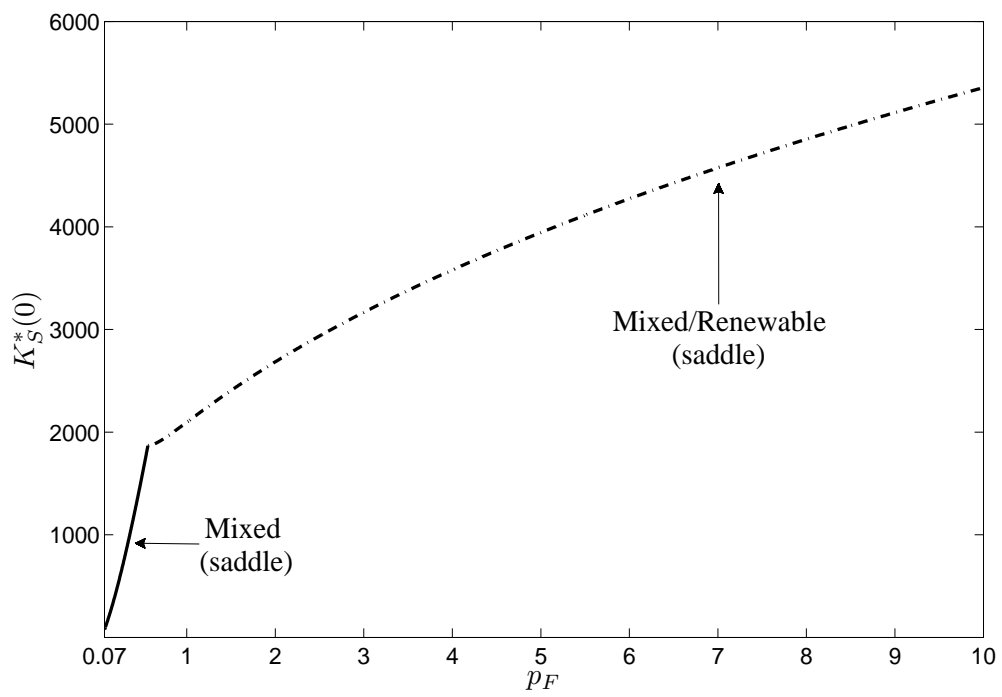


Figure 3.12: Sensitivity analysis of the canonical system with respect to a fossil energy price $p_F \geq 0.07$.

As we have already mentioned, the stability of a long-term periodic solution is equivalent to the stability of the fixed point of the corresponding Poincaré map, and a periodic solution is stable if all eigenvalues (Floquet multipliers) ξ_1, \dots, ξ_n of the Jacobian of the locally defined map $P: \mathbb{R}^n \rightarrow \mathbb{R}^n$ evaluated at the fixed point are located within the unit circle, $|\xi| < 1$. Hence, a local bifurcation occurs when an eigenvalue crosses the unit circle (see for this Reithmeier, 1991).

Figure 3.13 shows the norm of the eigenvalues of each periodic solution along the p_F -axis. As we already have shown in Section 3.2.3, the monodromy matrix and hence the eigenvalues of any fossil solution in this model approach are independent of the periodic solution itself, as no state nor costate occurs in the Jacobian matrix for this case. Hence, the eigenvalues of the fossil periodic solution in Figure 3.13 shown in dark gray are constant for varying values of the fossil energy price p_F and are given by $\xi_1 = e^{-\delta s}$, $\xi_2 = e^{r+\delta s}$. As one eigenvalue lies within and the other one outside the unit circle, which in Figure 3.13 is plotted as black horizontal line, the fossil solution is of saddle-type over its whole interval of existence.

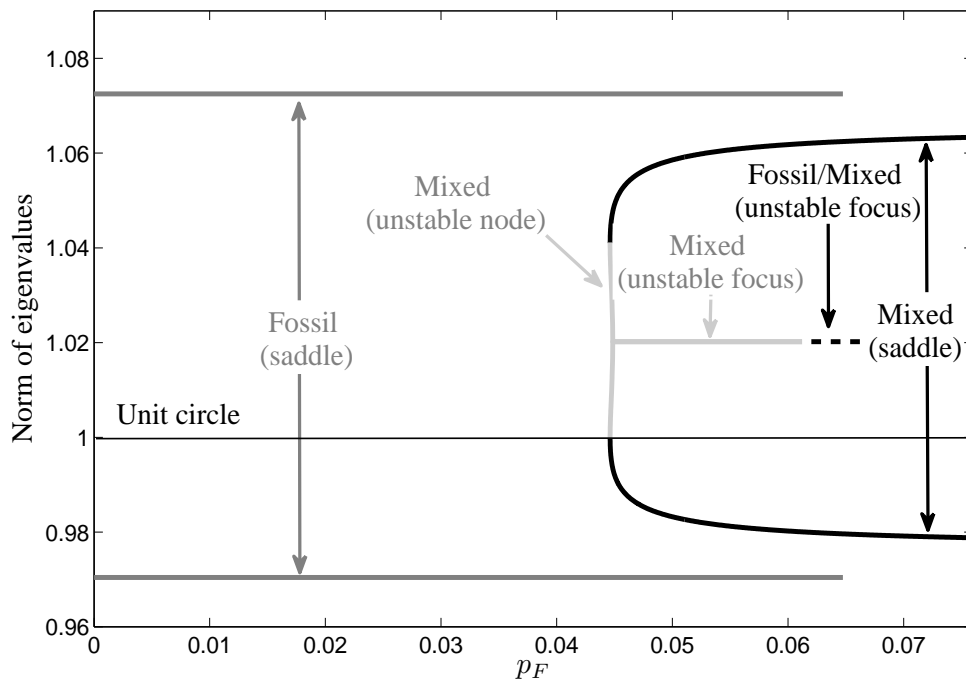


Figure 3.13: Norms of eigenvalues of the obtained periodic solutions for a fossil energy price $p_F \leq 0.07$.

The probably most interesting result can be observed at the fossil energy price $p_F = 0.044$ where an additional pair of mixed periodic solutions occurs. This sudden appearance of a pair of solutions is also known as *fold-bifurcation*, see Grass et al. (2008). While below that price the only periodic solution is given by the fossil one, there exist three periodic solutions beyond this price. The eigenvalues corresponding to the upper mixed periodic solution are shown in Figure 3.13 as black line, where again one is lying within and the other one outside the unit circle, which specifies the solution to be of saddle-type. The lower the fossil energy price p_F , the higher gets the stable eigenvalue until finally, at $p_F = 0.044$, it crosses the unit circle. The lower mixed solution whose two eigenvalues are plotted as light gray lines in Figure 3.13 and lie outside the unit circle, consequently is unstable. At the beginning they are real and hence the lower mixed periodic solution is an unstable node, but very soon they get complex and the mixed periodic solution turns into an unstable focus. At $p_F = 0.0612$, the lower mixed periodic solution turns into a fossil-mixed solution whose eigenvalues are shown as black dashed line. Also here, the eigenvalues are complex and their real parts are outside of the unit circle, which specifies this solution as unstable focus as well.

3.4.2 Learning-by-Doing Coefficient α

As already mentioned at the beginning of this section, not only the fossil energy price plays an important role for the optimal portfolio composition, but also the reducing impact of the learning-by-doing effect on the investment costs of renewable energy, which is determined by the learning-by-doing coefficient α . In the literature, many research papers can be found that investigate the correct size of the learning-by-doing coefficient for different types of technologies (see, for example, McDonald and Schratzenholzer, 2001). However, opinions strongly differ. To analyze how sensitive the optimal portfolio composition is with respect to different assumptions on the learning-by-doing coefficient, we here conduct a sensitivity analysis with respect to the learning-by-doing coefficient α .

For that purpose we keep the fossil energy price constant at $p_F = 0.05$ and use again numerical continuation in order to calculate the periodic solutions as well as the indifference threshold points if existent, for a varying α . The results can be seen in Figure 3.14. For a learning-by-doing coefficient of $\alpha < 0.2068$, which corresponds to a learning-by-doing rate of $LDR < 13.35\%$, the optimal long-run periodic solution is always given by the fossil periodic solution. The reason for this is the fact that the cost-reducing effect of learning by doing is too weak to offset the initially high investment costs. It therefore is optimal to stop investments immediately and cover the whole

demand with fossil energy in the long run.

For learning-by-doing coefficients $\alpha > 0.2068$, three periodic solutions exist of which one is the fossil solution and the other two are the two mixed solutions where the higher one is of saddle-type and the lower one is unstable. Up to $\alpha = 0.282$, indifference threshold points separate again the areas of attraction. The economic interpretation of this result is that the historical renewable energy capital efforts that are necessary in order to make renewable energy investments profitable, decline with the intensity of the learning-by-doing effect, as a lower initial renewable energy capital stock then already is sufficient. Until $\alpha = 0.2505$, which corresponds to a learning-by-doing rate of $LDR = 15.94\%$, the indifference threshold curve lies beyond the unstable mixed solution. Also here, the path leading into the fossil periodic solution has to be continued to a mixed-arc path in order to get the indifference threshold point. For $\alpha > 0.2505$, the indifference threshold curve lies below the unstable mixed solution and further declines with α until finally, at $\alpha = 0.282$ and hence at a learning-by-doing rate $LDR = 17.75\%$, it coincides with the unstable mixed solution. For higher learning-by-doing coefficients the mixed periodic solution dominates the fossil one as fossil energy is too expensive to be in the portfolio exclusively.

3.4.3 Global Radiation Intensity

So far we have investigated the impact of price and learning-by-doing effects on the optimal portfolio composition. However, we so far have fixed site-specific aspects concerning the supply of global radiation. Therefore, an interesting aspect on which we focus in the following is how the solutions change when geographical conditions vary.

Figure 3.15 shows the different global radiation scales in Europe for the year 2007. For the estimation of the parameter values τ and ν for the analysis so far, we have used Austrian data, which lie quite in the middle of the scale as can be seen in Figure 3.15. However, how would the results of our analysis change if estimations for geological sites higher in the north or lower in the south were used instead? To do so, we use global radiation data for Hamburg (Scenario 1) as an example of a northern site and for Athens (Scenario 2) as an example for a southern site, marked as red circles in Figure 3.15 (source of data see SODA, 2014). Figure 3.16 shows the average daily global radiation for Hamburg and Athens from 1985-2004. Comparing this with the basic scenario for which we used global radiation data of Austria as shown in Figure 2.1a, the strong differences immediately get obvious. While the radiation in winter in Hamburg is less than half the one in Austria, the radiation in Athens at this time of the year is around 50% higher. In summer, the global radiation in Athens rises up to around 7 kWh/m^2 , while in Hamburg it reaches only

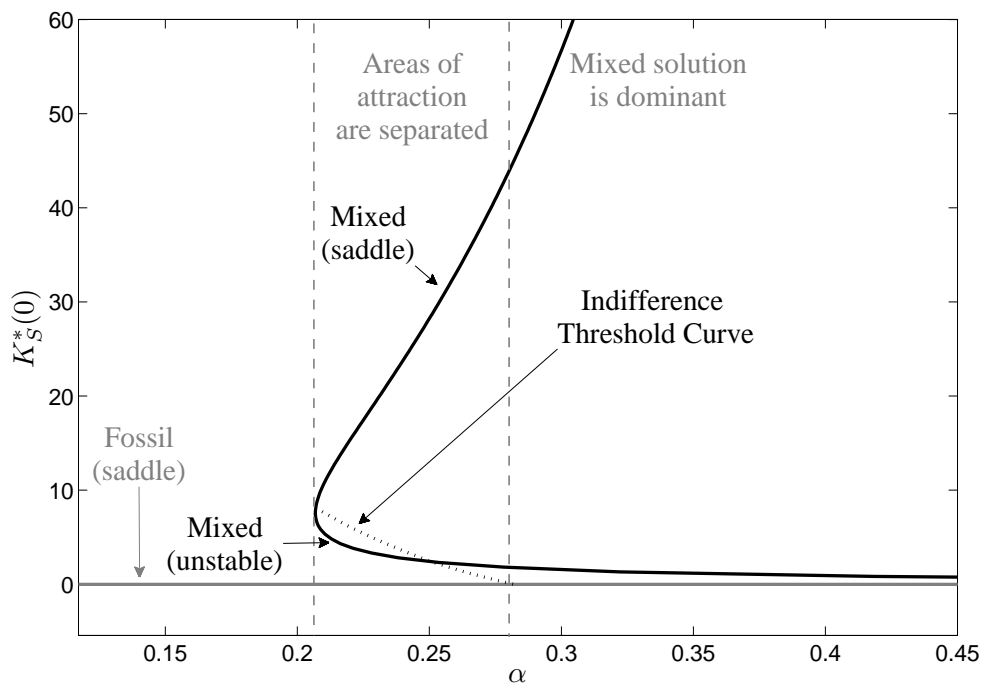


Figure 3.14: Bifurcation diagram of the canonical system with respect to the learning-by-doing coefficient α .

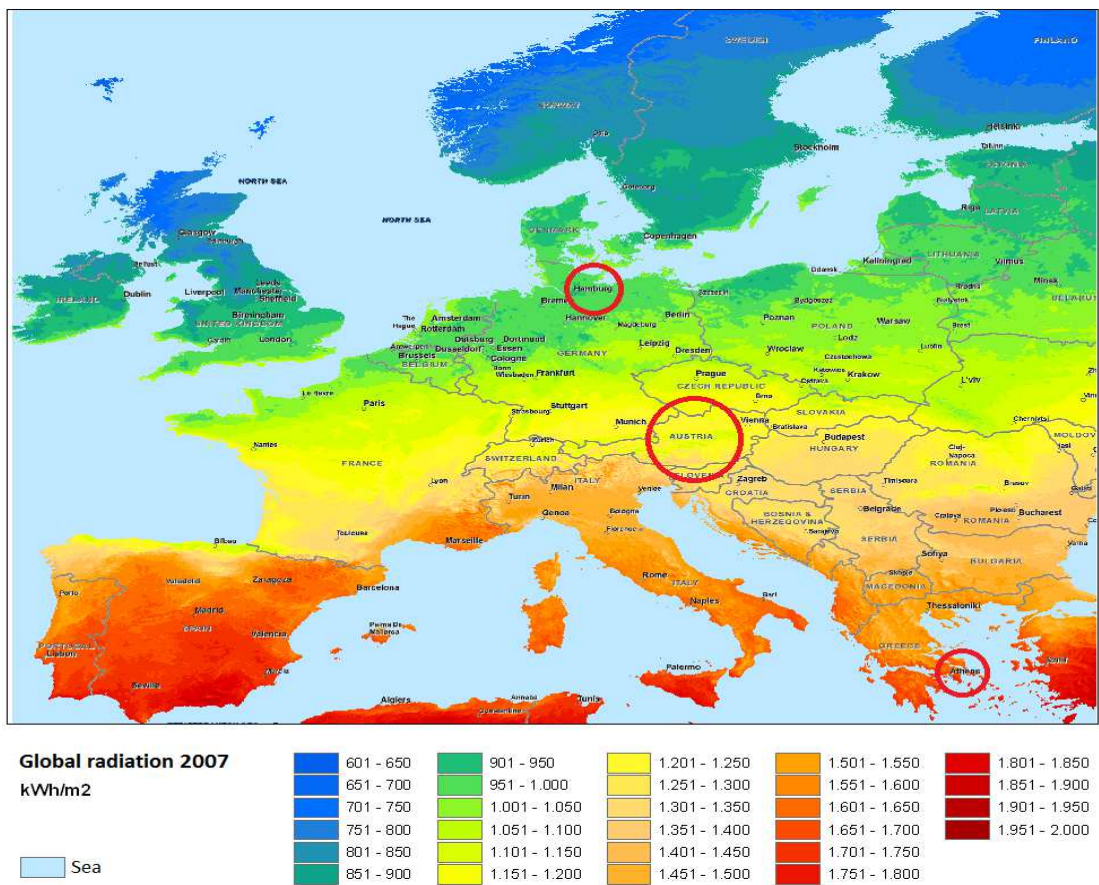


Figure 3.15: Global radiation in Europe.

(Source: <http://www.focussolar.de/Maps/RegionalMaps/Europe/Europe>, 4.Feb.2014)

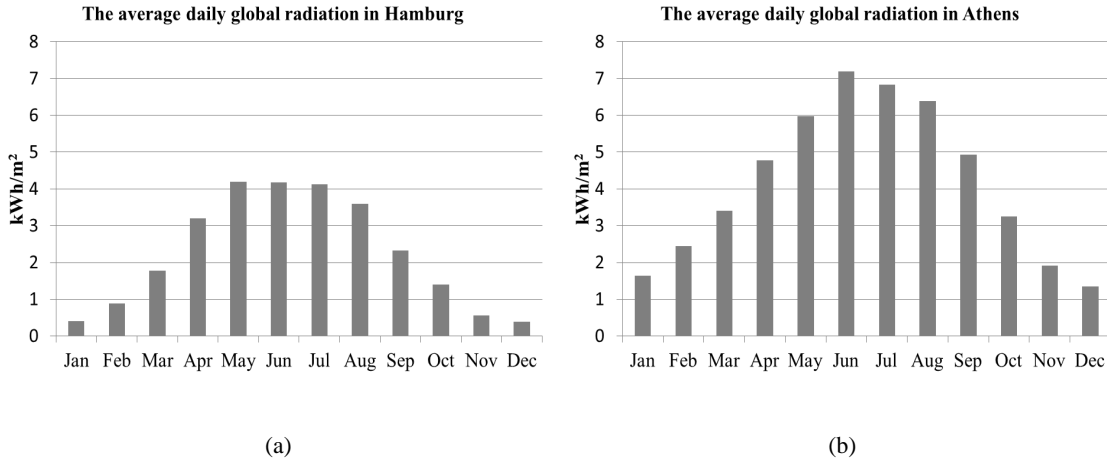


Figure 3.16: (a) Average daily global radiation in Hamburg (Scenario 1). (b) Average daily global radiation in Athens (Scenario 2).

around 4.3 kWh/m². Given these data, we estimate the parameter values τ and ν for these two new scenarios, respectively. The results are summarized in Table 3.3 together with those of the basic scenario for Austria. Further on, Figure 3.17 shows the deterministic functions for Scenario 1, Scenario 2 and the basic scenario.

	τ	ν
Basic Scenario	0.79	4.56
Scenario 1	0.21	4.08
Scenario 2	1.35	5.64

Table 3.3: Estimates for τ and ν for Scenarios 1 and 2 and the basic scenario for Austria.

In order to investigate the changes in the optimal portfolio composition when site-specific parameters change, we conduct the same sensitivity analysis with respect to the fossil energy price p_F , as done in Section 3.4.1, and compare the different outcomes.

Sensitivity Analysis for Scenarios 1 and 2

Figure 3.18 shows the results of the sensitivity analysis for Scenarios 1 and 2, respectively, compared to the results we have obtained for the parameters estimated for Austria.

First, we focus on Scenario 1 with a less intensive supply of global radiation. We first can observe that the qualitative behavior is the same. For a low fossil energy price, only the fossil

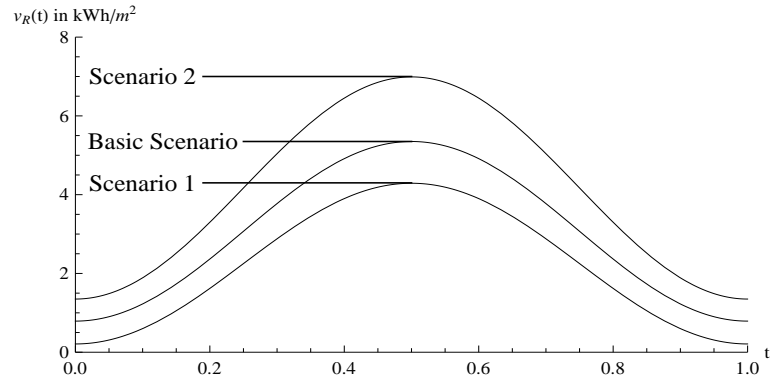


Figure 3.17: Deterministic functions for global radiation.

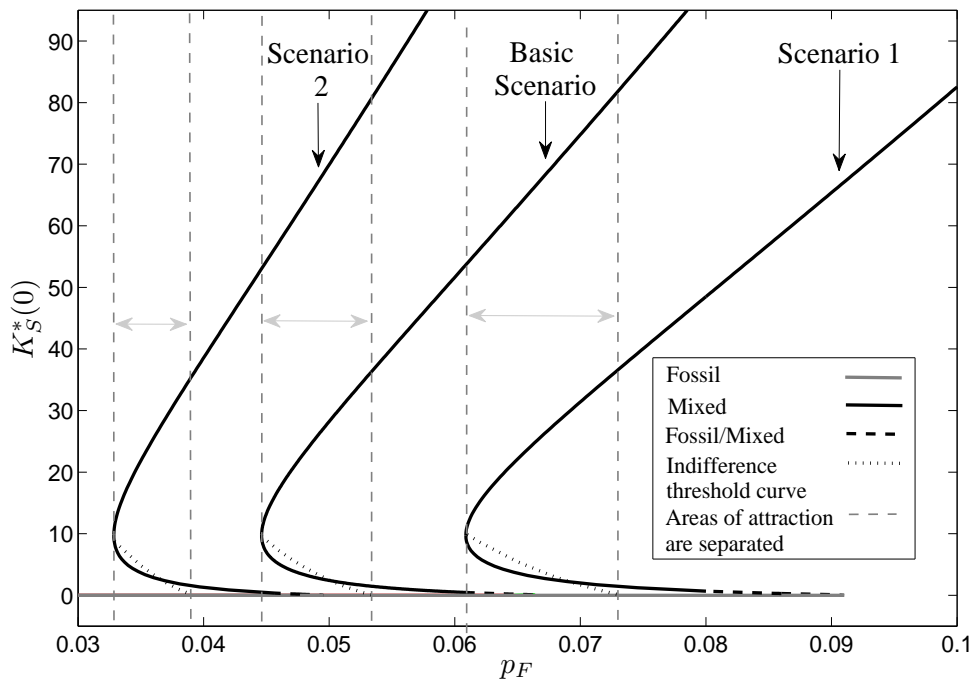


Figure 3.18: Bifurcation diagram with respect to the fossil energy price p_F for the Scenarios 1 and 2 in comparison with the basic scenario.

solution exists, while at a specific price level the two mixed solutions, with one being unstable and the other one being of saddle-type, occur and the areas of attraction are separated by indifference threshold points up to a certain level of p_F . However, a look on the price axis makes clear that remarkable changes concerning the position of the solutions occur. While the first bifurcation point at which these two additional mixed periodic solutions exists has been at $p_F = 0.0446$ for the original parameter set, this happens here at a comparably higher price $p_F = 0.0609$. Although the intensity of the learning-by-doing effect is the same and therefore the investment costs per unit capital decline at the same speed, the lower global radiation supply leads to a lower renewable energy generation and hence, to higher investment costs per unit of power. This aspect shifts the interval, in which the mixed periodic solutions as well as the indifference threshold curve exist, to the right as the fossil energy price has to be much higher in order to make further investments cost-effective. Consequently, also the price level at which the high mixed solution gets dominant because fossil energy as single source to cover the demand is too expensive, shifts to the right. For the original parameter set this has happened at $p_F = 0.0535$, while here the price level for this bifurcation is much higher at $p_F = 0.0739$. Finally, at $p_F = 0.091$, the optimal long-run periodic solution is given by the high mixed periodic solution only. Furthermore, the slope with which the high mixed periodic solution increases with the fossil energy price is lower compared to the basic scenario for Austria. The reason for this is given by the fact that due to the lower global radiation less renewable energy can be generated and, hence, the optimal renewable energy capital stock is lower at the same fossil energy price. Additionally, one can see that also the interval gets larger in which the indifference threshold curve separates the areas of attraction of the two periodic solutions being of saddle-type. This is because also the capital stock at which the mixed periodic solution starts to dominate the fossil one is reached at a comparably higher fossil energy price.

Second, we investigate Scenario 2 with a higher intensity of global radiation. Also for this case, the qualitative outcome does not change, but again the price boundaries are of special interest. While the interval, in which all three periodic solutions exist and the area of attraction is separated by the indifference threshold curve has started at $p_F = 0.0446$ in the original set and at $p_F = 0.0609$ in Scenario 1, one can observe in Figure 3.18 that this here happens already at a comparably lower price $p_F = 0.0328$. As the supply of global radiation is higher, the investment costs per unit of power for an equal capital stock here are even lower than for the other two cases. Hence, investments into renewable energy get profitable already at a lower fossil energy price. For this reason, also the indifference threshold curve has shifted to the left. The high mixed solution in Scenario 2 gets dominant at $p_F = 0.0449$, a price at which in the original set a mixed portfolio just starts to be an alternative to the pure fossil one, not to mention Scenario 1 where this possibility

does not exist at all at this price level. Starting at $p_F = 0.0495$, the high mixed solution is the optimal long-run periodic solution only. Here, the slope with which the high mixed periodic solution increases with the fossil energy price is higher compared to the basic scenario for Austria. Due to the higher global radiation more renewable energy can be generated and hence, a higher renewable energy capital stock is profitable already at a lower fossil energy price. Consequently, the interval in which the indifference threshold curve separates the areas of attraction of the two periodic solutions being of saddle-type gets smaller because the capital stock, at which the mixed periodic solution with research starts to dominate the fossil one, is reached at a lower fossil energy price.

Varying the intensity of the site-specific global radiation has shown some interesting aspects. While in all three cases, the original scenario as well as the two alternative scenarios, the intensity of the learning-by-doing effect is exactly the same, the outcomes and their possible consequences for political decisions are completely different. For southern countries the inclusion of renewable energy into the portfolio happens quite early along the fossil energy price axis. While in the case that the capital stock is below the indifference threshold curve, possible subsidies during the start-up period could easily help to induce the switch to the mixed portfolio in southern countries, for the northern countries the fossil energy price first has to increase enough to make such subsidies even reasonable. Another consequence could be that possible taxes on fossil energy would have to be much higher in order to induce this shift in northern countries. But as the supply of global radiation is lower, the profitability will never be the same as the one for the southern countries.

3.5 Summary

In this chapter, we have investigated how accumulated experience can reduce the investment costs of renewable (solar) energy capital and how different the results can be if such a learning-by-doing aspect is included into an energy portfolio planning model. We have extended the non-autonomous optimal control model of Chapter 2 by including a one-factor log-linear learning curve into the objective function so that the accumulated renewable energy capital, which is supposed to reflect the collected experience, has a diminishing impact on the investment costs. Investigating again the impact of the fossil energy price p_F on the optimal portfolio composition has shown that there exist price intervals in which multiple periodic solutions occur, and whose areas of attraction are separated by an indifference threshold point. Further on, it turns out that these results are not only sensitive with respect to the fossil energy price but also to the intensity of the learning-by-doing effect as well as to the geographical site conditions concerning the global radiation.

The occurrence of an indifference threshold point yields important aspects for the economic interpretation of the obtained results. We have seen that whether investments into renewable energy capital are worthwhile or not may depend on the initial capital stock. Due to this history dependence, investments into renewable energy generation from the very beginning would never be optimal in our approach as the initial investment costs would be too high. The level of the capital stock at which such investments get worthwhile shifts even further up if global radiation is lower, as for the northern countries, or if the learning-by-doing effect is weaker, meaning that the learning-by-doing coefficient is assumed to be lower. One important conclusion of these results is that financial support in form of subsidies during the start-up period of a new technology could play a major role for the successful introduction of this technology into the market. The profitability, however, strongly depends on the site-specific conditions. Experience in this approach has been the driving force for the reduced investment costs. But this is not the only source for technological learning, as we already have mentioned. So far we have completely neglected the aspect of R&D efforts, which will be the focus of the next chapter.

The Effect of Learning by Searching in Renewable Energy Generation

This chapter deals with the second aspect of learning which is driven by the accumulation of knowledge due to R&D efforts. As we have already mentioned in the introduction in Chapter 1, such learning effects can be included in form of a two-factor learning curve, which will be the extension of our model in this chapter.

4.1 The Model

To additionally include the aspects of learning by searching, we introduce a second state variable $K_R(t)$, reflecting the stock of knowledge and described by

$$\dot{K}_R(t) = I_R(t) - \delta_R K_R(t).$$

$I_R(t)$ are the R&D expenditures at time t which increase the stock of knowledge and which are introduced as third control in our model. Also here, forgetting by not doing occurs and the knowledge stock depreciates over time with the depreciation rate δ_R . This loss of knowledge can also be understood in the sense that R&D expenditures of the past gradually become outdated and hence their impact declines (cf. Berglund and Söderholm, 2006). Incorporating the fact that knowledge reduces the investment costs of renewable energy, the corresponding Cobb-Douglas-type function of the two-factor learning curve, as already presented in (1.2), is included into the instantaneous objective function given by

$$C_t = I_S(t) (b + cI_S(t)) (K_S(t) + \varepsilon_1)^{-\alpha_1} (K_R(t) + \varepsilon_2)^{-\alpha_2},$$

where we distinguish between α_1 and α_2 as the learning-by-doing and learning-by-searching coefficients, respectively, as well as ε_1 and ε_2 as the initial investment costs and the initial R&D expenditures when the corresponding stock is zero. This concerns, of course, only the investment costs for renewable energy. Further on, however, also the R&D expenditures come at some cost, which are modeled in a similar way using, also here, a linear and a quadratic cost term,

$$C_{R\&D_t} = dI_R(t) + eI_R(t)^2,$$

where the latter one reflects the aspect that a rapid increase in knowledge is expensive.

To sum up, the adapted optimal control model with three controls and two states reads as

$$\begin{aligned} \max_{E_F(t), I_S(t), I_R(t)} \int_0^\infty e^{-rt} \left(-I_S(t) \left(b + cI_S(t) \right) \left(K_S(t) + \varepsilon_1 \right)^{-\alpha_1} \left(K_R(t) + \varepsilon_2 \right)^{-\alpha_2} \right. \\ \left. - I_R(t) \left(d + eI_R(t) \right) - p_F E_F(t) \right) dt \end{aligned} \quad (4.1)$$

$$\text{s.t.: } \dot{K}_S(t) = I_S(t) - \delta_S K_S(t), \quad (4.1a)$$

$$\dot{K}_R(t) = I_R(t) - \delta_R K_R(t), \quad (4.1b)$$

$$E_F(t) + E_S(K_S(t), t) - E \geq 0, \quad (4.1c)$$

$$E_S(K_S(t), t) = (\nu \sin^2(t\pi) + \tau) K_S(t) \eta, \quad (4.1d)$$

$$E_F(t), I_S(t), I_R(t) \geq 0. \quad (4.1e)$$

4.2 Solution

4.2.1 Canonical System and Necessary First Order Conditions

To solve the optimal control problem (4.1) we use Pontryagin's maximum principle for infinite time horizon problems (cf. Grass et al., 2008) analogously to the previous model approaches and

consider the Lagrangian given by

$$\begin{aligned} \mathcal{L}(K_S, K_R, E_F, I_S, I_R, \lambda_1, \lambda_2, \lambda_0, \mu_1, \mu_2, \mu_3, t) = \\ \lambda_0 \left(-(bI_S(t) + cI_S(t)^2)(K_S(t) + \varepsilon_1)^{-\alpha_1} (K_R(t) + \varepsilon_2)^{-\alpha_2} - (dI_R(t) + eI_R(t)^2) - p_F E_F(t) \right) \\ + \lambda_1 (I_S(t) - \delta_S K_S(t)) + \lambda_2 (I_R(t) - \delta_R K_R(t)) + \mu_1 (E_F(t) + (v \sin^2(t\pi) + \tau) K_S(t) \eta - E) \\ + \mu_2(t) E_F(t) + \mu_3 I_S(t) + \mu_4(t) I_R(t). \end{aligned}$$

Note that as of here, we will often omit the time argument t if necessary for the readability of the expressions. In this approach we have two costates, $\lambda_1(t)$ and $\lambda_2(t)$, both assumed to be continuous and piecewise continuously differentiable functions, and a constant $\lambda_0 \geq 0$, so that for all $t \geq 0$

$$(\lambda_0, \lambda_1(t), \lambda_2(t)) \neq 0,$$

$$\mathcal{L}(K_S^*, K_R^*, E_F^*, I_S^*, I_R^*, \lambda_1, \lambda_2, \lambda_0, \mu_1, \mu_2, \mu_3, t) = \max_{E_F, I_S, I_R} \mathcal{L}(K_S^*, K_R^*, E_F, I_S, I_R, \lambda_1, \lambda_2, \lambda_0, \mu_1, \mu_2, \mu_3, t).$$

We further require that the limiting transversality conditions

$$\lim_{t \rightarrow \infty} \lambda_1(t) e^{-rt} = 0, \quad (4.2)$$

$$\lim_{t \rightarrow \infty} \lambda_2(t) e^{-rt} = 0, \quad (4.3)$$

are satisfied. $\mu_1(t), \mu_2(t), \mu_3(t)$, and $\mu_4(t)$ are again the piecewise continuous Lagrange multipliers for the mixed-path constraint and the non-negativity conditions, respectively, so that the complementary slackness conditions

$$\mu_1(t) (E_F^*(t) + E_S^*(K_S^*(t), t) - E) = 0, \quad \mu_1(t) \geq 0,$$

$$\mu_2(t) E_F^*(t) = 0, \quad \mu_2(t) \geq 0,$$

$$\mu_3(t) I_S^*(t) = 0, \quad \mu_3(t) \geq 0,$$

$$\mu_4(t) I_R^*(t) = 0, \quad \mu_4(t) \geq 0.$$

hold.

Proposition 3. *Without loss of generality we can set $\lambda_0 = 1$ for the subsequent analysis.*

Proof. Similar to the proof for the first model approach in Chapter 2, for $\lambda_0 = 0$ we get the switching functions and the adjoint equations

$$\begin{aligned}\frac{\partial \mathcal{L}}{\partial E_F(t)} &= \mu_1(t) + \mu_2(t), \\ \frac{\partial \mathcal{L}}{\partial I_S(t)} &= \lambda_1(t) + \mu_3(t), \\ \frac{\partial \mathcal{L}}{\partial I_R(t)} &= \lambda_2(t) + \mu_4(t), \\ \dot{\lambda}_1(t) &= (r + \delta_S)\lambda_1(t) - \mu_1(t)\eta(v \sin^2(t\pi) + \tau), \\ \dot{\lambda}_2(t) &= (r + \delta_R)\lambda_2(t).\end{aligned}$$

As $\mu_1(t), \mu_2(t) \geq 0$, in case of no fossil energy, $E_F(t) = 0$, it follows that $\mu_1(t) = \mu_2(t) = 0$. For $E_F(t) > 0$ the condition

$$\frac{\partial \mathcal{L}}{\partial E_F(t)} = \mu_1(t) = 0$$

has to hold. For both cases, this yields the solution for $\lambda_1(t)$ as

$$\lambda_1(t) = \lambda_1(0)e^{(r+\delta_S)t}.$$

Similarly, the solution for $\lambda_2(t)$ is given by

$$\lambda_2(t) = \lambda_2(0)e^{(r+\delta_R)t}.$$

As the transversality conditions in (4.2)-(4.3) have to hold, the only feasible initial values $\lambda_1(0) = 0$ and $\lambda_2(0) = 0$ imply that $\lambda_1(t) = \lambda_2(t) = 0 \forall t$. Hence, this is contradictory to the condition that $(\lambda_0, \lambda_1(t), \lambda_2(t)) \neq 0$. \square

The necessary first order conditions then read as

$$\begin{aligned}\frac{\partial \mathcal{L}}{\partial I_S} &= -(b + 2cI_S)(K_S + \varepsilon_1)^{-\alpha_1}(K_R + \varepsilon_2)^{-\alpha_2} + \lambda_1 + \mu_3 = 0 \\ &\Leftrightarrow I_S = \frac{(K_S + \varepsilon_1)^{\alpha_1}(K_R + \varepsilon_2)^{\alpha_2}(\lambda_1 + \mu_3) - b}{2c},\end{aligned}\tag{4.4}$$

$$\frac{\partial \mathcal{L}}{\partial I_R} = -d + \lambda_2 + \mu_4 - 2eI_R = 0 \quad \Leftrightarrow \quad I_R = \left(\frac{-d + \lambda_2 + \mu_4}{2e} \right),\tag{4.5}$$

$$\begin{aligned} \dot{\lambda}_1 &= (r + \delta_S)\lambda_1 - \left(b + \frac{1}{2}(-b + (K_S + \varepsilon_1)^{\alpha_1}(K_R + \varepsilon_2)^{\alpha_2}(\lambda_1 + \mu_3)) \right) \\ &\quad \frac{\alpha_1}{2c}(K_S + \varepsilon_1)^{-\alpha_1-1}(K_R + \varepsilon_2)^{\alpha_2}(-b + (K_S + \varepsilon_1)^{\alpha_1}(K_R + \varepsilon_2)^{\alpha_2}(\lambda_1 + \mu_3)) \\ &\quad - \eta\mu_1(v \sin^2(t\pi) + \tau), \end{aligned} \quad (4.6)$$

$$\begin{aligned} \dot{\lambda}_2 &= (r + \delta_R)\lambda_2 - \left(b + \frac{1}{2}(-b + (K_S + \varepsilon_1)^{\alpha_1}(K_R + \varepsilon_2)^{\alpha_2}(\lambda_1 + \mu_3)) \right) \\ &\quad \frac{\alpha_2}{2c}(K_S + \varepsilon_1)^{-\alpha_1}(K_R + \varepsilon_2)^{\alpha_2-1}(-b + (K_S + \varepsilon_1)^{\alpha_1}(K_R + \varepsilon_2)^{\alpha_2}(\lambda_1 + \mu_3)). \end{aligned} \quad (4.7)$$

Similar to the previous model approach described in Chapter 3, also in this approach only the satisfaction of the necessary and not the sufficient conditions can be guaranteed, and the economic interpretation of the obtained results is used to justify the assumption that they are in fact optimal.¹ Due to the linearity of the Lagrangian in $E_F(t)$, also in this approach the optimal fossil energy amount is determined by the switching function

$$\frac{\partial \mathcal{L}}{\partial E_F(t)} = -p_F + \mu_1(t) + \mu_2(t).$$

As follows from the proof of Proposition 2, also for this extended model version this proposition applies, implying that a solution lying completely in the interior of the feasible domain with all three controls positive and the mixed-path constraint satisfied with inequality can never be optimal. The reason for this is again the possibility to reduce costs by reducing the fossil energy amount until finally the mixed-path constraint is satisfied with equality or the fossil energy amount is zero. The proof for this is similar to the one of Proposition 2. We therefore distinguish again between the different boundaries of the feasible domain, but this time, as we have a third control, we have six instead of three different boundaries: fossil with and without research, mixed with and without research, and renewable with and without research. Referring to one of these cases, we will in the following always mention additionally if research is included, otherwise the already established terms (fossil, mixed, and renewable) always mean that they are without research. The canonical system is given as follows:

$$\begin{aligned} \dot{K}_S &= A_1 - \delta_S K_S, \\ \dot{K}_R &= A_2 - \delta_R K_R, \end{aligned}$$

¹In this model approach, however, $\frac{\partial^2 \mathcal{L}}{\partial I_S(t)^2} = -2c(K_S(t) + \varepsilon_1)^{-\alpha_1}(K_R(t) + \varepsilon_2)^{\alpha_2} < 0$ and $\frac{\partial^2 \mathcal{L}}{\partial I_R(t)^2} = -2e < 0$ holds and, therefore, the Lagrangian is at least concave with respect to $I_S(t)$ and $I_R(t)$ and the first order conditions (4.4) and (4.5) indeed deliver maxima.

$$\begin{aligned}\dot{\lambda}_1 &= (r + \delta_S)\lambda_1 + A_3 + A_4, \\ \dot{\lambda}_2 &= (r + \delta_R)\lambda_2 + A_5,\end{aligned}$$

where

$$A_1 = \frac{(K_S + \varepsilon_1)^{\alpha_1} (K_R + \varepsilon_2)^{\alpha_2} \lambda_1 - b}{2c},$$

$$\begin{aligned}A_3 &= -\left(b + \frac{1}{2}(-b + (K_S + \varepsilon_1)^{\alpha_1} (K_R + \varepsilon_2)^{\alpha_2} \lambda_1)\right) \\ &\quad \frac{\alpha_1}{2c} (K_S + \varepsilon_1)^{-\alpha_1 - 1} (K_R + \varepsilon_2)^{\alpha_2} (-b + (K_S + \varepsilon_1)^{\alpha_1} (K_R + \varepsilon_2)^{\alpha_2} \lambda_1), \\ A_5 &= -\left(b + \frac{1}{2}(-b + (K_S + \varepsilon_1)^{\alpha_1} (K_R + \varepsilon_2)^{\alpha_2} \lambda_1)\right) \\ &\quad \frac{\alpha_2}{2c} (K_S + \varepsilon_1)^{-\alpha_1} (K_R + \varepsilon_2)^{\alpha_2 - 1} (-b + (K_S + \varepsilon_1)^{\alpha_1} (K_R + \varepsilon_2)^{\alpha_2} \lambda_1),\end{aligned}$$

for all cases with positive investments in renewable energy capital (mixed, mixed with research, renewable, renewable with research). Otherwise, $A_1 = A_3 = A_5 = 0$. Further on,

$$A_2 = \left(\frac{-d + \lambda_2}{2e}\right),$$

for all cases with research, otherwise $A_2 = 0$, and finally

$$A_4 = -\eta p_F (v \sin^2(t\pi) + \tau),$$

for all fossil and mixed cases, both with and without research, otherwise, $A_4 = 0$.

4.2.2 Periodic Solution

Similar to the previous chapters, we calculate the instantaneous equilibrium points, $K_S^{IEP}(t)$, $K_R^{IEP}(t)$, $\lambda_1^{IEP}(t)$, $\lambda_2^{IEP}(t)$, as starting solution for the subsequent boundary value problem,

$$\begin{aligned}\dot{K}_S &= f^{K_S}(t, K_S, K_R, \lambda_1, \mu_3), & \text{with } K_S(0) &= K_S(1), \\ \dot{K}_R &= f^{K_R}(t, K_S, K_R, \lambda_2, \mu_4), & \text{with } K_R(0) &= K_R(1), \\ \dot{\lambda}_1 &= f^{\lambda_1}(t, K_S, K_R, \lambda_1, \mu_1, \mu_3), & \text{with } \lambda_1(0) &= \lambda_1(1), \\ \dot{\lambda}_2 &= f^{\lambda_2}(t, K_S, K_R, \lambda_1, \lambda_2, \mu_3), & \text{with } \lambda_2(0) &= \lambda_2(1),\end{aligned}$$

in order to calculate candidates for the optimal long-run periodic solution of the model. For the calculation of periodic solutions that exist of several arcs, we solve again for $i = 1, \dots, n + 1$, $j = 1, \dots, n$, $s \in [i - 1, i]$, together with the linear time transformation $T(s)$ of (2.28), the switching times τ_i with the boundary points $\tau_0 = 0$, $\tau_{n+1} = 1$, and an index

$$a_i = \begin{cases} 1, & \text{for the fossil region with research,} \\ 2, & \text{for the mixed region with research,} \\ 3, & \text{for the renewable region with research,} \\ 4, & \text{for the fossil region,} \\ 5, & \text{for the mixed region,} \\ 6, & \text{for the renewable region,} \end{cases} \quad (4.8)$$

to distinguish between the canonical systems for the six boundary cases of the feasible domain, the multi-point boundary problem

$$\begin{aligned} \dot{K}_{S_i}(s) &= (\tau_i - \tau_{i-1}) f_{a_i}^{K_S}(T(s), K_{S_i}(s), K_{R_i}(s), \lambda_{1_i}(s), \mu_{3_i}(s)), \\ \dot{K}_{R_i}(s) &= (\tau_i - \tau_{i-1}) f_{a_i}^{K_R}(T(s), K_{R_i}(s), \lambda_{2_i}(s), \mu_{4_i}(s)), \\ \dot{\lambda}_{1_i}(s) &= (\tau_i - \tau_{i-1}) f_{a_i}^{\lambda_1}(T(s), K_{S_i}(s), K_{R_i}(s), \lambda_{1_i}(s), \mu_{1_i}(s), \mu_{3_i}(s)), \\ \dot{\lambda}_{2_i}(s) &= (\tau_i - \tau_{i-1}) f_{a_i}^{\lambda_2}(T(s), K_{S_i}(s), K_{R_i}(s), \lambda_{1_i}(s), \lambda_{2_i}(s), \mu_{3_i}(s)), \\ 0 &= (K_{S_j}(\tau_j), K_{R_j}(\tau_j), \lambda_{1_j}(\tau_j), \lambda_{2_j}(\tau_j)) - (K_{S_{j+1}}(\tau_j), K_{R_{j+1}}(\tau_j), \lambda_{1_{j+1}}(\tau_j), \lambda_{2_{j+1}}(\tau_j)), \\ 0 &= (K_{S_{n+1}}(1), K_{R_{n+1}}(1), \lambda_{1_{n+1}}(1), \lambda_{2_{n+1}}(1)) - (K_{S_1}(0), K_{R_1}(0), \lambda_{1_1}(0), \lambda_{2_1}(0)), \\ 0 &= c(a_j, a_{j+1}). \end{aligned}$$

Note, however, that the index a_i no longer satisfies condition (2.27) claiming that only switches between neighboring regions are allowed, as now the third control describing the R&D investments can be chosen independently of the current portfolio composition. However, what still holds is the fact that a switch from a fossil case (with or without research) to a renewable case (with or without research) always has to happen over a mixed case (with or without research) as a direct switch is not possible. The conditions for the continuity of the controls with respect to time are given for $j = 1, \dots, n$ as

$$c(a_j, a_{j+1}) = \left\{ \begin{array}{l} \frac{(K_{S_j}(\tau_j) + \varepsilon_1)^{\alpha_1}}{(K_{R_j}(\tau_j) + \varepsilon_2)^{-\alpha_2}} \lambda_{1_j}(\tau_j) - b = 0 \\ \lambda_{2_j}(\tau_j) - d = 0 \\ E_S(K_{S_j}(\tau_j), \tau_j) - E = 0 \end{array} \right\} \text{ if } \{a_j, a_{j+1}\} \in \left\{ \begin{array}{l} \{\{1, 2\}, \{4, 5\}, \{2, 1\}, \\ \{5, 4\}\} \\ \{\{1, 4\}, \{2, 5\}, \{3, 6\}, \\ \{4, 1\}, \{5, 2\}, \{6, 3\}\} \\ \{\{2, 3\}, \{5, 6\}, \{3, 2\}, \\ \{6, 5\}\} \end{array} \right\}. \quad (4.9)$$

4.2.3 Stability

In order to investigate the stability of a periodic solution $\Gamma(t)$, we have to calculate the monodromy matrix, as done in the previous chapters. The Jacobian matrix for the fossil case and the fossil case with research is given by

$$J(t) = \begin{pmatrix} -\delta_S & 0 & 0 & 0 \\ 0 & -\delta_R & 0 & \frac{\partial f^{K_R}}{\partial \lambda_2} \\ 0 & 0 & r + \delta_S & 0 \\ 0 & 0 & 0 & r + \delta_R \end{pmatrix} (\Gamma(t)),$$

where

$$\frac{\partial f^{K_R}}{\partial \lambda_2} = \begin{cases} 0, & \text{for the fossil case ,} \\ \frac{1}{2e}, & \text{for the fossil case with research.} \end{cases}$$

The monodromy matrix then is given by

$$M(1) = e^{J(1)} = \begin{pmatrix} e^{-\delta_S} & 0 & 0 & 0 \\ 0 & e^{-\delta_R} & 0 & A \\ 0 & 0 & e^{r+\delta_S} & 0 \\ 0 & 0 & 0 & e^{r+\delta_R} \end{pmatrix},$$

where

$$A = \begin{cases} 0, & \text{for the fossil case ,} \\ \frac{e^{-\delta_R}(e^{r+2\delta_R}-1)}{(r+2\delta_R)2e}, & \text{for the fossil case with research.} \end{cases}$$

Both monodromy matrices have the same eigenvalues given by

$$\xi_1 = e^{-\delta_S} < 1, \quad \xi_2 = e^{-\delta_R} < 1, \quad \xi_3 = e^{r+\delta_S} > 1, \quad \xi_4 = e^{r+\delta_R} > 1.$$

This implies that also in the current model approach, every fossil solution but also every fossil solution with research is of saddle-type. For all the other cases, the Jacobian explicitly depends on the periodic solution and, therefore, a general statement on the stability is not possible. The Jacobian for the mixed case with research reads as

$$J(t) = \begin{pmatrix} \frac{\partial f^{K_S}}{\partial K_S} & 0 & \frac{\partial f^{K_S}}{\partial \lambda_1} & 0 \\ 0 & -\delta_R & 0 & \frac{(\lambda_2 - d)^2}{2e} \\ \frac{\partial f^{\lambda_1}}{\partial K_S} & \frac{\partial f^{\lambda_1}}{\partial K_R} & \frac{\partial f^{\lambda_1}}{\partial \lambda_1} & 0 \\ \frac{\partial f^{\lambda_2}}{\partial K_S} & \frac{\partial f^{\lambda_2}}{\partial K_R} & \frac{\partial f^{\lambda_2}}{\partial \lambda_1} & r + \delta_R \end{pmatrix} (\Gamma(t)),$$

where

$$\begin{aligned} \frac{\partial f^{K_S}}{\partial K_S} &= -\delta_R + \frac{\alpha_1 (K_S + \varepsilon_1)^{\alpha_1 - 1} (K_R + \varepsilon_2)^{\alpha_2} \lambda_1}{2c}, \\ \frac{\partial f^{K_S}}{\partial \lambda_1} &= \frac{(K_S + \varepsilon_1)^{\alpha_1} (K_R + \varepsilon_2)^{\alpha_2}}{2c}, \\ \frac{\partial f^{\lambda_1}}{\partial K_S} &= -\frac{\alpha_1 (b^2 (1 + \alpha_1) + (\alpha_1 - 1) (K_S + \varepsilon_1)^{2\alpha_1} (K_R + \varepsilon_2)^{2\alpha_2} \lambda_1^2)}{4c (K_S + \varepsilon_1)^{\alpha_1 + 2} (K_R + \varepsilon_2)^{\alpha_2}}, \\ \frac{\partial f^{\lambda_1}}{\partial K_R} &= -\frac{\alpha_1 \alpha_2 (b^2 + (K_S + \varepsilon_1)^{2\alpha_1} (K_R + \varepsilon_2)^{2\alpha_2} \lambda_1^2)}{4c (K_S + \varepsilon_1)^{\alpha_1 + 1} (K_R + \varepsilon_2)^{\alpha_2 + 1}}, \\ \frac{\partial f^{\lambda_1}}{\partial \lambda_1} &= r + \delta_S - \frac{\alpha_1 (K_S + \varepsilon_1)^{\alpha_1 - 1} (K_R + \varepsilon_2)^{\alpha_2} \lambda_1}{2c}, \\ \frac{\partial f^{\lambda_2}}{\partial K_S} &= -\frac{\alpha_1 \alpha_2 (b^2 + (K_S + \varepsilon_1)^{2\alpha_1} (K_R + \varepsilon_2)^{2\alpha_2} \lambda_1^2)}{4c (K_S + \varepsilon_1)^{\alpha_1 + 1} (K_R + \varepsilon_2)^{\alpha_2 + 1}}, \\ \frac{\partial f^{\lambda_2}}{\partial K_R} &= -\frac{\alpha_2 (b^2 (1 + \alpha_2) + (\alpha_2 - 1) (K_S + \varepsilon_1)^{2\alpha_1} (K_R + \varepsilon_2)^{2\alpha_2} \lambda_1)}{4c (K_S + \varepsilon_1)^{-\alpha_1} (K_R + \varepsilon_2)^{\alpha_2 + 2}}, \\ \frac{\partial f^{\lambda_2}}{\partial \lambda_1} &= -\frac{\alpha_2 \lambda_1}{2c (K_S + \varepsilon_1)^{-\alpha_1} (K_R + \varepsilon_2)^{1 - \alpha_2}}. \end{aligned}$$

4.2.4 Optimal Paths

For the calculation of trajectories that lead into a periodic solution, we use again the Moore-Penrose method, as also done in the previous chapter. For this approach, however, we have an additional state and an additional control to consider. Assume that we have again N continuation steps. Then, in order to get a trajectory that starts at the initial capital stocks $\{K_{S_0}, K_{R_0}\}$, at each step $n = 1, \dots, N$ the system

$$\begin{aligned} 0 &= K_S^n(0) - K_{S_0}^n, \\ 0 &= K_R^n(0) - K_{R_0}^n, \\ 0 &= F' \left(\begin{pmatrix} K_S^n(1) \\ K_R^n(1) \\ \lambda_1^n(1) \\ \lambda_2^n(1) \end{pmatrix} - \begin{pmatrix} K_S^*(0) \\ K_R^*(0) \\ \lambda_1^*(0) \\ \lambda_2^*(0) \end{pmatrix} \right), \end{aligned}$$

has to be solved.

For the calculations of trajectories that consist of multiple arcs, we have again to solve in addition the marginal conditions guaranteeing the continuity of the paths, as done in Section 3.4.1. As the numbers of states and controls for this model approach have changed, we will once again formulate the complete boundary value problem. Let I_n denote the number of necessary arcs for the n -th continuation step and let

$$\tau_0^n := 0 < \tau_1^n < \tau_2^n < \dots < \tau_{I_n-1}^n < 1 =: \tau_{I_n}^n,$$

be again the switching times as well as the two boundary points. We use the index of (4.8) to distinguish between the six different boundary cases of the feasible domain, and the time transformation

$$T(s) = T_p((\tau_i - \tau_{i-1})(s - i) + \tau_i)$$

with T_p being the truncation time, as we have done in Section 3.4.1 so that $s \in [i-1, i]$ for $i = 1, \dots, I_n$. Then, at each continuation step $n = 1, \dots, N$, a path is searched that consists of I_n arcs

and that solves for $i = 1, \dots, I_n$ and for $j = 1, \dots, I_n - 1$ the boundary value problem

$$\dot{K}_{S_i}(s) = T_p(\tau_i - \tau_{i-1})f_{a_i}^{K_S}(T(s), K_{S_i}(s), K_{R_i}(s), \lambda_{1_i}(s), \mu_{3_i}(s)), \quad (4.10)$$

$$\dot{K}_{R_i}(s) = T_p(\tau_i - \tau_{i-1})f_{a_i}^{K_R}(T(s), K_{R_i}(s), \lambda_{2_i}(s), \mu_{4_i}(s)), \quad (4.11)$$

$$\dot{\lambda}_{1_i}(s) = T_p(\tau_i - \tau_{i-1})f_{a_i}^{\lambda_1}(T(s), K_{S_i}(s), K_{R_i}(s), \lambda_{1_i}(s), \mu_{1_i}(s), \mu_{3_i}(s)), \quad (4.12)$$

$$\dot{\lambda}_{2_i}(s) = T_p(\tau_i - \tau_{i-1})f_{a_i}^{\lambda_2}(T(s), K_{S_i}(s), K_{R_i}(s), \lambda_{1_i}(s), \lambda_{2_i}(s), \mu_{3_i}(s)), \quad (4.13)$$

$$0 = K_{S_j}^n(\tau_j) - K_{S_{j+1}}^n(\tau_j), \quad (4.14)$$

$$0 = K_{R_j}^n(\tau_j) - K_{R_{j+1}}^n(\tau_j), \quad (4.15)$$

$$0 = \lambda_{1_j}^n(\tau_j) - \lambda_{1_{j+1}}^n(\tau_j), \quad (4.16)$$

$$0 = \lambda_{2_j}^n(\tau_j) - \lambda_{2_{j+1}}^n(\tau_j), \quad (4.17)$$

$$0 = c(a_j, a_{j+1}), \quad (4.18)$$

$$0 = K_{S_1}^n(0) - K_{S_0}^n, \quad (4.19)$$

$$0 = K_{R_1}^n(0) - K_{R_0}^n, \quad (4.20)$$

$$0 = F' \left(\begin{pmatrix} K_{S_{I_n}}^n(1) \\ K_{R_{I_n}}^n(1) \\ \lambda_{1_{I_n}}^n(1) \\ \lambda_{2_{I_n}}^n(1) \end{pmatrix} - \begin{pmatrix} K_S^*(0) \\ K_R^*(0) \\ \lambda_1^*(0) \\ \lambda_2^*(0) \end{pmatrix} \right), \quad (4.21)$$

where (4.18) are the same continuity conditions as in (4.9).

4.3 Results

In what follows, we present the results of the numerical analysis of the model for which we set the parameters as summarized in Table 4.1. Similar to the model approach in Chapter 3, also here multiple periodic solutions can be found. For the current parameter set, we obtain a fossil solution, a mixed solution, and a mixed solution with research. The first solution exhibits no investments, neither in renewable energy capital nor in R&D efforts. Hence, the whole energy demand is covered by fossil energy in the long run. In the second periodic solution, investments in renewable energy capital are made and, therefore, both types of energy are used in the portfolio to cover the demand, while there are still no R&D efforts to improve the renewable energy technology. In the third periodic solution, however, also R&D investments are positive and, hence, as a positive knowledge stock reduces the investment costs, more renewable energy capital is affordable, and therefore more renewable energy can be generated.

Interpretation	Parameter	Value	Interpretation	Parameter	Value
Investment costs	b	0.6	LS* ² coefficient	α_2	0.2
Adjustment costs	c	0.3	Depreciation rate of K_S	δ_S	0.03
Linear research costs	d	0.3	Depreciation rate of K_R	δ_R	0.02
Non-linear research costs	e	0.6	Initial investment costs for K_S	ε_1	1
Energy demand	E	2000	Initial research costs for K_R	ε_2	1
Fossil energy price	p_F	0.047	Degree of efficiency	η	0.2
Discount rate	r	0.04	Maximal radiation increment	ν	4.56
LD* ¹ coefficient	α_1	0.25	Minimal radiation in winter	τ	0.79

*¹... learning by doing *²... learning by searching

Table 4.1: Parameter values used for the numerical analysis.

Considering the stability of the obtained periodic solutions, we already have analytically proven in Section 4.2.3 that the fossil periodic solution always is of saddle-type. For the two other periodic solutions the numerical calculation of the monodromy matrix shows that they are of saddle-type as well. The mixed periodic solution, however, has only a 1-dimensional stable manifold, while the mixed periodic solution with research as well as the fossil periodic solution have a 2-dimensional manifold. The three periodic solutions are plotted in the state space in Figure 4.1, and their state and control values together with the corresponding eigenvalues are summarized in Table 4.2. Further on, the time-control and time-state paths for these three periodic solutions are plotted in Figure 4.2. Note that also the R&D investments as well as the stock of knowledge slightly fluctuate over the year in accordance with the investments in renewable energy capital so that the slightly higher knowledge stock compensates for the slightly lower renewable energy capital stock. Moreover, also here the fluctuations in knowledge as well as in renewable energy capital already imply forgetting by not doing. But similar to the results obtained in Chapter 3, the fluctuations are so small that this forgetting process is negligibly small as well.

Summing up, we have two periodic solutions of saddle-type with a 2-dimensional stable manifold whose areas of attraction probably are separated, induced by the periodic solution of saddle-type in-between with only a 1-dimensional manifold. In contrast to the previous model approach, however, this separation here is not further given by a single indifference threshold point but by an indifference threshold curve, as we have two states in the current approach.

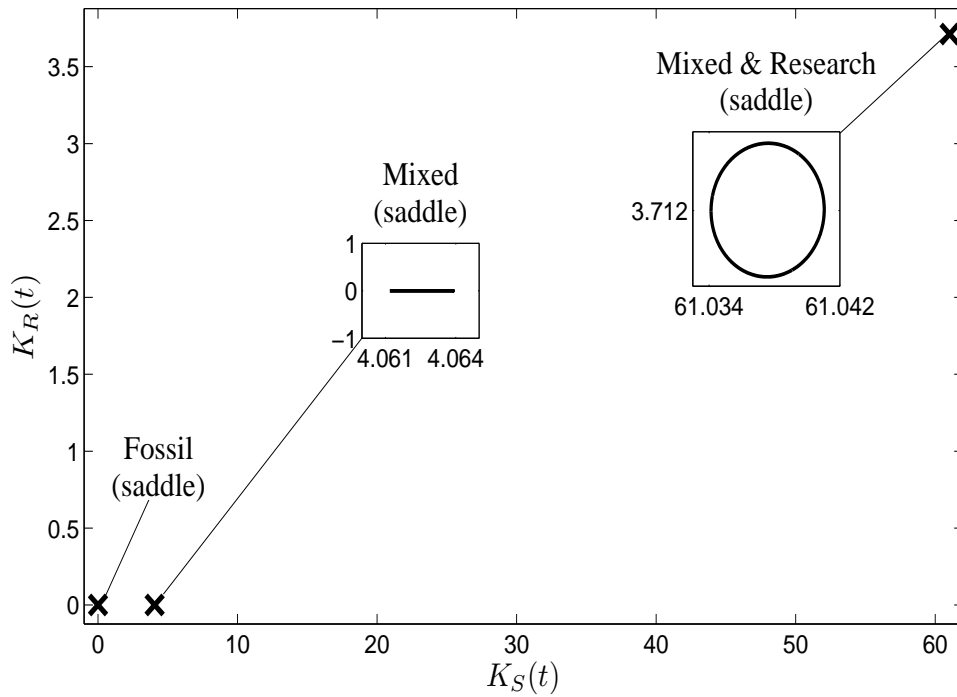


Figure 4.1: The three detected periodic solutions for a fossil energy price $p_F = 0.047$ in the state-space.

Solution	$K_S^*(0)$	$K_R^*(0)$	$E_F^*(0)$	$I_S^*(0)$	$I_R^*(0)$	Eigenvalues	Objective function
Fossil	0.0000	0.0000	2000.0	0.0000	0.0000	{0.9704, 0.9802, 1.0618, 1.0725}	-92.1448
Mixed	4.0612	0.0000	1999.36	0.1218	0.0000	{1.0618, 0.9802, 1.0195+0.0390i, 1.0195-0.0390i}	-92.0806
Mixed & Research	61.0341	3.7120	1990.36	1.8309	0.0743	{0.9513, 0.9824, 1.0941, 1.0594}	-90.9825

Table 4.2: Multiple periodic solutions for $p_F = 0.047$.

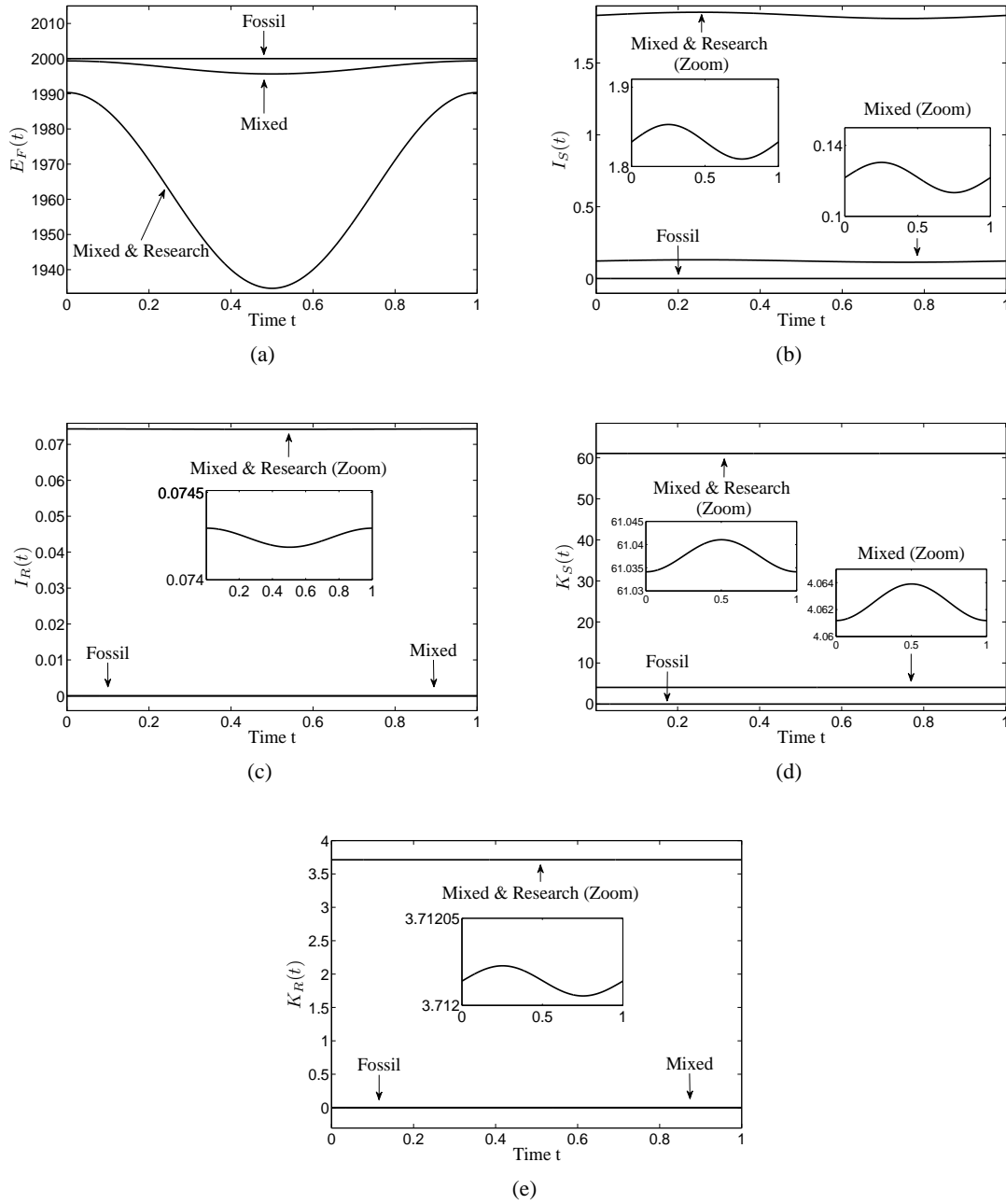


Figure 4.2: Time-control paths for the three obtained periodic solutions for a fossil energy price $p_F = 0.047$ in (a) fossil energy amount $E_F(t)$, (b) renewable energy investments $I_S(t)$, and (c) research investments $I_R(t)$, as well as time-state paths in (d) renewable energy capital $K_S(t)$, and (e) knowledge $K_R(t)$.

4.3.1 Calculation of the Indifference Threshold Curve

An indifference threshold curve in our model approach is a curve that lies in the K_S - K_R -state space and separates the areas of attraction of two periodic solutions in the sense that two paths having the same initial states on the indifference threshold curve and leading into the two periodic solutions, respectively, have the same objective values. Hence, along this curve one is indifferent between these two periodic solutions.

In order to investigate whether an indifference threshold curve exists, we first have to find out if any of the obtained periodic solutions is dominated. To begin with, we focus on the mixed periodic solutions with only a 1-dimensional stable manifold. Therefore, we try to calculate a path that starts at this periodic solution and leads into the mixed periodic solution with research. For the calculation of the objective values, we enlarge again the canonical system by introducing the differential equation

$$\dot{c}(t) = e^{-rt} \left(-I_S(t) \left(b + cI_S(t) \right) \left(K_S(t) + \varepsilon_1 \right)^{-\alpha_1} \left(K_R(t) + \varepsilon_2 \right)^{-\alpha_2} - I_R(t) \left(d + eI_R(t) \right) - p_F E_F(t) \right),$$

as done in Section 3.3.1. The continuation of the path is possible and is plotted in Figure 4.3a, while Figure 4.3b shows the objective values along the continuation of this path, compared to the objective value if the decision is to stay in the mixed periodic solution. As one can see, the path leading into the mixed periodic solution with research has a better performance and, consequently, the mixed periodic solution is dominated. In what follows, we will therefore refer to it as the dominated periodic solution.

Considering the other two solutions, the fossil and the mixed one with research, we try to continue a path starting at one periodic solution and leading into the other one as far as possible and vice versa, until either the continuation process aborts as the path reaches some boundary of the feasible domain, the path is bending back, or the target value starting at the other periodic solution is reached. Figure 4.4 shows the resulting paths for $p_F = 0.046$. In this case, the continuation process stops as both paths reach boundaries of the feasible domain. One can see that there exist intervals for both states where the paths overlap. Within these intervals we compare the objective value curves, which is illustrated in Figures 4.5a and 4.5b. As it turns out, none of the two periodic solutions is dominated by the other and an indifference threshold point occurs, which is determined by the intersection of these two curves. Given this first indifference threshold point, the goal is to continue the indifference threshold curve along one of the two states. To do so, we use this indifference threshold point as starting solution for solving the boundary value problem presented

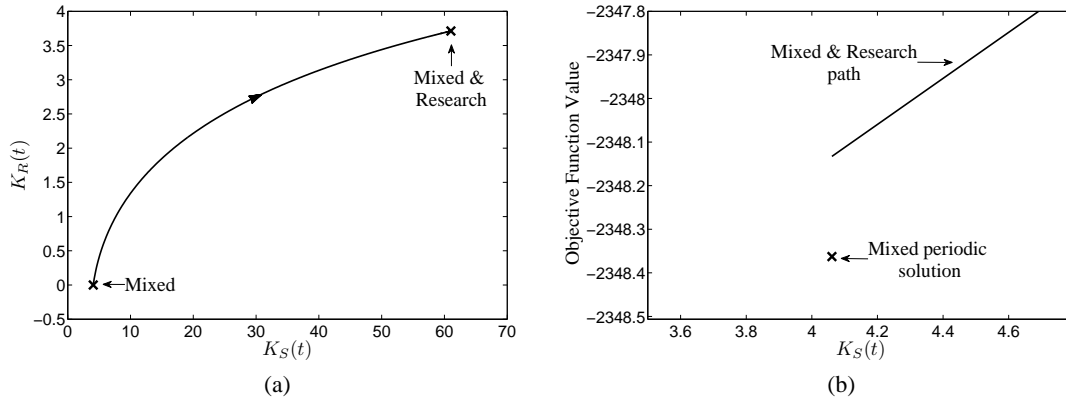


Figure 4.3: Dominance over the mixed periodic solution for a fossil energy price $p_F = 0.047$: **(a)** Continued path leading from the mixed periodic solution into the mixed periodic solution with research. **(b)** Comparison of the objective values.

in what follows.

Let

$$y_1(t) := (K_S^1(t), K_R^1(t), \lambda_1^1(t), \lambda_2^1(t)), \quad t \in [0, T_p^1],$$

$$y_2(t) := (K_S^2(t), K_R^2(t), \lambda_1^2(t), \lambda_2^2(t)), \quad t \in [0, T_p^2],$$

define the fossil path and the mixed-path with research, respectively, leading into the corresponding periodic solution and starting at the first obtained indifference threshold point. T_p^1 and T_p^2 are the truncation times of these two paths. It holds that

$$0 = F_1'(y_1(T_p^1) - \Gamma_1(0)), \quad (4.22)$$

$$0 = F_2'(y_2(T_p^2) - \Gamma_2(0)), \quad (4.23)$$

where F_i , $i \in \{1, 2\}$, are the orthogonal complements to the stable eigenspace, respectively, and Γ_i , $i \in \{1, 2\}$, denote the periodic solutions. As both paths start at the indifference point, they have the same objective value, denoted as $OV(\cdot)$ in the following, so

$$OV(y_1(T_p^1)) = OV(y_2(T_p^2)). \quad (4.24)$$

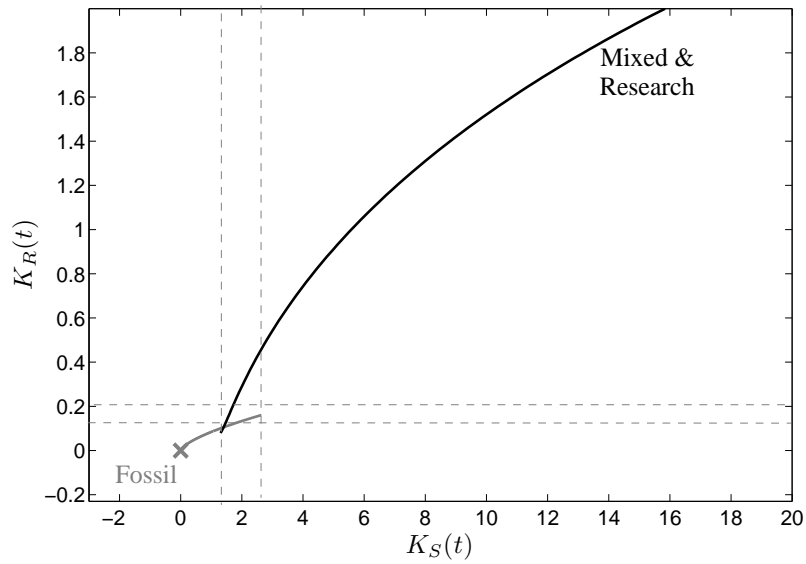


Figure 4.4: Overlap of trajectories leading into the two periodic solutions for a fossil energy price $p_F = 0.047$.

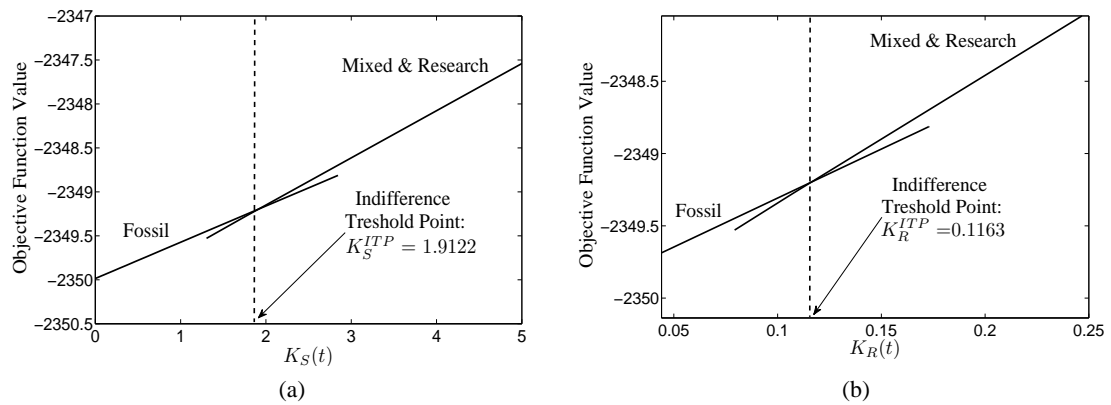


Figure 4.5: Indifference threshold point for a fossil energy price $p_F = 0.047$: Intersection of the objective function values along the (a) K_S -axis, (b) K_R -axis.

Therefore, in order to find another point on the indifference threshold curve, another pair of solution paths $\{\hat{y}_1(t), \hat{y}_2(t)\}$ has to be found that satisfies (4.22)-(4.24) with both having the same initial state values. Let $f_{a_i}(t, y_i(t))$ denote in general notation the canonical system for the different regions according to the introduced index in (4.8), $T(s)$ be the linear time transformation of (3.20) but this time only for two arcs so $i = 1, 2$, let further $T_p = T_p^1 + T_p^2$ be the total truncation time, and τ be the switching time between the two arcs. Further assume that N continuation steps are needed in order to continue the indifference threshold curve separating the areas of attraction of the fossil periodic solution and the mixed periodic solution with research, until it finally reaches the required state value. Then, at each step $n = 1, \dots, N$, the following boundary value problem has to be solved,

$$\dot{y}_1(s) = T_p \tau f_4(T(s), y_1(s)), \quad s \in [0, 1], \quad (4.25)$$

$$\dot{y}_2(s) = T_p (1 - \tau) f_2(T(s), y_2(s)), \quad s \in [1, 2], \quad (4.26)$$

$$0 = y_1^n(0)_{\{1,2\}} - y_2^n(1)_{\{1,2\}}, \quad (4.27)$$

$$0 = OV(y_1^n(1)) - OV(y_2^n(2)), \quad (4.28)$$

$$0 = F_1'(y_1^n(1) - \Gamma_1(0)), \quad (4.29)$$

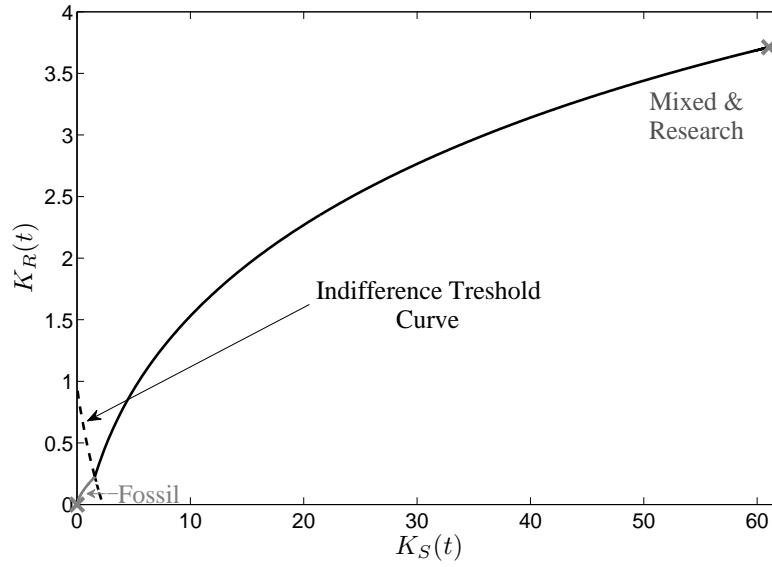
$$0 = F_2'(y_2^n(2) - \Gamma_2(0)), \quad (4.30)$$

$$0 = y_1^n(0)_{\{1\}} - K_{S_0}^n, \quad \text{or} \quad 0 = y_1^n(0)_{\{2\}} - K_{R_0}^n. \quad (4.31)$$

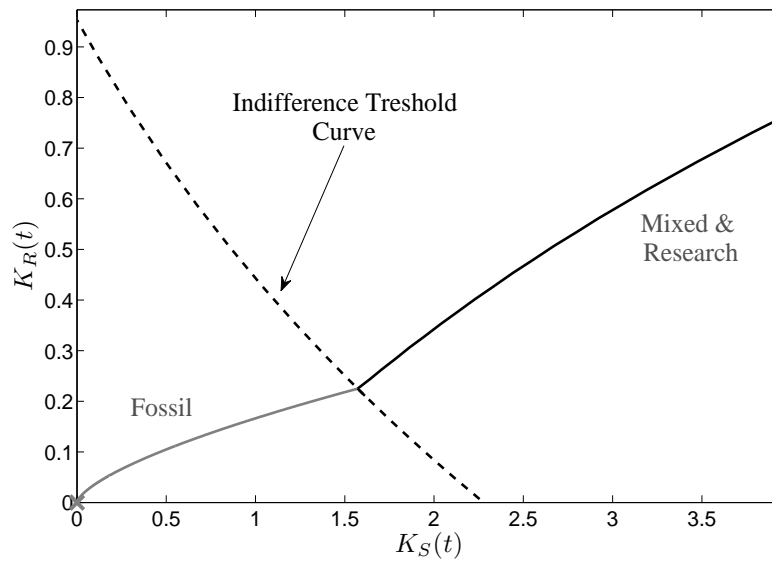
The subscripts in $\{.\}$ refer to the coordinates of the paths, $\{K_S(t), K_R(t), \lambda_1(t), \lambda_2(t)\}$. As already mentioned, the continuation takes place along one state, while the other one is left unrestricted. Therefore, in (4.31) both possibilities are mentioned. For more details on the continuation of the indifference threshold curve see Grass (2012). Numerically, the problem is solved again with the Moore-Penrose method. Solving this for the current parameter set yields the indifference threshold curve, shown in Figures 4.6a and 4.6b.

4.3.2 Economic Interpretation of the Indifference Threshold Curve

Similar to the interpretation of the indifference threshold point in Chapter 3, also here the indifference threshold curve supplies information whether a portfolio with renewable energy is profitable in the long run or not, depending on the starting point. But while in Chapter 3 this decision has been based only on the initial stock of renewable energy capital, it here also depends on the accumulated stock of knowledge that contributes to the performance of renewable energy generation



(a)



(b)

Figure 4.6: (a) Indifference threshold curve separating the areas of attraction of the fossil periodic solution and the mixed and research periodic solution for a fossil energy price $p_F = 0.047$, (b) Zoom.

in form of reduced investment costs. The indifference threshold curve is shown in Figures 4.6a and 4.6b as black dashed line. If the initial states lie beyond this curve, this implies that the stock of renewable energy capital as well as the stock of knowledge are high enough to compensate for the initially very high investment costs of the renewable energy technology, and hence a portfolio of both energy types is profitable in the long run in order to cover the given energy demand. If they lie beneath, the available knowledge and the renewable energy capital stock are too low and, hence, due to the still very high investment costs it is better to stop all investments and only use fossil energy in the long run to cover the given energy demand. Note that also here the accumulation of new capital, the maintenance of already existing capital, as well as R&D efforts stop and, consequently, forgetting by not doing in both factors increase again the investment costs. If one starts exactly on the curve, one is indifferent whether to include renewable energy in the long run into the portfolio or not.

Further on, one can observe that a marginal reduction in the stock of renewable energy capital can be compensated by a marginal increase in the stock of knowledge in terms of profitability, and vice versa. In the extreme case, when the initial stock of renewable energy capital is zero, one can see that still a portfolio with both energy types can be optimal in the long run, if the initial stock of knowledge is high enough. Note that this is in contrast to the results of Chapter 3, where it turned out that a start with renewable energy generation from the very beginning never can be optimal. Here, it can be optimal, postulated that at least R&D efforts have already been done and the accumulated knowledge is high enough to reduce the initially high investment costs. This, of course, also holds the other way round. If there haven't been R&D efforts so far, but the initial stock of renewable energy capital is high enough, it still can be optimal to invest further in renewable energy capital and, in addition, make R&D investments.

These results underline the fact that not only subsidies for investments into renewable energy capital can be helpful for the introduction of a new energy technology into the market, as suggested in Chapter 3, but also subsidies for R&D efforts on this field. As investment costs for a new technology are very high and, hence, the competitiveness with conventional technologies is not given, subsidizing R&D efforts would increase the stock of knowledge and simultaneously decline the investment costs a bit, until, finally, a start-up with the new technology is profitable.

4.3.3 Break-Even Analysis

In order to investigate how the investment costs decline along the path leading into the mixed optimal long-run periodic solution with research, we next conduct a similar analysis as in Sec-

tion 3.3.3. This time, however, we have two effects that simultaneously reduce the investment costs of renewable energy. On the one hand, there is the learning-by-doing effect which we have considered extensively in Chapter 3. On the other hand, we have the learning-by-searching effect that also contributes to the cost reduction but requires additional R&D investments. To see how the costs change along such a path when also learning by searching is included, we consider the investment costs per unit of generated renewable energy (unit investment costs) given by the term

$$\frac{I_S^*(t)(b + cI_S^*(t))(K_S^*(t) + \varepsilon_1)^{-\alpha_1}(K_R^*(t) + \varepsilon_2)^{-\alpha_2} + I_R^*(t)(d + eI_R^*(t))}{(v \sin^2(t\pi) + \tau)K_S^*(t)\eta}, \quad (4.32)$$

along the mixed-path with research plotted in Figure 4.6.

The result can be seen in Figure 4.7. As the generation of renewable energy occurs in the denominator of Equation (4.32), the fluctuation in global radiation is also reflected in the unit investment costs. At the beginning of the path, the unit investment costs are very high as almost no renewable energy capital is available and also the knowledge stock is very low. As it gets obvious in the K_S - K_R -plane, along the first part of the path, the focus rather lies on accumulation of knowledge by R&D investments although they come at some cost and cause an initial increase in the unit investment cost function. This is because the considered learning effects are only with respect to investment costs for renewable energy capital, not for R&D efforts. Therefore, in case the initial point lies above the indifference threshold curve, it is always profitable to first increase the knowledge stock up to a sufficiently high level to then fully utilize the learning effect for the accumulation of renewable energy capital. This is also in accordance with the observed aspect that in this model approach with learning in two factors, a complete start-up with renewable energy generation can be profitable as long as already sufficient knowledge is accumulated. Due to the learning-by-searching effect, knowledge reduces the high investment costs, so that accumulation of renewable energy capital gets profitable. From then on, also the learning-by-doing effect contributes to this decline and a change in the investment regime can be observed. While at the beginning R&D investments were dominant, they saturate along the path and investments for renewable energy capital strongly increase, until finally the break-even point, where the unit investment costs are equal to the fossil energy price, is reached and the path ends in the optimal long-run periodic solution. Note, however, that the unit investment costs do not stay at the competitive level of the fossil energy price over the whole year. Similar to the results in Chapter 3, also here they lie above the fossil energy price in winter and slightly below it in summer.

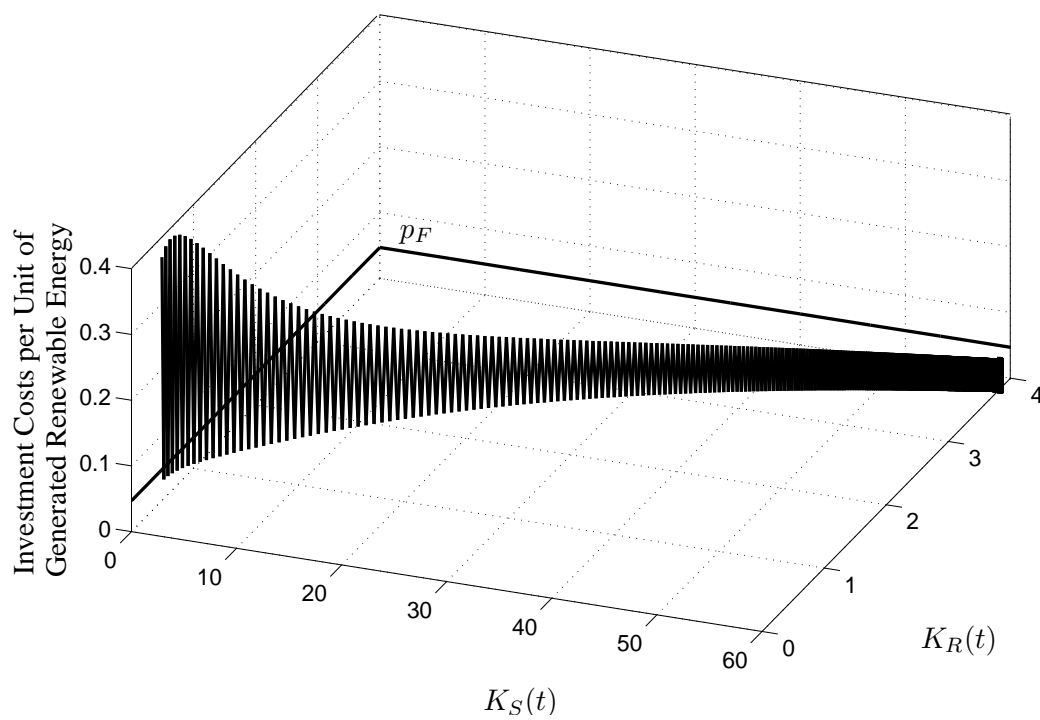


Figure 4.7: Investment costs per unit of generated renewable energy along the path leading into the mixed optimal long-run periodic solution with research for a fossil energy price $p_F = 0.047$.

4.4 Sensitivity Analysis

As the results of the previous section have shown, also in this approach with both learning by doing and learning by searching included into the model, history dependence occurs. However, this time the analysis was carried out not only with respect to the initially installed renewable energy capital but also with respect to the initial knowledge stock. Whether it is profitable or not to further invest in renewable energy generation in order to approach the mixed periodic solution is indicated by the indifference threshold curve which separates the areas of attraction. This profitability, of course, is strongly dependent on the competitiveness of the renewable technology with the conventional one. Similar to the sensitivity analysis of the previous chapters, in this section we also focus on the investigation of the changes in the optimal portfolio composition and the shift of the indifference threshold curve, when the fossil energy price p_F changes. Further on, we use again the different scenarios of Section 3.4.3 to investigate the changes in the optimal portfolio composition when the global radiation intensity varies due to different geographical conditions.²

4.4.1 Fossil Energy Price p_F

Before we start with the continuation of the periodic solutions along the fossil energy price axis, we first consider the calculation of the indifference threshold curve for a slightly lower fossil energy price $p_F = 0.046$, which exhibits some specialties.

Calculation of the Indifference Threshold Curve for $p_F = 0.046$

As we have done in Section 4.3.1, we first continue the fossil path and the mixed-path with research as far as possible. If we get a sufficiently large overlap so that an intersection point of the objective function values along the paths occurs, we can find a first indifference threshold point. With these first starting solutions we solve the boundary value problem (4.25)-(4.31) in order to calculate the corresponding indifference threshold curve, first towards the K_R -axis and second towards the K_S -axis, respectively. In both directions, however, the continuation process aborts as one of the paths gets infeasible. Figure 4.8a shows the Lagrange multiplier μ_3 along the fossil paths starting at the so far calculated indifference threshold curve. As one can see, it declines towards zero and hence the path reaches the feasible boundary of the mixed case with positive investments in renewable energy capital I_S . We therefore calculate a multi-arc path by continuing the fossil path into the

²As the learning-by-searching effect is identically modeled as the learning-by-doing effect, a sensitivity analysis with respect to the learning-by-searching coefficient would not provide new insights qualitatively. We therefore neglect this aspect in the carried out analysis.

mixed region. However, very soon investments get zero again and hence, a switch back to the fossil region happens. The complete path therefore is a multi-arc path consisting of two fossil arcs and one mixed arc in-between, shown as black line in Figure 4.8a. The resulting path in the state-control space can be seen in Figure 4.8b. During the continuation of the indifference threshold

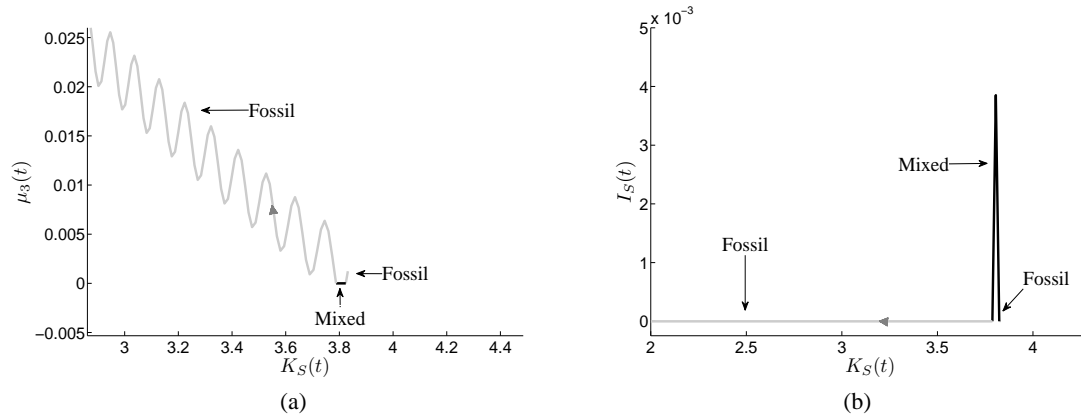


Figure 4.8: Multi-arc path consisting of two fossil arcs and one mixed arc in-between leading into the fossil periodic solution for a fossil energy price $p_F = 0.046$: **(a)** the Lagrange multiplier along the path, **(b)** the path in the state-control space.

curve towards the K_R -axis, the mixed-path with research gets infeasible as R&D investments get zero, therefore the Lagrange multiplier μ_4 gets positive, and hence the feasible boundary of the mixed case is reached, as shown in Figure 4.9a. Therefore, also here a switch happens to the mixed region, where still investments in renewable energy capital are made, but no further investments in knowledge accumulation. The resulting path consequently consists of two arcs, one belonging to the mixed case with research and the second one corresponding to the mixed case (without research), as shown in Figure 4.9b.

Given these new and corrected paths, the continuation of the indifference threshold point can be carried on. This time, however, we do not only have to consider the marginal conditions that guarantee the indifference along the curve, but also the marginal conditions for the continuity of the multi-arc paths. To demonstrate this in more detail, assume that we have two paths, $y_1(t)$ and $y_2(t)$, consisting of m and k arcs, respectively, and leading with the truncation times of T_p^1 and T_p^2 into the two periodic solutions, which are denoted as $\Gamma_1(t)$ and $\Gamma_2(t)$ in what follows. Further on, assume that N continuation steps are needed for the calculation of the indifference threshold curve. Then, at each step $n = 1, \dots, N$, we have to consider the time transformation $T(s)$ of (3.20)

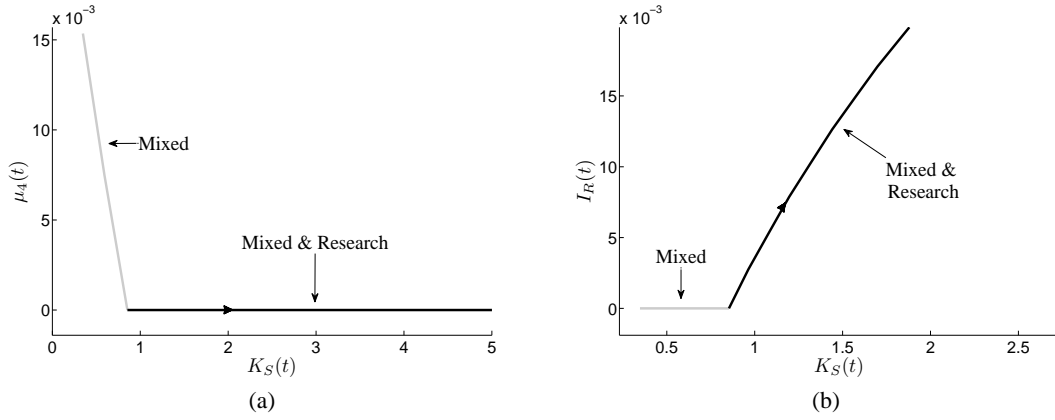


Figure 4.9: Multi-arc path consisting of a mixed arc and a mixed arc with research leading into the mixed periodic solution with research for a fossil energy price $p_F = 0.046$: **(a)** the Lagrange multiplier along the path, **(b)** the path in the state-control space.

and the $m + k - 1$ switching times,

$$\tau_0 := 0 < \tau_1 < \dots < \tau_m < \tau_{m+1} < \dots < \tau_{m+k-1} < 1 =: \tau_{m+k},$$

for which we have to solve for $T_p = T_p^1 + T_p^2$, $u = 1, \dots, m$, and $v = 1, \dots, k$,

$$\dot{y}_{1u} = T_p(\tau_u - \tau_{u-1})f_{a_u}(T(s), y_{1u}(s)), \quad s \in [u-1, u], \quad (4.33)$$

$$\dot{y}_{2_{m+v}} = T_p(\tau_{m+v} - \tau_{m+v-1})f_{a_{m+v}}(T(s), y_{2_{m+v}}(s)), \quad s \in [m+v-1, m+v], \quad (4.34)$$

$$0 = y_{1_1}^n(0)_{\{1,2\}} - y_{2_{m+1}}^n(m)_{\{1,2\}}, \quad (4.35)$$

$$0 = OV(y_{1_m}^n(m)) - OV(y_{2_{m+k}}^n(m+k)), \quad (4.36)$$

$$0 = F_1'(y_{1_m}^n(m)) - \Gamma_1(0), \quad (4.37)$$

$$0 = F_2'(y_{2_{m+k}}^n(m+k)) - \Gamma_2(0), \quad (4.38)$$

$$0 = y_{1_1}^n(0)_{\{1\}} - K_{S_0}^n, \quad \text{or} \quad 0 = y_{1_1}^n(0)_{\{2\}} - K_{R_0}^n, \quad (4.39)$$

$$0 = y_{1_i}^n(\tau_i) - y_{1_{i+1}}^n(\tau_{i+1}), \quad \forall i = 1, \dots, m-1 \quad (4.40)$$

$$0 = y_{2_{m+j}}^n(\tau_{m+j}) - y_{2_{m+j+1}}^n(\tau_{m+j+1}), \quad \forall j = 1, \dots, k-1 \quad (4.41)$$

$$0 = c(a_i, a_{i+1}), \quad \forall i = 1, \dots, m-1 \quad (4.42)$$

$$0 = c(a_{m+j}, a_{m+j+1}), \quad \forall j = 1, \dots, k-1, \quad (4.43)$$

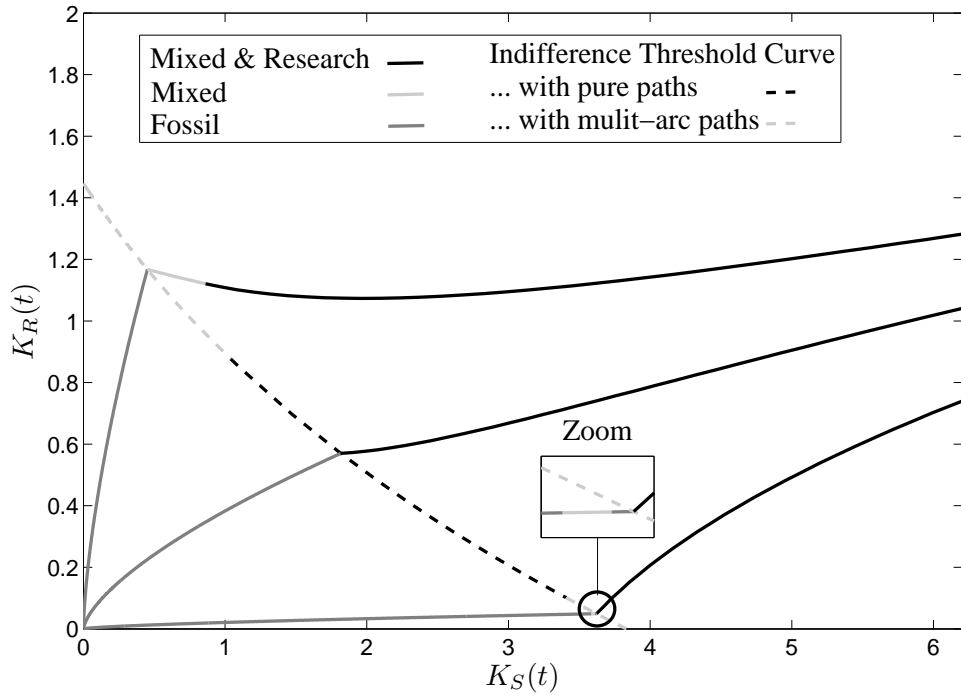


Figure 4.10: Indifference threshold curve for a fossil energy price $p_F = 0.046$ along which multi-arc solution paths occur.

where y_{1_u} and y_{2_v} denote the current arc solution and \dot{y}_{1_u} and \dot{y}_{2_v} are the corresponding canonical system equations, depending on the current region. Note that (4.35)-(4.39) are the same conditions as in (4.27)-(4.31), while (4.40)-(4.43) correspond to the continuity conditions of (4.14)-(4.18).

Solving this boundary value problem for the calculated paths with multiple arcs yields the complete indifference threshold curve that is shown in Figure 4.10. The black part of the indifference threshold curve belongs to the region where both paths leading into the periodic solutions consist of only one arc (pure path), while along the two gray parts one of the two involved paths has several arcs. To illustrate this in more detail, for each part of the indifference threshold curve a pair of paths is plotted in Figure 4.10.

Continuation of the Periodic Solutions along the p_F -Axis

In order to continue the obtained periodic solutions along the p_F -axis, we use also here the single shooting method explained in Section 3.4.1 to find a fixed point of the Poincaré map of the slightly

perturbed canonical system. Figures 4.11a and 4.11b show the results for the starting points $K_S^*(0)$ and $K_R^*(0)$ of the periodic solutions, respectively. To avoid ambiguity, note that we will consider the changes of the indifference threshold curve separately later and focus here only on the changes in the number and the position of the periodic solutions that can be found.

For a fossil energy price $p_F < 0.0409$ the only long-term periodic solution that exists is the fossil one, which is of saddle-type. Here, fossil energy is so cheap that neither investments into renewable energy capital nor into R&D efforts are profitable, and hence it is optimal to cover the whole energy demand with fossil energy in the long run.

As soon as $p_F > 0.0409$, two additional periodic solutions occur, where both correspond to the mixed case with research and are of saddle-type, but the higher one has a 2-dimensional stable manifold while the lower one only has a 1-dimensional one. If the fossil energy price further increases, the higher mixed periodic solution with research also increases as investments in both, renewable energy capital as well as R&D efforts, get more profitable. In contrast, the lower periodic solution declines until finally at $p_F = 0.0448$ the investments into R&D efforts get zero and hence a transition to a mixed periodic solution without research occurs, which is also of saddle-type with a 1-dimensional stable manifold and responsible for the tiny kink in Figure 4.11a. This periodic solution further decreases in p_F until also the investments into renewable energy capital get zero at $p_F = 0.063$ and a transition to a multi-arc solution with fossil and mixed arcs occurs. Also this multi-arc solution is of saddle-type and has a 1-dimensional stable manifold.

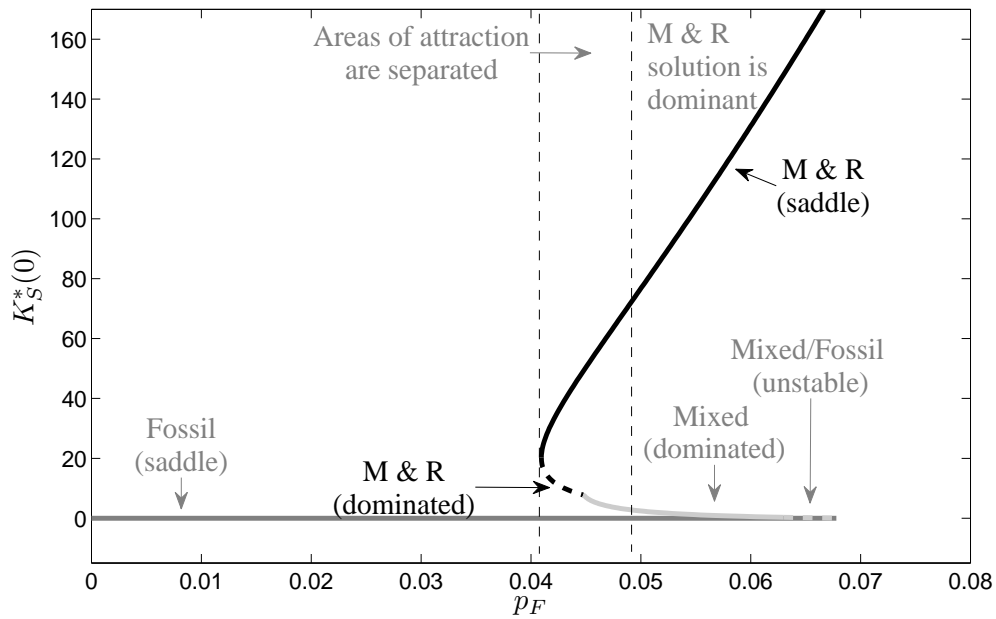
From Figures 4.11a and 4.11b one can observe that also for this two-factor model, the fossil solution is only existent up to a specific fossil energy price. Similar to the calculation in Section 3.4.1 we will determine this price level in what follows. As the first adjoint equation of this two-factor model for the fossil case coincides with the adjoint equation of the one-factor model for the fossil case, the analytical solution for $\lambda_1(t)$ is equal to (3.29), given by

$$\lambda_1(t) = \frac{p_F \eta \left((4\pi^2 + (r + \delta_S)^2)(v + 2\tau) + (r + \delta_S)v(2\pi \sin(2\pi t) - (r + \delta_S) \cos(2\pi t)) \right)}{2(r + \delta_S)(4\pi^2 + (r + \delta_S)^2)}.$$

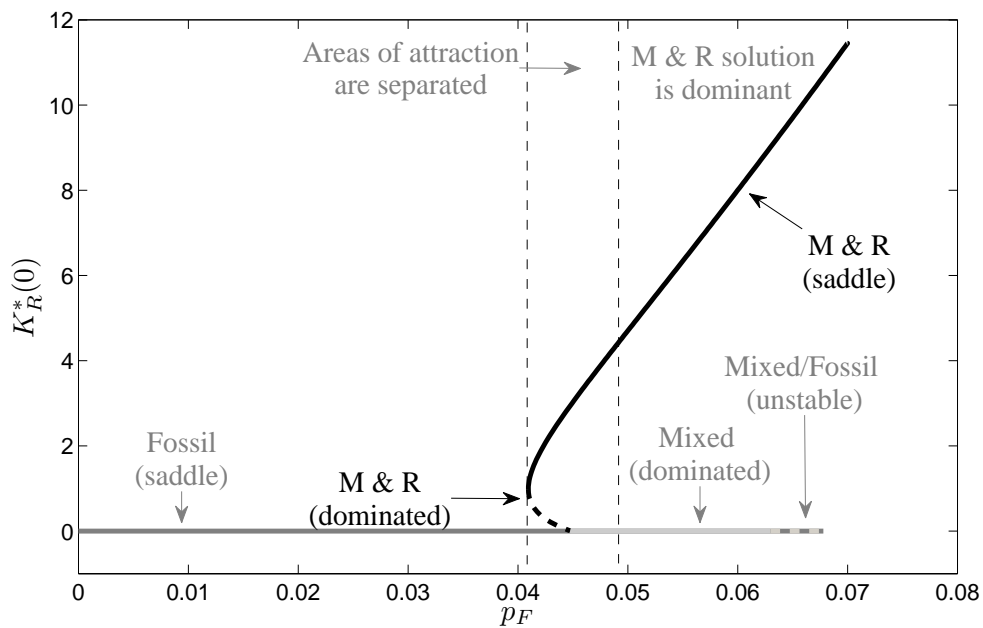
The equation for the Lagrange multiplier,

$$\mu_3(t) = b(K_S(t) - \varepsilon_1)^{-\alpha_1} (K_R(t) - \varepsilon_2)^{-\alpha_2} - \lambda(t), \quad (4.44)$$

shows that also here the reason for the limited existence of the fossil solution is given by $\mu_3(t)$



(a)



(b)

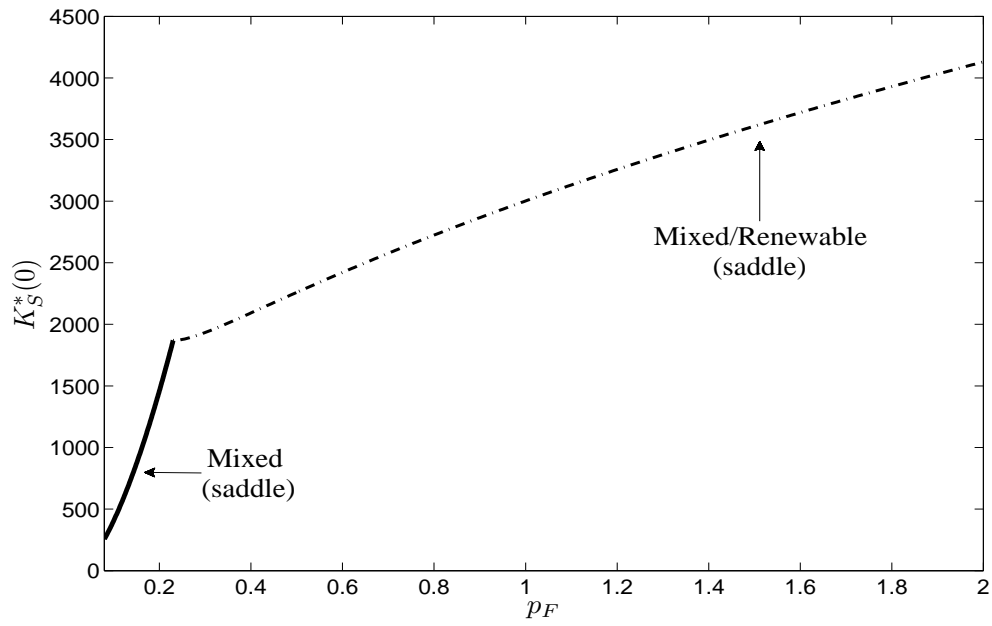
Figure 4.11: Bifurcation diagram of the canonical system with respect to a fossil energy price $p_F \leq 0.08$, showing (a) $K_S(0)$, (b) $K_R(0)$.

getting negative at some fossil energy price level, which can be calculated as

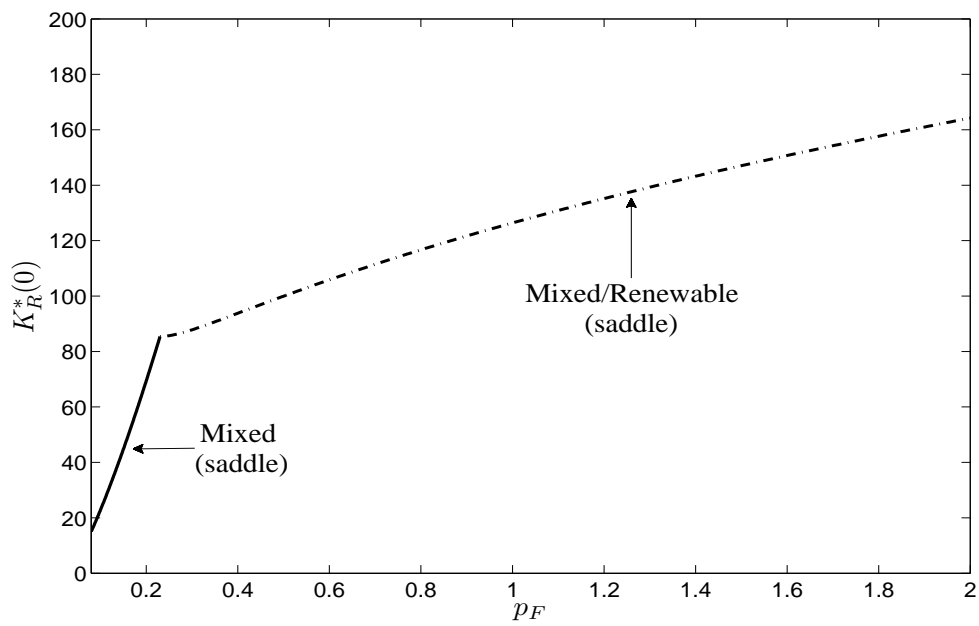
$$\bar{p}_F(\cdot) = \frac{2b(r + \delta_S)(4\pi^2 + (r + \delta_S)^2)(K_S(t) + \varepsilon_1)^{-\alpha_1}(K_R(t) + \varepsilon_2)^{-\alpha_2}}{\eta((4\pi^2 + (r + \delta_S)^2)(v + 2\tau) + (r + \delta_S)v(2\pi \sin(2\pi t) - (r + \delta_S)\cos(2\pi t)))},$$

which is a function of $K_S(t)$, $K_R(t)$, and time t . As the derivative of (4.44) with respect to λ_1 is negative, similar to Section 3.4.1 the first violation of $\mu_3 \geq 0$ when p_F is increased occurs at a peak of the periodic fluctuations of λ_1 . Inserting the corresponding time point t_{max} together with $K_S(t_{max}) = 0$ and $K_R(t_{max}) = 0$ yields, for the current parameter set, $\bar{p}_{F,t_{max}} = 0.0678$ until which the fossil solution is feasible. For a higher fossil energy price, however, a fossil-mixed periodic solution still is feasible, if the part along which $\mu_3(t)$ gets negative is again replaced by a mixed arc. As soon as $\mu_3(t)$ is already negative at the minimum of the periodic fluctuations of $\lambda_1(t)$ at some t_{min} , also this mixed-arc solution is not further feasible, which happens for the used parameter set at $\bar{p}_{F,t_{min}} = 0.0689$. For a fossil energy price even beyond this level, the only periodic solution is given by the mixed periodic solution with research being of saddle-type.

Figure 4.12 shows what happens if the fossil energy price p_F increases even further. As renewable energy generation progressively gets profitable due to the reduced investment costs by the accumulated experience as well as the accumulated knowledge so far, a strong increase both in renewable energy capital and the knowledge stock can be observed. Nevertheless, both energy types still are needed over the whole period in order to cover the given energy demand. Similar to the results in Section 3.4.1, also here there exists a price level at which renewable energy capital is so high that during summer, when global radiation reaches its maximum, the demand can even be covered without fossil energy. This here happens at $p_F = 0.2301$. At this point, the feasible boundary of the mixed case is reached and, consequently, a optimal long-run periodic solution occurs that consists of two mixed arcs and a renewable arc in-between, where the demand is covered only by renewable energy. If the fossil energy price increases even further, still both, the renewable energy capital stock as well as the knowledge stock, increase but obviously at a decreasing rate. Also here, the reason for this is that the marginal benefit of an additional unit of renewable energy capital declines due to the generated surpluses over summer, and consequently, also the marginal benefit of R&D investments decreases.



(a)



(b)

Figure 4.12: Sensitivity analysis of the canonical system with respect to a fossil energy price $p_F \geq 0.08$, showing (a) $K_S(0)$, (b) $K_R(0)$.

Changes in the Indifference Threshold Curve with Respect to the Fossil Energy Price p_F

So far we have only considered how the solutions of the canonical system change with a varying fossil energy price p_F but not how the optimal long-run solution changes. To analyze this we first calculate the indifference threshold curves for different fossil energy price scenarios and see how the areas of attraction are separated, which are plotted in Figure 4.13. It gets obvious that for a low fossil energy price, the initial stocks of knowledge and renewable energy capital have to be very high, so that the learning-by-doing and learning-by-searching effect are strong enough to sufficiently reduce the investment costs in order to make further investments in renewable energy capital profitable at all. In these scenarios, the introduction of the renewable energy technology into the market is only possible with appropriately high financial support for example in form of subsidies, either for R&D investments or for investments in renewable energy capital. The higher the fossil energy price, the lower are the necessary initial stocks of knowledge and renewable energy capital at which further investments in renewable energy generation start to be profitable. Consequently, a parallel shift of the indifference curve towards the origin occurs. At a fossil energy price $p_F = 0.049$, however, the mixed periodic solution with research finally gets dominant and therefore, from here on the areas of attraction are not further separated.

To show these results also in 3 dimensions, we used these calculated indifference threshold curves to interpolate the indifference threshold surface for the considered fossil energy price interval $[0.046, 0.049]$,³ which is plotted in Figure 4.14. The black solid line shows the fossil periodic solution, while the position of the higher mixed periodic solution can only be indicated by an arrow for scaling reasons. The intersection of a 2-dimensional hyperplane in the K_S - K_R -space for a specific fossil energy price with the indifference threshold surface then yields the indifference threshold curve for this case.

Finally, looking at the rather small interval, in which an indifference curve exists, we conclude that the solution is fairly sensitive with respect to the fossil energy price p_F in that respect.

³Note that the indifference threshold surface in fact exists on the whole interval of $[0.04, 0.049]$, but due to reasons of clarity and accuracy, we only picked out this sub-interval to give a hint how the indifference threshold surface lies within the 3-dimensional space.

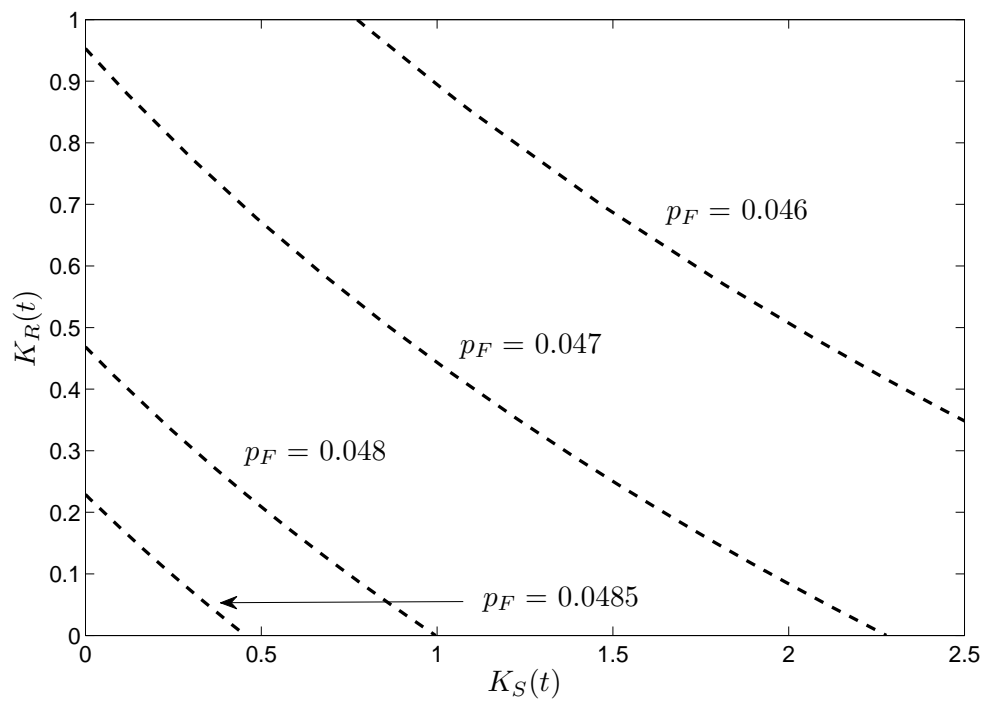


Figure 4.13: Indifference threshold curves for different fossil energy prices p_F .

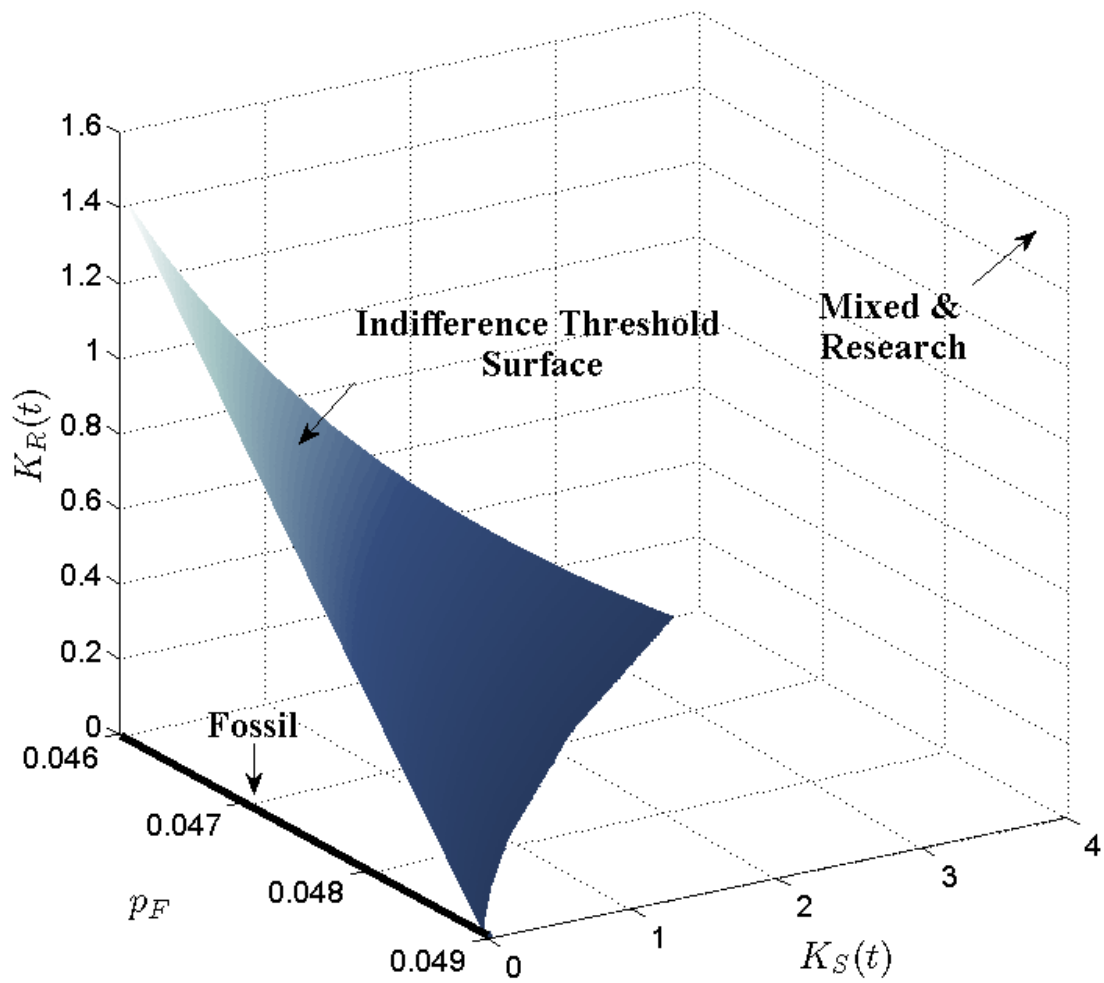


Figure 4.14: Indifference threshold surface separating the areas of attraction of the fossil periodic solution and the mixed periodic solution with research.

Bifurcation Analysis

Given the previous results, we investigate again the local behavior of the monodromy matrix to see how the optimal vector field changes along the p_F -axis. Figure 4.15 shows again the norms of the eigenvalues of the obtained periodic solutions. In contrast to the analysis in Chapter 3, we here have four eigenvalues for each periodic solution. According to the definition of stability for periodic solutions, described in Section 2.2.3, a periodic solution is of saddle-type, if at least one eigenvalue lies within and one outside the unit circle. As already determined in Section 4.2.3, every fossil solution that can be found for the current model approach is of saddle-type. In Figure 4.15, one can see that for the fossil case indeed the norms of two eigenvalues are above and two below 1. At $p_F = 0.0409$ again a fold-bifurcation occurs where an additional pair of mixed periodic solutions with research appears. The higher one is of saddle-type, as two eigenvalues lie within and two outside the unit circle. At the bifurcation point one eigenvalue crosses the unit circle. The lower mixed periodic solution with research consequently has only a 1-dimensional stable manifold, but it is still of saddle-type and is dominated, as we have already mentioned. At $p_F = 0.0448$, the R&D investments of this dominated mixed periodic solution with research get zero, and hence it changes to a mixed periodic solution without research, which also has only a 1-dimensional manifold as there are still three eigenvalues (one real and a pair of complex eigenvalues) outside and only one inside the unit circle. Note that the one inside the unit circle coincides with one eigenvalue of the fossil solution. This transition to another canonical system is also the reason for the small discontinuity in the complex eigenvalues. Finally, also the investments in renewable energy generation of this dominated mixed periodic solution get zero and it turns into a mixed/fossil solution at $p_F = 0.063$, which also has a 1-dimensional manifold and is dominated.

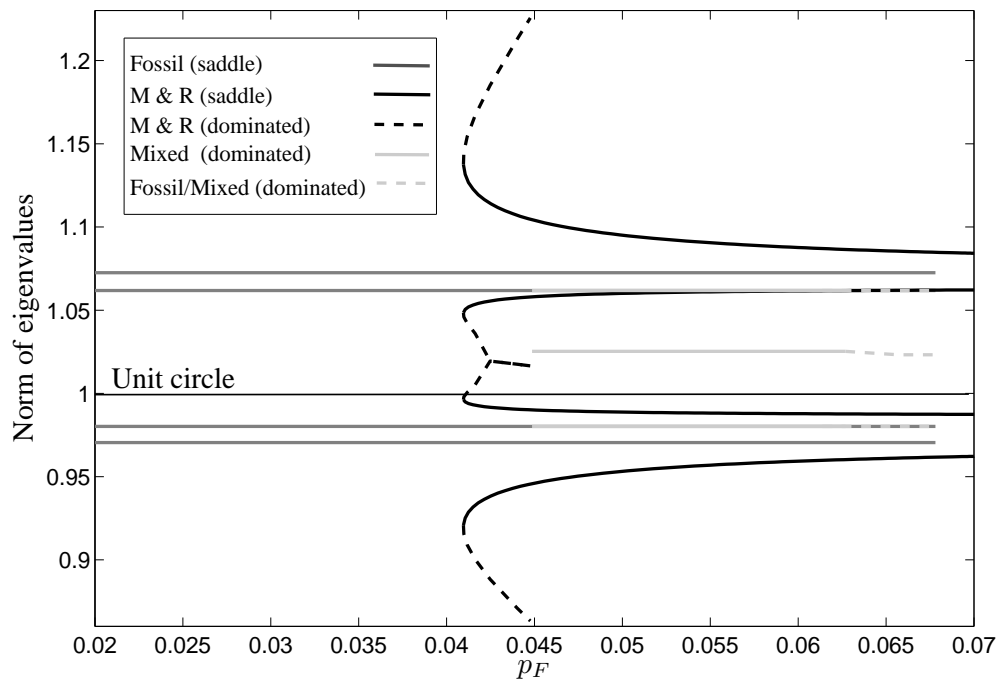


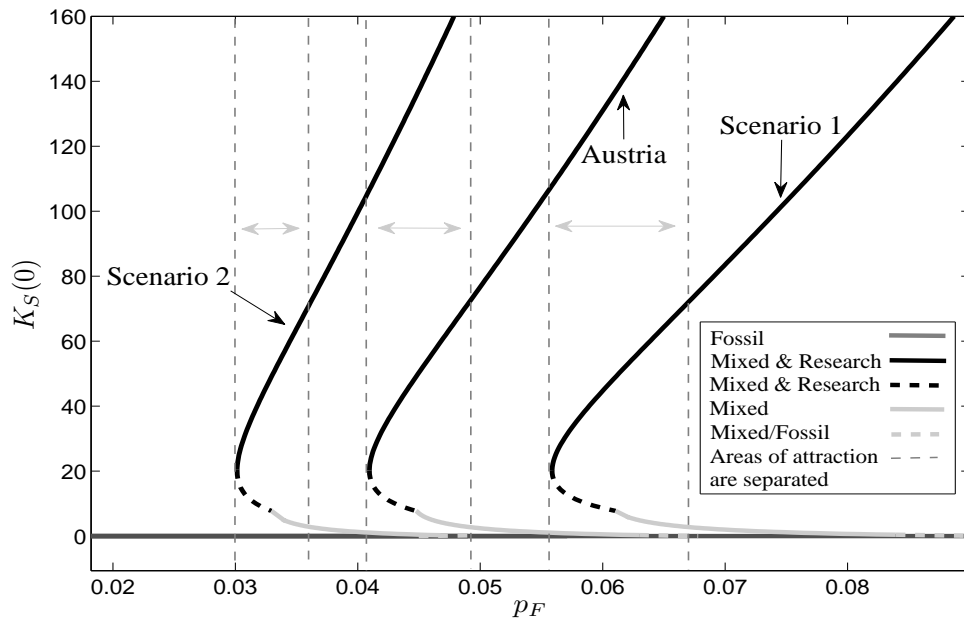
Figure 4.15: Norms of eigenvalues of the obtained periodic solutions along the p_F -axis.

4.4.2 Global Radiation Intensity

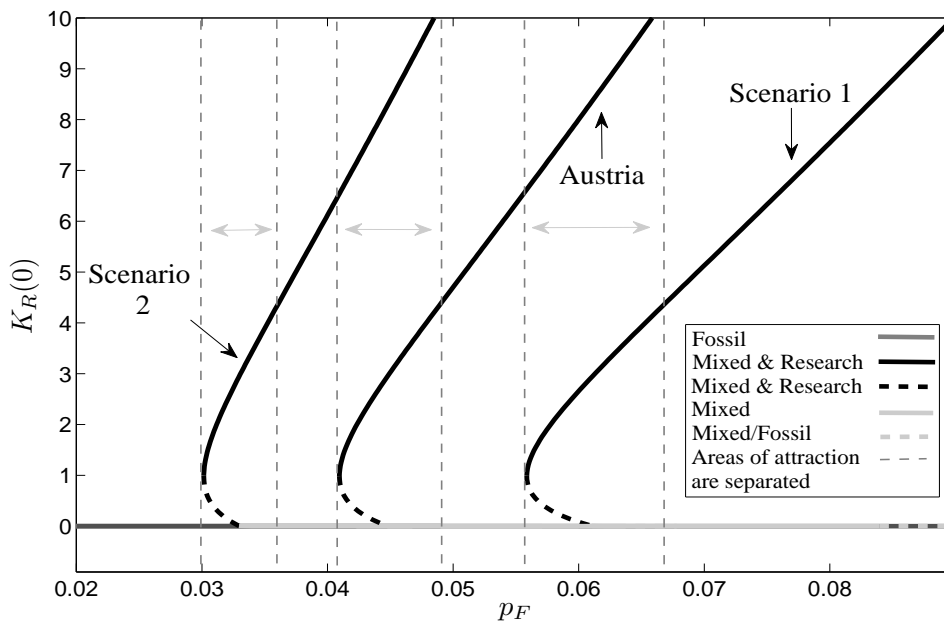
To investigate the changes in the bifurcation diagram in Figure 4.11 when the intensity of global radiation varies, we use again the two scenarios summarized in Table 3.3, where the first one corresponds to a northern country with a lower supply, and the second one to a southern country with a higher supply, compared to the original scenario for Austria.

Figure 4.16 shows the obtained results for all three scenarios both for $K_S(0)$ and $K_R(0)$. Similar to the results in Section 3.4.3, one can see that the changes in the global radiation intensity also here induce a shift along the p_F -axis, but this time in both states.

The interpretation is the following: In a northern country, where the global radiation intensity is lower, less renewable energy can be generated. Therefore, the fossil energy price at which renewable energy generation gets a considerable alternative and could be profitable in case capital and knowledge are sufficiently available, is higher than in the original scenario for Austria. This induces a shift to the right and implies that in order to foster renewable energy generation, a higher financial support for example in form of subsidies would be necessary than in the basic scenario. As for this reason the slope with which both states increase with the fossil energy price is lower, the fossil energy price interval in which the areas of attraction of the two periodic solutions are separated, is larger than in the original scenario for Austria. In contrast, for a southern country where the global radiation intensity and therefore the renewable energy generation is higher, the inclusion of renewable energy into the portfolio is a considerable alternative already at a lower fossil energy price than in the original scenario. This induces the shift to the left. Consequently, the need for financial support is lower and the interval, in which the areas of attraction of the two periodic solutions are separated, is smaller due to the higher slope with which both states increase with the fossil energy price.



(a)



(b)

Figure 4.16: Bifurcation diagram of the canonical system with respect to the fossil energy price p_F for Scenario 1 and 2 in comparison with the basic scenario in (a) $K_S(0)$, (b) $K_R(0)$.

4.5 Summary

In addition to the effect of learning by doing we have included in this Chapter the effect of learning by searching into the model by using a two-factor log-linear learning curve and adding a second state and a third control to the considered non-autonomous optimal control model. The representative energy-sector decision maker therefore does not only decide on the investments into renewable (solar) energy capital and the fossil energy amount that is bought, but also on R&D investments in order to accumulate knowledge and as consequently to reduce in addition investment costs for renewable energy capital.

The obtained results show that again history dependence occurs due to the learning effects, but this time not only for the renewable energy capital but also for the knowledge stock. We have seen from the calculated indifference threshold curves that an initially low renewable energy capital can be compensated by an initially higher knowledge stock and vice versa, in order to make further investments in both stocks profitable. Even if one of the two stocks is initially zero, an investment policy for renewable energy generation still can be profitable as long as the other initial stock is high enough. This is in contrast to the results of Chapter 3, where investments into renewable energy generation from the very beginning never would be optimal. If both investment stocks are too low or maybe even zero, however, also in this approach fossil energy is optimal and no further investments for renewable energy capital or R&D investments would be made. In this case, financial support for example in form of subsidies, would play a major role for a successful introduction of the renewable energy technology into the market, but this time not only support for investments into renewable energy capital but also for R&D efforts would be helpful during the start-up period of the new technology.

Discussion and Conclusion

In this thesis we have analyzed three different non-autonomous optimal control models in which we investigate the optimal composition of a portfolio consisting of fossil and renewable (solar) energy to cover a given energy demand of a small country, given that the supply of the renewable source is seasonally fluctuating and the considered representative energy-sector decision maker acts as price taker. The three model approaches differ in the aspect whether and how learning effects are included into the energy planning decision. While in Chapter 2 we have investigated the optimal composition of the portfolio under the assumption that the investment costs for renewable energy generation capital do not change, we have extended the model in Chapter 3 by including the effect of learning by doing and in Chapter 4 additionally the effect of learning by searching in order to investigate how the portfolio composition changes and what impact the inclusion of learning effects has on the solution. For both learning effects we have used a log-linear learning curve, for the learning-by-doing approach with one-factor, and for the learning-by-searching approach with two factors by including into the model an additional state for knowledge. Sensitivity analysis with respect to the fossil energy price, the efficiency of the renewable energy technology, the learning-by-doing coefficient, and geographical differences in the global radiation intensity have given insights on how the optimal portfolio composition changes and what this implies for possible policy decisions. As seasonal fluctuations are included into the models, they are non-autonomous, and consequently the analysis of these models differs from the usual steady-state analysis and exhibits some specialties. This chapter will provide a summary of the important findings and insights of the conducted investigations, considering both methodological as well as economic aspects.

5.1 Methodological Aspects of Non-Autonomous Optimal Control Models

As the canonical systems considered in this thesis are not only non-autonomous but also 1-periodic, candidates for the optimal long-run solutions have been given by periodic solutions with a period of one year, the stability of which is reflected by the eigenvalues of the monodromy matrix. In Section 2.2.3 we have introduced the equivalent but more geometric view of the Poincaré map. Here, the first specialty of non-autonomous problems in comparison to autonomous ones occurs. For autonomous problems the Poincaré map is defined on a hyperplane Σ of co-dimension one which is orthogonal to the periodic orbit at the starting point x_0 and, given the Poincaré map as $P: \Sigma \rightarrow \Sigma$, x_0 is a fixed point. To get the analogous interpretation for non-autonomous, 1-periodic problems,

$$\dot{x} = f(t, x), \quad f(t+1, x) = f(t, x), \quad (t, x) \in \mathbb{R} \times \mathbb{R}^n,$$

however, we have seen that the system first has to be transformed into the $(n+1)$ -dimensional autonomous system

$$\begin{aligned} \dot{\theta} &= 1, \\ \dot{x} &= f(\theta, x), \end{aligned} \tag{5.1}$$

which lies on the cylindrical manifold $X = \mathbb{S}^1 \times \mathbb{R}^n$ with the coordinates $(t(\text{mod } 1), x)$. In this space, a 1-dimensional cross-section then can be set as

$$\Sigma = \{(t, x) \in X : t = 0\}.$$

Defining the Poincaré map on this cross-section finally yields the same geometric interpretations as in the autonomous case. The eigenvalues of the monodromy matrix then coincide with the eigenvalues of the Poincaré map and therefore reflect the stability of the periodic solution.

Here, a second aspect can be observed that is different between autonomous and non-autonomous problems. As we have explained in Section 2.2.3, the monodromy matrix in the autonomous case always has the trivial eigenvector 1, as perturbations along the periodic orbit have eigenvalue 1. Due to the time dimension, however, this is not the case for non-autonomous problems. Only if the system is again transformed to the $(n+1)$ -dimensional autonomous system of (5.1), this trivial Floquet multiplier occurs.

In Section 3.3.1 we discussed the third specialty of non-autonomous optimal control problems,

which will be pointed out next. It concerns the calculation of the objective values. We have seen that for a trajectory solving a non-autonomous system, the relation for autonomous problems given by

$$\int_0^{\infty} e^{-rt} F(x(t), u(t)) dt = \frac{1}{r} H^0(x(0), \lambda(0)),$$

with $F(\cdot, \cdot)$ being the objective function and H^0 being the maximized Hamiltonian, does not hold as the calculation of the objective values is not time-invariant for non-autonomous problems. Instead, we have added an additional differential equation for the objective value function to the canonical system and solved this system for the necessary boundary value problems. This aspect of time-dependence is however not only important for the calculation of the objective values but also for the determination of the indifference threshold point/curve. We have seen that it is not sufficient to compare only the objective values of the involved trajectories along the path of the last continuation step, which would be sufficient for autonomous problems, but instead we have to consider the last objective values of each continuation step. Further on, also the term \hat{c} has to be added to the objective value of the path on $[0, T_p]$, including the remaining objective values for the periodic solution in the interval $[T_p, \infty)$ with T_p being the truncation time of the path and r being the discount rate. This term is given by the weighted objective value of the periodic solution over one period (c_{per}),

$$\hat{c} = \frac{e^{-rT_p}}{1 - e^{-r}} c_{per}. \quad (5.2)$$

5.2 Economic Interpretation of the Results

The results have shown that learning effects indeed have a strong impact on energy planning decisions. While for the first model in Chapter 2 without learning effects we have found only one optimal long-run periodic solution, two periodic solutions occurred in the second and third model where one corresponds to the pure fossil solution and the other one to a mixed portfolio with both fossil and renewable energy used to cover the given energy demand. In the latter two cases the areas of attraction are separated by an indifference threshold point/curve, respectively. The results for the three different model approaches are summarized in Table 5.1. The induced history dependence in Models 2 and 3 has consequences on the optimal long-run solution in two respects. First, the separation of the areas of attraction implies that renewable energy generation from the very beginning never would be optimal, which means that renewable energy would not be included into the portfolio, if the initial renewable energy generation capital stock is zero and, in case of the third model if also no knowledge has been accumulated. In this case, the initial

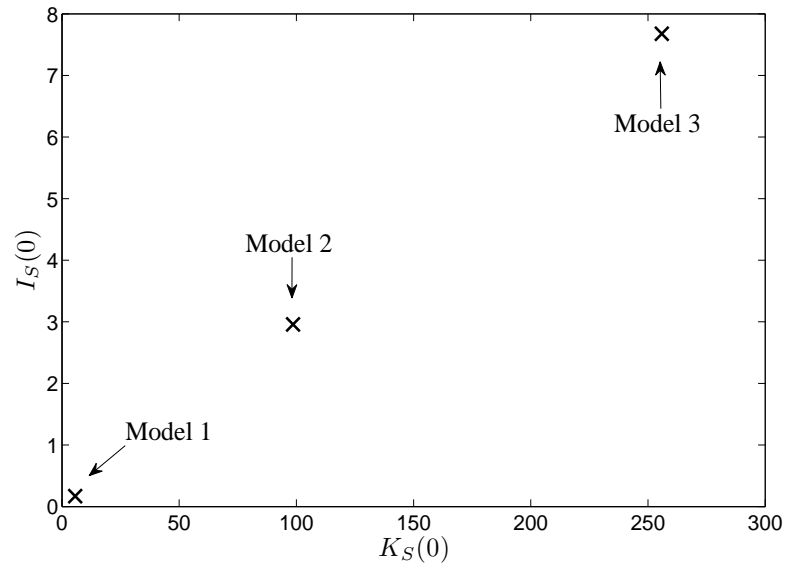
	Learning by doing	Learning by searching	Multiple periodic solutions	Indifference threshold point/curve
Model 1	×	×	×	×
Model 2	✓	×	✓	✓
Model 3	✓	✓	✓	✓

Table 5.1: Overview of the considered three different model approaches and their results.

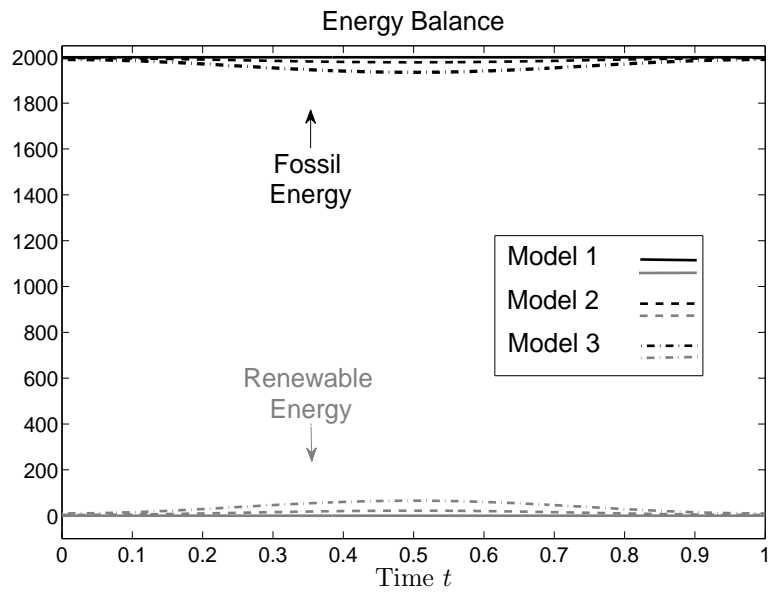
investment costs of renewable energy generation are too high so that it is profitable to use the pure fossil solution to cover the demand. In contrast, a start-up with renewable energy generation from the very beginning is possible in the first model approach without learning.

The results of the sensitivity analysis with respect to the fossil energy price highlight another difference, which is given by the rapidness of adapting renewable energy into the portfolio if the fossil energy price increases. Although a start-up is possible in the first model, the marginal increase in renewable energy generation capital with a higher fossil energy price is very low compared to the solutions with a mixed portfolio that lies beyond the indifference threshold point/curve in the two other model approaches. This means that in the models with learning, as soon as the indifference threshold point/curve is reached for example due to the support of subsidies, the adaption of the new technology in the portfolio happens at a much higher speed than in the basic model, although the fossil energy price is assumed to be the same. The reason for this is given by the ongoing reduction of investment costs due to the learning effects. This is shown in more detail in Figure 5.1, where Figure 5.1a depicts the periodic solutions with a mixed portfolio for the three different model approaches at a fossil energy price $p_F = 0.08$. While in the first model approach, very little is invested in renewable energy capital and, consequently, the capital stock is very low, the investments and hence the capital stock of the mixed periodic solution of the second model approach are many times larger for the same fossil energy price. As the investment costs in Model 1 stay high over the whole planning period, independent of the efforts in renewable energy generation, a further increase therefore is not optimal, while in Model 2 these investment costs get smaller with every additional unit of renewable energy capital that is accumulated.

If also learning by searching is considered, one can see that the investments in renewable energy capital and the capital stock for Model 3 are even almost three times larger than for the second model approach at the same fossil energy price. This underlines the fact that additional investments into R&D efforts can strongly foster the success of renewable energy generation. Although additional costs occur, the even stronger decrease in the investment costs for renewable energy capital can compensate for this and make further investments profitable.



(a)



(b)

Figure 5.1: Comparison of the mixed portfolio of the three considered model approaches for a fossil energy price $p_F = 0.08$: **(a)** State-control space. **(b)** Energy balance.

Figure 5.1b shows the energy balance for the obtained periodic solutions of the three model approaches. Also here, it gets obvious that the inclusion of both learning effects strongly encourages renewable energy generation and plays an important role in the adaption of renewable energy into the portfolio.

One of the main conclusions of the obtained results is the necessity of support for a successful adaption into the system during the start-up period of a new renewable energy technology. Here, the main difference between Model 2 and Model 3 has been the form of support that would be needed. While in Model 2 subsidizing investments into renewable energy capital would be helpful to overcome this difficult period, we have seen in Model 3 that also supports for R&D efforts could compensate for a too small stock in renewable energy capital.

In addition to this aspect, sensitivity analysis with respect to the global radiation intensity has shown that the effect of such supports and consequently their significance strongly depends on geographical conditions. As we have concluded from the obtained results in Sections 3.4.3 and 4.4.2, the fossil energy price boundary at which renewable energy is even a considerable alternative, shifts to the right if global radiation is less intensive. Therefore, in this case subsidies possibly would have no effect if the fossil energy price lies below this boundary. Only if the fossil energy price would increase, subsidies would have an impact. On the other hand, in a region with a high global radiation intensity, subsidies might be overshooting as this price boundary shifts to the left and, hence, already at a lower fossil energy price renewable energy generation is profitable. These aspects underline the difficulty of a proper subsidizing policy, because in practice these boundaries cannot be determined easily.

Regardless of whether learning effects are included or not, the results of all three model approaches have shown that even in case of a very high fossil energy price the exclusive coverage of the energy demand with renewable energy is not possible. Due to the seasonally fluctuating supply there are always periods of shortfalls in which fossil energy is needed, independent of the shape of the demand. Of course this also is due to the stringent assumption that storage is not possible in our model. However, it reflects quite well the current situation on the markets, where on the one hand subsidized renewable energy generation keeps down the electricity prices, which consequently makes conventional energy generation non-economical due to the high commodity prices, but on the other hand conventional energy forms are needed to cover up in these periods of shortfalls.

5.3 Conclusion

The considered models underline the major challenges of a renewable but simultaneously secure energy supply. In this work we have focused on solar energy, but seasonal fluctuations are also a big problem for other types of renewable energy as for example hydro power plants. Here, the seasonal fluctuations are induced by snow melting and dry periods and are also a matter of geographical aspects. The results of the models have shown that the coverage of the demand only with renewable (solar) energy for the considered country is not possible. However, combinations with other renewable sources, which in the case of hydro-pump-storage power plants for example would even imply storage possibilities, could of course at least diminish these fluctuations. Nevertheless, technology and policy efforts are not yet sufficient to reach complete independence of fossil energy sources.

One important aspect is given by a proper subsidy system, which is a delicate issue and if applied in the wrong way might cause even a counteracting imbalance. What we further on have seen from the sensitivity analysis with respect to the global radiation intensity is, that such portfolio combinations and policy decisions always have to be a local issue in the geographical sense, as a global solution to the energy problem never can cover all these regional specialties. The differences in the results obtained due to the inclusion of learning effects into the model have shown that such aspects of learning are indeed important to be included into energy planning decisions, because a far-sighted view is crucial for the success of including a new technology into the system.

To sum up, a switch to renewable energy is essential to mitigate climate change, but the implementation has to be planned carefully and far-sighted, while solutions have to be adapted to local conditions so that the inclusion into the system can be successful.

List of Figures

1.1	Break-even points for different learning rates.	7
2.1	Average global radiation per month in Austria and its deterministic approximation.	15
2.2	Fossil, mixed, and renewable solutions to cover the given energy demand.	22
2.3	Poincaré map.	27
2.4	Searching for a solution path.	31
2.5	Continuation algorithms searching along different hyperplanes.	33
2.6	Periodic solution, time paths for investments and capital over one year and renewable energy generation for a fossil energy price $p_F = 0.08$	35
2.7	Phase portrait for a fossil energy price $p_F = 0.08$	36
2.8	Maintenance investments along the solution paths for a fossil energy price $p_F = 0.08$	37
2.9	Energy balance for a fossil energy price $p_F = 0.08$	37
2.10	Solution for a fossil energy price $p_F = 0.01$	39
2.11	Periodic solution for a fossil energy price $p_F = 0.0068$	41
2.12	Periodic solution for a fossil energy price $p_F = 2.7$	41
2.13	Periodic solution for a fossil energy price $p_F = 5.5$	42
2.14	Periodic solution for a fossil energy price $p_F = 10$	43
2.15	Development of the cost function along the optimal long-run periodic solutions for different fossil energy price scenarios.	44
2.16	Periodic solution for different degrees of efficiency η	46
2.17	Combined effects with changes in both the fossil energy price as well as efficiency.	47
2.18	Seasonally fluctuating energy demand with a peak during the winter period, a peak during the summer period and both peaks, respectively.	49
2.19	Periodic solution for a fossil energy price $p_F = 4$ and a seasonally fluctuating energy demand with a winter peak.	50

2.20	Periodic solution for a fossil energy price $p_F = 4$ and a seasonally fluctuating energy demand with a summer peak.	51
2.21	Periodic solution for a fossil energy price $p_F = 7.5$ and a seasonally fluctuating energy demand with both, a winter and a summer peak.	51
3.1	One continuation step with the Moore-Penrose method.	60
3.2	The three detected periodic solutions for a fossil energy price $p_F = 0.051$	62
3.3	Time-control and time-state paths for the two detected periodic solutions of saddle-type for a fossil energy price $p_F = 0.051$	63
3.4	Search for the indifference threshold point for a fossil energy price $p_F = 0.051$	67
3.5	Indifference threshold point for a fossil energy price $p_F = 0.051$	68
3.6	Investment costs per unit of generated renewable energy along the mixed path for a fossil energy price $p_F = 0.051$	70
3.7	Search for the indifference threshold point for a fossil energy price $p_F = 0.05$	72
3.8	Search for the indifference threshold point for a fossil energy price $p_F = 0.05$	75
3.9	Indifference threshold point for a fossil energy price $p_F = 0.05$	76
3.10	Shooting method to locate periodic solutions.	78
3.11	Bifurcation diagram of the canonical system with respect to the fossil energy price $p_F \leq 0.07$	79
3.12	Sensitivity analysis of the canonical system with respect to a fossil energy price $p_F \geq 0.07$	82
3.13	Norms of eigenvalues of the obtained periodic solutions for a fossil energy price $p_F \leq 0.07$	83
3.14	Bifurcation diagram of the canonical system with respect to the learning-by-doing coefficient α	86
3.15	Global radiation in Europe.	87
3.16	Average daily global radiation in Hamburg and Athens.	88
3.17	Deterministic functions for global radiation.	89
3.18	Bifurcation diagram with respect to the fossil energy price p_F for the Scenarios 1 and 2 in comparison with the basic scenario.	89
4.1	The three detected periodic solutions for a fossil energy price $p_F = 0.047$	105
4.2	Time-control and time-state paths for the three detected periodic solutions for a fossil energy price $p_F = 0.047$	106
4.3	Dominance over the mixed periodic solution for a fossil energy price $p_F = 0.047$	108

4.4	Overlap of trajectories leading into the two periodic solutions for a fossil energy price $p_F = 0.047$	109
4.5	Indifference threshold point for a fossil energy price $p_F = 0.047$	109
4.6	Indifference threshold curve for a fossil energy price $p_F = 0.047$	111
4.7	Investment costs per unit of generated renewable energy along the mixed path with research for a fossil energy price $p_F = 0.047$	114
4.8	Fossil/Mixed path for a fossil energy price $p_F = 0.046$	116
4.9	Mixed/Mixed & Research path for a fossil energy price $p_F = 0.046$	117
4.10	Indifference threshold curve for a fossil energy price $p_F = 0.046$	118
4.11	Bifurcation diagram of the canonical system with respect to a fossil energy price $p_F \leq 0.08$	120
4.12	Sensitivity analysis of the canonical system with respect to a fossil energy price $p_F \geq 0.08$	122
4.13	Indifference threshold curves for different fossil energy prices p_F	124
4.14	Indifference threshold surface.	125
4.15	Norms of eigenvalues of the obtained periodic solutions along the p_F -axis.	127
4.16	Bifurcation diagram of the canonical system with respect to the fossil energy price p_F for Scenario 1 and 2 in comparison with the basic scenario.	129
5.1	Comparison of the three considered model approaches.	135

List of Tables

2.1	Parameter values used for the numerical analysis of the basic model.	34
3.1	Parameter values used for the numerical analysis of the extended model with learning by doing.	61
3.2	Multiple periodic solutions for $p_F = 0.051$	62
3.3	Estimates for τ and ν for Scenarios 1 and 2 and the basic scenario for Austria. . .	88
4.1	Parameter values used for the numerical analysis of the extended model with learning by searching.	104
4.2	Multiple periodic solutions for $p_F = 0.047$	105
5.1	Overview of the considered three different model approaches and their results. . .	134

Bibliography

- Allgower, E. L. and Georg, K. (1997). Numerical path following. In Ciarlet, P. and Lions, J., editors, *Techniques of Scientific Computing (Part 2)*, volume 5 of *Handbook of Numerical Analysis*, pages 3 – 207. Elsevier.
- Argote, L., Beckman, S. L., and Epple, D. (1990). The persistence and transfer of learning in industrial settings. *Management Science*, 36(2):140–154.
- Argote, L. and Epple, D. (1990). Learning Curves in Manufacturing. *Science*, 247:920–924.
- Arrow, K. J. (1962). The economic implications of learning by doing. *The Review of Economic Studies*, 29(3):155–173. Available at SSRN: <http://ssrn.com/abstract=1506343>.
- Baloff, N. (1970). Startup management. *IEEE Transactions on Engineering Management*, EM-17(4):132–141.
- Barreto, L. (2001). *Technological learning in energy optimisation models and deployment of emerging technologies*. PhD thesis, ETH Zürich. Nr. 14151.
- Barreto, L. and Kypreos, S. (1999). *Technological learning in energy models: experience and scenario analysis with MARKAL and the ERIS model prototype*. Wurenlingen, Switzerland: Paul Scherrer Institut.
- BCG (1970). *Perspectives on Experience*. The Boston Consulting Group, Boston.
- Benkard, C. L. (2000). Learning and forgetting: The dynamics of aircraft production. *American Economic Review*, 90(4):1034–1054.
- Berglund, C. and Söderholm, P. (2006). Modeling technical change in energy system analysis: analyzing the introduction of learning-by-doing in bottom-up energy models. *Energy Policy*, 34(12):1344–1356.

- Carr, J. (1982). Applications of centre manifold theory. In Marsden, J. E. and Sirovich, L., editors, *Applied Mathematical Sciences*, volume 35. Springer, New York.
- Chakravorty, U., Leach, A., and Moreaux, M. (2008). "Twin peaks" in energy prices: A hotelling model with pollution and learning. IDEI Working Papers 52, Institut d'Économie Industrielle (IDEI), Toulouse.
- Chakravorty, U., Leach, A., and Moreaux, M. (2011). Would hotelling kill the electric car? *Journal of Environmental Economics and Management*, 61(3):281–296.
- Chakravorty, U., Magné, B., and Moreaux, M. (2006). A hotelling model with a ceiling on the stock of pollution. *Journal of Economic Dynamics and Control*, 30(12):2875–2904.
- Chakravorty, U., Magné, B., and Moreaux, M. (2012). Resource use under climate stabilization: Can nuclear power provide clean energy? *Journal of Public Economic Theory*, 14(2):349–389.
- Cohen, W. M. and Levinthal, D. A. (1989). Innovation and learning: The two faces of R&D. *Economic Journal*, 99(397):569–596.
- Coulomb, R. and Henriot, F. (2011). Carbon price and optimal extraction of a polluting fossil fuel with restricted carbon capture. Working paper 322, Banque de France, Paris.
- Cunha-e Sá, M. A., Leitão, A., and Reis, A. B. (2010). Innovation and environmental policy: Clean vs. dirty technical change. FEUNL Working Paper Series wp548, Universidade Nova de Lisboa, Faculdade de Economia.
- Dechert, W. D. (1983). Increasing returns to scale and the reverse flexible accelerator. *Economics Letters*, 13(1):69 – 75.
- Dechert, W. D. and Nishimura, K. (1983). A complete characterization of optimal growth paths in an aggregated model with a non-concave production function. *Journal of Economic Theory*, 31(2):332–354.
- Deshmukh, M. K. and Deshmukh, S. S. (2008). Modeling of hybrid renewable energy systems. *Renewable and Sustainable Energy Reviews*, 12(1):235–249.
- Dhooge, A., Govaerts, W., Kuznetsov, Y. A., Mestrom, W., Riet, A. M., and Sautois, B. (2006). MATCONT and CL_MATCONT: continuation toolboxes in MATLAB.
- Diamond, J. (1993). Ten thousand years of solitude. *Discover*, March.

- Epple, D., Argote, L., and Devadas, R. (1991). Organizational learning curves: A method for investigating intra-plant transfer of knowledge acquired through learning by doing. *Organization Science*, 2(1):58–70.
- Feichtinger, G. and Hartl, R. F. (1986). *Optimale Kontrolle ökonomischer Prozesse: Anwendungen des Maximumprinzips in den Wirtschaftswissenschaften*. de Gruyter, Berlin.
- Feichtinger, G., Hartl, R. F., Kort, P. M., and Veliov, V. M. (2006). Anticipation effects of technological progress on capital accumulation: a vintage capital approach. *Journal of Economic Theory*, 126(1):143–164.
- Gerlagh, R. and Van der Zwaan, B. (2003). Gross world product and consumption in a global warming model with endogenous technological change. *Resource and Energy Economics*, 25(1):35–57.
- Grass, D. (2012). Numerical computation of the optimal vector field: Exemplified by a fishery model. *Journal of Economic Dynamics and Control*, 36(10):1626–1658.
- Grass, D., Caulkins, J. P., Feichtinger, G., Tragler, G., and Behrens, D. A. (2008). *Optimal Control of Nonlinear Processes: With Applications in Drugs, Corruption, and Terror*. Springer, Berlin.
- Greiner, A., Grüne, L., and Semmler, W. (2014). Economic growth and the transition from non-renewable to renewable energy. *Environment and Development Economics*, 19(04):417–439.
- Grimaud, A., Lafforgue, G., and Magné, B. (2011). Climate change mitigation options and directed technical change: A decentralized equilibrium analysis. *Resource and Energy Economics*, 33(4):938 – 962. Special section: Sustainable Resource Use and Economic Dynamics.
- Grübler, A. and Messner, S. (1998). Technological change and the timing of mitigation measures. *Energy Economics*, 20(5-6):495–512.
- Guckenheimer, J. and Holmes, P. (1990). *Nonlinear oscillations, dynamical systems, and bifurcations of vector fields*, volume 42 of *Applied mathematical sciences*. Springer, Berlin.
- Hale, J. and Koçak, H. (1991). *Dynamics and Bifurcations*. Springer, New York.
- Han, M., Feichtinger, G., and Hartl, R. F. (1994). Non-concavity and proper optimal periodic control. *Journal of economic dynamics & control*, 18(5):975–990.

- Harmon, C. (2000). Experience curves of photovoltaic technology. IIASA Interim Report IR-00-014. http://www.iiasa.ac.at/publication/more_IR-00-014.php.
- Hartl, R. F. (1993). On the properness of one-dimensional periodic control problems. *Systems & Control Letters*, 20(5):393 – 395.
- Hartley, P. R., Medlock, K. B., Temzelides, T., and Zhang, X. (2010). Innovation, renewable energy, and macroeconomic growth. Working paper, James A. Baker III Institute for Public Policy, Rice University, Houston.
- Heinzel, C. and Winkler, R. (2011). Distorted time preferences and time-to-build in the transition to a low-carbon energy industry. *Environmental & Resource Economics*, 49(2):217–241.
- IPCC (1998). *The Regional Impacts of Climate Change: An Assessment of Vulnerability*. Cambridge University Press. Special Reports, Working Group II, Watson, R.T., Zinyowera, M.C. and Moss, R.H., editors, Cambridge.
- IPCC (2014). *Climate Change 2014: Mitigation of Climate Change*. Cambridge University Press. Fifth Assessment Report, Working Group III, Edenhofer, O., Pichs-Madruga, R., Sokona, Y., Farahani, E., Kadner, S., Seyboth, K., Adler, A., Baum, I., Brunner, S., Eickemeier, P., Kriemann, B., Savolainen, J., Schlmer, S., von Stechow, C., Zwickel T. and Minx, J.C., editors, Cambridge.
- Joosten, R., Peters, H., and Thuijsman, F. (1995). Unlearning by not doing: Repeated games with vanishing actions. *Games and Economic Behavior*, 9(1):1–7.
- Ju, N., Small, D., and Wiggins, S. (2003). Existence and computation of hyperbolic trajectories of aperiodically time dependent vector fields and their approximations. *International Journal of Bifurcation and Chaos*, 13(6):1449–1457.
- Kahouli-Brahmi, S. (2008). Technological learning in energy-environment-economy modelling: A survey. *Energy Policy*, 36(1):138–162.
- Keachie, E. C. and Fontana, R. J. (1966). Effects of learning on optimal lot size. *Management Science*, 13(2):B–102–B–108.
- Kiseleva, T. (2011). *Structural Analysis of Complex Ecological Economic Optimal Control Problems*. PhD thesis, University of Amsterdam, Center for Nonlinear Dynamics in Economics and Finance (CeNDEF).

- Kiseleva, T. and Wagener, F. O. O. (2010). Bifurcations of optimal vector fields in the shallow lake model. *Journal of Economic Dynamics and Control*, 34(5):825–843.
- Köhler, J., Grubb, M., Popp, D., and Edenhofer, O. (2006). The transition to endogenous technical change in climate-economy models: A technical overview to the innovation modeling comparison project. *The Energy Journal*, Special Issue: Endogenous Technological Change and the Economics of Atmospheric Stabilization:17–56.
- Kouvaritakis, N., Soria, A., and Isoard, S. (2000). Modelling energy technology dynamics: methodology for adaptive expectations models with learning by doing and learning by searching. *International Journal of Global Energy Issues*, 14(1-4):104–115.
- Kuznetsov, Y. A. (1998). *Elements of Applied Bifurcation Theory, Second Edition*, volume 112 of *Applied Mathematical Sciences*. Springer, New York.
- McDonald, A. and Schrattenholzer, L. (2001). Learning rates for energy technologies. *Energy Policy*, 29(4):255–261.
- Messner, S. (1997). Endogenized technological learning in an energy systems model. *Journal of Evolutionary Economics*, 7(3):291–313.
- Miketa, A. and Schrattenholzer, L. (2004). Experiments with a methodology to model the role of R&D expenditures in energy technology learning processes; first results. *Energy Policy*, 32(15):1679–1692.
- Moser, E., Grass, D., Tragler, G., and Prskawetz, A. (2014). Optimal control models of renewable energy production under fluctuating supply. In Lirkov, I., Margenov, S., and Waniewski, J., editors, *Large-Scale Scientific Computing*, Lecture Notes in Computer Science, pages 133–142. Springer, Berlin.
- Neij, L. (1997). Use of experience curves to analyse the prospects for diffusion and adoption of renewable energy technology. *Energy Policy*, 25(13):1099–1107.
- Nema, P., Nema, R. K., and Rangnekar, S. (2009). A current and future state of art development of hybrid energy system using wind and PV-solar: A review. *Renewable and Sustainable Energy Reviews*, 13(8):2096–2103.
- Nemet, G. F. (2006). Beyond the learning curve: factors influencing cost reductions in photovoltaics. *Energy Policy*, 34(17):3218–3232.

- Popp, D. (2006). ENTICE-BR: the effects of backstop technology R&D on climate policy models. *Energy Economics*, 28(2):188–222.
- Rasmussen, T. N. (2001). CO₂ abatement policy with learning-by-doing in renewable energy. *Resource and Energy Economics*, 23(4):297–325.
- Rauscher, M. (2009). Green R&D versus end-of-pipe emission abatement: A model of directed technical change. Thünen-Series of Applied Economic Theory 106, University of Rostock, Institute of Economics.
- Reichenbach, J. and Requate, T. (2012). Subsidies for renewable energies in the presence of learning effects and market power. *Resource and Energy Economics*, 34(2):236–254.
- Reithmeier, E. (1991). *Periodic Solutions of Nonlinear Dynamical Systems*, volume 1483 of *Lecture Notes in Mathematics*. Springer, Berlin.
- Rong-Gang, C. (2013). An optimization model for renewable energy generation and its application in china: A perspective of maximum utilization. *Renewable and Sustainable Energy Reviews*, 17(C):94–103.
- Sethi, S. P. (1977). Nearest feasible paths in optimal control problems: Theory, examples, and counterexamples. *Journal of Optimization Theory and Applications*, 23(4):563–579.
- Sethi, S. P. (1979). Optimal advertising policy with the contagion model. *Journal of Optimization Theory and Applications*, 29(4):615–627.
- Skiba, A. K. (1978). Optimal Growth with a Convex-Concave Production Function. *Econometrica*, 46(3):527–39.
- SODA (2014). Solar radiation data. Downloaded on 5th of February 2014 from http://www.soda-is.org/eng/services/service_invoke/gui.php?xml_descript=hc1_month.xml&Submit=HC1month.
- Sturm, R. (1993). Nuclear power in Eastern Europe: Learning or forgetting curves? *Energy Economics*, 15(3):183–189.
- Van der Ploeg, F. and Withagen, C. A. (2012). Is there really a green paradox? *Journal of Environmental Economics and Management*, 64(3):342–363. 2010 Monte Verita Conference on Sustainable Resource Use and Economic Dynamics (SURED).

Van der Zwaan, B. C. C., Gerlagh, R., Klaassen, G., and Schrattenholzer, L. (2002). Endogenous technological change in climate change modelling. *Energy Economics*, 24(1):1–19.

Wene, C. O. (2000). *Experience Curves for Energy Technology Policy*. OECD/IEA.

Wright, T. P. (1936). Factors affecting the cost of airplanes. *Journal of the Aeronautical Sciences (Institute of the Aeronautical Sciences)*, 3(4):122–128.

ZAMG (2012). Klimadaten. Downloaded on 16th of February 2012 from http://www.zamg.ac.at/fix/klima/oe71-00/klima2000/klimadaten_oesterreich_1971_frame1.htm.

Curriculum Vitae

Elke Moser

Date of Birth: 20th of November 1985

Place of Birth: Wels

Nationality: Austria

Education

- | | |
|----------------------|--|
| Since February 2011 | PhD studies in Technical Mathematics at the Institute for Mathematical Methods in Economics, Vienna University of Technology |
| December 2010 | Graduation, Degree: Dipl.-Ing.
Thesis: <i>Optimal Controls in Models of Economic Growth and the Environment</i> , at the Institute for Mathematical Methods in Economics, Vienna University of Technology |
| Feb. 2009-July 2009 | National and Kapodistrian University of Athens (Greece), Erasmus program |
| Oct. 2004-Nov. 2010 | Studies in Technical Mathematics, focus on Mathematical Methods in Economics, Vienna University of Technology |
| Sept. 1996-July 2004 | Secondary school, Wirtschaftliches Realgymnasium der Kreuzschwesternschule Linz |

Awards and Scholarships

Nov. 2011	OeGOR Prize, Prize of the Austrian Society of Operations Research, awarded for the diploma thesis
April 2012	VERBUND Women's Scholarship for PhD-students

Professional Experience

Since March 2013	e&t ENERGIE HANDESLGESELLSCHAFT m.b.H., Quantitative analyst
Feb. 2013	VERBUND Trading AG, Internship in risk management
Jan. 2011-Dec. 2012	Vienna Institute of Demography, Austrian Academy of Sciences, Project assistant
Nov. 2009-Mar. 2010	Austrian Environmental Expert Group, Forschungsinstitut für Energie und Umweltplanung, Research assistant
July/August 2008	Schenker Hörsching, Internship in cost and cash accounting
July 2007	DSM Fine Chemicals in Linz, Internship in process management

Publications

- Moser, E., Prskawetz, A., and Tragler, G., 2012,
Optimal Controls in Models of Economic Growth and the Environment,
In Lirkov, I., Margenov, S., and Wasniewski, J. (Eds.),
Large-Scale Scientific Computing, 7116, 139-146, Springer Heidelberg.
- Moser, E., Prskawetz, A., and Tragler, G., 2013,
Environmental Regulations, Abatement and Economic Growth,
In Crespo Cuaresma, J., Palokangas, T. and Tarasyev, A. (Eds.)
Green Growth and Sustainable Development, 14, 87-111, Springer Heidelberg.
- Moser, E., Seidl, A., and Feichtinger, G., 2013,
History-dependence in production-pollution-trade-off models: a multi-stage approach,
Annals of Operations Research, 1-25, Springer US.
- Moser, E., Grass, D., Tragler, G., and Prskawetz, A., 2014,
Optimal Control Models of Renewable Energy Production Under Fluctuating Supply,
In Lirkov, I., Margenov, S., and Wasniewski, J. (Eds.),
Large-Scale Scientific Computing, 133-142, Springer Heidelberg.

Edited Volumes

- Moser, E., Semmler, W., Tragler, G., Veliov, V.M. (Eds.), 2014,
Dynamic Optimization in Environmental Economics,
Series *Dynamic Modeling and Econometrics in Economics and Finance*,
Vol.15, Springer Heidelberg.

Talks, Workshops and Schools

- June 3-4, 2011 NoeG 2011, Annual Meeting of the Austrian Economic Association,
Talk on *Environmental Regulations, Abatement and Economic Growth*, University of Graz
- Nov.4, 2011 OeGOR Jahrestagung,
Annual Meeting of the Austrian Society of Operations Research,
Talk on the diploma thesis in the course of the OeGOR Prize awards
- Dec. 9-10, 2011 IIASA Symposium on *Green Growth and Sustainable Development*,
Talk on *Environmental Regulations, Abatement and Economic Growth*, IIASA, Laxenburg
- Jan. 22-27, 2012 Arctic Frontiers 2012 - Energy of the High North,
Talk on *Seasonal Varying Renewable Energy Supply in a Firm-based Model*, University of Tromsø, Norway
- Jan. 22-Feb. 2, 2012 Arctic Frontiers Workshop on Research Proposal Writing,
Young Scientist Forum, University of Tromsø, Norway
- May 30-June 2, 2012 12th Viennese Workshop
on Optimal Control, Dynamic Games and Nonlinear Dynamics,
Talk on *Optimal control models of renewable energy production under fluctuating supply*, Vienna University of Technology, Austria
- Sept. 4-7, 2012 Operations Research 2012,
Energy, Markets and Mobility,
Talk on *Optimal control models of renewable energy production under fluctuating supply*, Leibniz Universität Hannover, Germany
- April. 8-12, 2013 CIRM School
on *Stochastic Control for the Management of Renewable Energies*,
Centre International de Rencontres Mathématiques, Marseille, France
- July, 1-4, 2013 26th European Conference on Operational Research,
Talk on *Optimal control models of renewable energy production under fluctuating supply*, SAPIENZA University of Rome, Italy